EK-1

NANODESENLİ HÜCRE İSKELELERİ ÜRETİMİ VE DOKU MÜHENDİSLİĞİ YÖNTEMİYLE YAPAY DAMAR YAPIMINDA KULLANIMI

Proje No: 108T576

Prof. Dr. Vasıf HASIRCI
Prof. Dr. Nesrin HASIRCI
Pınar ZORLUTUNA
Hayriye ÖZÇELİK

ARALIK 2010
ANKARA

TÜBİTAK

PROJE ÖZET BİLGİ FORMU

Proje No:108T576
Proje Başlığı: Nanodesenli Hücre İskeleleri Üretimi Ve Doku Mühendisliği Yöntemiyle Yapay Damar Yapımında Kullanımı
Proje Yürütücüsü ve Araştırmacılar: Prof. Dr. Vasıf Hasırcı, Prof. Dr. Nesrin Hasırcı, Pınar Zorlutuna, Hayriye Özçelik
Projenin Yürütüldüğü Kuruluş ve Adresi: ODTÜ, FEF, Biyolojik Bilimler Bölümü, Biyoteknoloji Araştırma Birimi, Ankara 06531
Destekleyen Kuruluş(ların) Adı ve Adresi: TUBİTAK-TBAG
Projenin Başlangıç ve Bitiş Tarihleri: 01.12.2008-31.11.2010
Öz (en çok 70 kelime) **Bu çalışma nanoteknolojik yöntemler kullanılarak, hedeflenen doğal dokunun ekstraselüler matriks düzeyinde taklit edilmesi sonucunda doku mühendisliği yöntemi ile elde edilerek yapay dokunun işlevselliğini en üst düzeye çıkarmayı hedeflemiştir. Doğal damar dokusunda gerekli olan mekanik sağlamlığı sağlayan etken, damar düz kas hücrelerinin ve bu hücreler tarafından salgılanan ekstraselüler matriksin aynı yönde yerleşmiş ve yapılanmış olmalarıdır. Hazırlanan kollajen filmler üzerindeki nano-desenler sayesinde insan safen veninden izole edilen damar düz kas hücrelerinin yönlendirilmesi sağlanmış ve bu şekilde elde edilen yapay dokunun gerçek doku ile benzerliği bir çok farklı yöntemlerle incelenmiştir. Nano-desenlerin varlığı ve düzgünlüğü SEM ve AFM kullanılarak kanıtlanırken,**

iskeleler üzerindeki hücre miktarı Alamar Blue testi ile saptanmıştır. Hücre morfolojisi, fenotipi ve işlevselliği immün ve floresan boyamalar ve mikroskopik yöntemler (floresan, konfokal, SEM, ESEM ve TEM) kullanılarak incelenmiştir. Hücresiz ve hücreli yapı iskelelerin mekanik özellikleri belirlenmiştir. Çalışmanın nanokanallar içeren ayağına ek olarak çalışmaya mikron ve nano ölçekli çıkıntılar da dahil edilmiştir. Hücrelerin bu yapılara verdiği yüzeye tutunma ve yönelim davranışları floresan mikroskobu ile incelenmiştir. Hücreler üç farklı genişlikli film üstünde fenotiplerini korumuşlar ve kanallar yönünde uzanmışlardır. Damar düz kas hücrelerinin tıpkı doğal damar yapısındaki gibi yönlenmelerinin tasarımın mekanik özelliklerinin iyileştirilmesinde kullanılabileceği görülmüştür. Damar düz kas hücreleri nano ölçekli çıkıntıların boyutlarına göre oldukça büyük olduğundan belirgin bir uzanım gözlenmemiştir. Mikro çıkıntılar ise düz kas hücrelerinin uzanımlarından çok morfolojilerini etkilemiş, düz yüzeylerde tipik ince uzun yapılı olan hücreler bu çıkıntıların üzerine yayılarak geniş alanlı hücrelere dönüşmüşlerdir. Nanokanallı tasarımlardaki kadar olmasa bile asimetrik dağılım gösteren B tipi çıkıntılı yüzeylerde hücre yönlenmesi görülmüştür.

Anahtar Kelimeler: Damar doku mühendisliği, kollajen, mikro-nano-desen, hücre yönlenmesi

Fikri Ürün Bildirim Formu Sunuldu mu? **Evet** ☐ **Gerekli Değil** ☐
Fikri Ürün Bildirim Formu'nun tesliminden sonra 3 ay içerisinde patent başvurusu yapılmalıdır.

Projeden Yapılan Yayınlar: Ayrı bir dosya olarak (108T576_vasif hasirci_yayınlar) rapora eklenmiştir.

Önsöz

Damar doku mühendisliği araştırmalarındaki sorunların başında hücre ve iskeleden oluşan yapay damarın yetersiz ya da hastanın doku özellikleriyle uyumsuz (düşük) mekanik güce sahip olması gelmektedir. Bu projede önerilen yöntemle yapay damar üretimi daha önce yapılmamış ve bu sorunu çözmek için daha önce denenmemiştir. Proje 01.12.2008-01.12.2010 tarihleri arsında TÜBİTAK TBAG-108T576 koduyla laboratuvarımızda son 10 yılda elde edilen doku mühendisliği ile mikro ve nanodesenli dokular üzerindeki bilgi birikimi kullanılarak yapay damar geliştirmek amacıyla yürütülmüştür.

İÇİNDEKİLER

Abstract

One of the major causes of death in the Western societies is the diseases that affect small and medium sized blood vessels, most common among them being atherosclerosis. For reconstruction or substitution of small diameter blood vessels (< 6 mm) prosthetic vascular grafts (e.g. ePTFE or Dacron) can not be used mainly because of clogging. Therefore, in such cases autologous grafts have to be used. A functional tissue engineered vessel can be the ultimate solution to vascular reconstruction and all of the efforts for making it showed that if the natural vessel can be fully mimicked, this goal can be reached. Aim of this study was to develop a nanopatterned collagen film and to assess its interaction with vascular smooth muscle cells in order to use in vascular tissue engineering applications. X-ray interference lithography used for creating templates with nano-channels on silicon wafers. Collagen Type I was isolated from rat tails. Collagen films were produced by solvent casting using the templates and subsequent crosslinking performed by using chemical crosslinkers. Templates, patterned films, as well as unpatterned films, were examined under SEM and AFM for surface characterization and fidelity of the pattern. Collagen films seeded with vascular muscle cells which was isolated from human saphenous vein. Cells were characterized by immunostaining with antibodies that are specific to these cells, to prove the level of success of cell isolation. Material-cell interaction studied by various methods. To assess cell viability, cell numbers were determined by Alamar Blue. Immunostaining and other fluorescence stainings (i.e. DAPI) were performed with CLSM to examine cells to confirm the cell phenotype, cell functionality and degree of their guidance. SEM will also were used to observe cell guidance. These films were also subjected to mechanical testing to study their mechanical properties in untreated and in cell seeded form.

Cell culture studies with VSMCs showed that nanopatterned collagen films are good substrates for cell attachment and cell proliferation. The cells retained their phenotype and were aligned by the nanopatterns on all 3 nanopattern dimensions. It has been suggested that aligning VSMCs in the same way as they are in the natural tissue might be used to improve the mechanical properties. This study showed that this indeed is true, although alignment did not affect cell proliferation at the end of day 21, it increased the mechanical properties of the scaffolds. With the current approach, the good biological properties of collagen could be combined with the adequate mechanical properties obtained through cell guidance to create scaffolds for use in vascular tissue engineering.

Özet

Batılı ülkelerde en önde gelen ölüm sebeplerinden biri, başta aterosikleroz olmak üzere, küçük ve orta çaplı kan damarlarını etkileyen hastalıklardır. Küçük çaplı damarların (< 6 mm) rekonstrüksiyonunda ya da değiştirilmesinde, sebep oldukları tıkanmadan dolayı, prostetik greftlar (örneğin ePTFE ya da Dakron) kullanılamamaktadır. Dolayısı ile bu gibi durumlarda otolog greftler kullanılmak zorunda kalınmaktadır. Doku mühendisliği yöntemleri ile elde edilmiş bir vasküler greft, vasküler rekonstrüksiyon için en iyi çözüm olabilir. Bu amaca yönelik bütün çalışmalar doğal damar yapısı tamamen taklit edilebilirse bu hedefe ulaşılabilineceğini göstermiştir. Bu çalışmanın amacı, damar doku mühendisliği uygulamalarında kullanılmak üzere nano-desenli kollajenden yapılmış bir hücre taşıyıcısı (iskele) tasarlanması ve bu iskelenin damar düz kas hücreleri ile olan etkileşimlerinin incelenmesidir. Nano-kanallı yapıdaki silika temelli kalıplar X-ışını girişim litografisi yöntemi ile elde edilmiştir. Daha sonra bu kalıplar kullanılarak tip I kollajenden filmler hazırlanmış ve bu hücre iskelelerine insan safen veninden izole edilmiş olan damar kas hücreleri ekilmiştir. Kas hücreleri bu hücre tipine özgü antikorlarla boyanarak karakterize edilmiştir. Böylece izolasyonun başarısı tayin edilmiştir. Materyal ile hücrelerin etkileşimi iskele yüzeyine yapışan hücre miktarı, hücre sayısı ve hücre yönleniminin derecesiyle belirlenmiştir. Hücrenin işlevini ve canlılığını koruduğunu gözlemlemek amacıyla hücre sayısı Alamar Blue testi kullanılarak saptanmıştır. Hücreler immuno-boyama ve diğer floresan boyama (örneğin DAPI) yöntemleri kullanılarak konfokal mikroskopiyle incelenmiş ve böylece hücre yönleniminin derecesi gözlemlenmiştir. Hücre fenotipi ve hücre fonksiyonelliği kanıtlanmıştır. Hücre yönlenimi SEM kullanılarak da incelenmiştir. Taşıyıcının damarın mekanik özelliklerine yaklaşma derecesinin incelenmesi amacı ile hem hücresiz hem de üzerlerinde hücre ekilmiş film örnekleri mekanik testlere tabi tutulmuştur.

Sonuç olarak bu çalışma hücre yönlendirmesinin daha önce literatürde önerildiği üzere doku mühendisliği yöntemleri ile elde edilmiş damarların mekanik özelliklerinin arttırılmasında kullanılabileceğini ve damar doku mühendisliğinin en önemli sorunu olan yetersiz mekanik özellik sorununu aşmakta başarılı olabileceği görülmüştür.

Proje Ana Metni

Giriş ve Genel Bilgiler

Doku mühendisliği, zarar görmüş ya da hastalıklı dokuların yenisi ile değiştirilmesi amacı ile bu dokuları üretmek için biyomalzeme, hücre ve ekstraselüler matriks bileşenlerini kullanan disiplinler arası bir biyomedikal alandır. Doku mühendisliğinde genel yaklaşım, dokudan hücreleri almak, in vitro koşullarda büyütmek ve hücre yapışması, büyümesi, göç etmesi ve işlevselliği gibi konularda doğal ekstraselüler matriksi taklit edebilecek uygun hücre taşıyıcıları (iskeleleri) üzerine ekmektir. Iskele ve hücrelerden oluşan bu yapı in vitro koşullarda yeterince olgunlaştığında vücuda implante edilir. Daha sonra zamanla iskele vücut ortamında bozunur ve geriye hücreler, hücrelerin yeni oluşturdukları doğal matriks, kılcal damarlar vb. kalır (Freyman ve ark., 2001).

Doku mühendisliğinde kullanılan hücreler, hedeflenen dokuya özgü olmalıdır. İdeal hücre kaynağı hastanın kendi dokusundan alınan (otolog) hücrelerdir. Ökaryotik hücreler yaşamak için bir yüzeye tutunmak zorundadır. Doku mühendisliğinde bu yüzeyleri oluşturmak için genellikle doğal ya da yapay kökenli polimerler kullanılır. Bu amaçla denenmiş bir çok farklı polimer tipi vardır. En çok kullanılan doğal polimerler arasında yaygın bir hayvansal protein olan kollajen (Lee ve ark., 2001), doğal bir polisakkarit olan kitinden türetilmiş olan kitosan (Shi ve ark., 2006) ve bir çok mikroorganizmanın hücre içi enerji ve karbon kaynağı olarak depoladıkları, genetik olarak modifiye edildikten sonra bitkilere de ürettirilebilen polihidroksialkanoitler (PHA) (Williams ve ark., 1999) sayılabilir. En sık kullanılan sentetik polimerler arasında ise poli(L-laktik asit) (PLLA), poli(glikolik asit) (PGA) ve poli(laktik asit-*ko*-glikolik asit) (PLGA) gibi ABD Gıda ve İlaç Dairesi (FDA) tarafından klinik deneylerde kullanımı onaylanmış polyesterler vardır (Langer, 1993). Hücre iskeleleri 2 ya da 3 boyutlu olabilirler. İki boyutlu iskeleler genelde membran ya da film şeklinde olurken, 3 boyutlu olanlar genelde değişik gözeneklilikliere sahip köpük ya da sünger biçimindedir. Bazı çalışmalarda bu iskeleler sadece hücrelere yapışmaları için bir yüzey sağlamakla kalmaz aynı zamanda doğal ekstraselüler matriksin yaptığı gibi hormonlar ya da büyüme faktorleri gibi biyoaktif moleküller için de bir depo görevi üstlenirler (Quirk ve ark., 2004).

Kollajen başlıca memeli proteinidir ve toplam vücut proteinlerinin % 20-30'unu oluşturur Başlıca görevi ekstraselüler matriks içerisinde fibriler oluşumlar halinde düzenlenerek dokulara mekanik destek vermektir. Kollajen doğal bir molekül olduğu için, biyobozunur ve biyoemilirdir. Bu bozunma hızı çapraz bağlama derecesi kontrol edilerek ayarlanabilir. Doğal ekstraselüler matriksin bir parçası olduğu için hücre yapışmasında gerekli olan sinyal moleküllere de sahiptir (Lee ve ark., 2001).

Hücreler uygun hücre yapışma dizilimlerine sahip olmayan ve hidrofobik sentetik kaynaklı yüzeyleri sevmedikleri için doku mühendisliğinin başlangıcından beri hücre taşıyıcı yüzeyleri modifiye edilmişlerdir. Son yıllarda uygulanmaya başlanılan yeni bir yüzey modifikasyon yöntemi ise kimyasal ya da fiziksel yöntemler kullanarak hücre iskelesi yüzeyinin doğal ekstraselüler matriksin yapısını taklit etmesini sağlamak ve böylece hücrelerin organizasyonunu, doku oluşma hızını ve yeni oluşan dokunun işlevselliğini arttırmayı hedeflemektedir. Kimyasal yönlendirme RGD sekansı ya da başka hücre yapışma moleküllerinin önceden belirlenmiş bir düzen içerisinde yüzeye kaplanması ve bu yolla hücre yönleniminin istenilen şekilde olmasını içeren bir uygulamadır (Schmalenberg ve ark., 2004). Fiziksel yönlendirmede ise, bu iş için yüzey topografyası kullanılır ve tasarlanmış fiziksel yapılar kullanılarak hücreler yönlendirilir. Hücre morfolojisi aynı zamanda hücre işlevselliğini de etkilediği için doğal doku içerisindeki morfolojisine benzer morfolojiye sahip hücreler elde etmek oldukça önemlidir.

Hücre yönlendirilmesi için desenli iskele yüzeyleri kullanılması daha önce başarıyla uygulanmıştır (Pins ve ark., 2000, Dalton ve ark., 2001, Kenar ve ark., 2005). Şimdiye kadar kullanılan desenlerin çoğu bu desenlerin üretilmesinde kullanılan yöntemler nedeniyle mikro düzeydedir. Nano düzeydeki desenler ekstraselüler matriksi moleküler seviyede taklit edeceği için oldukça umut veren bir yöntem olarak görülmektedir (Craighead ve ark., 2001, Diehl ve ark., 2005). Polimerik yüzeyler üzerinde nano-boyutta özel değişimler yaratmak için günümüzde kullanılan metodlar arasında yumuşak litografi, sıcak damga litografisi ve daldırma nanolitografisi (DPN) sayılabilir (Hasirci ve ark., 2006). Bir başka 2 boyutlu nano-desenleme ise temassız (non-contact) modundaki bir AFM vasıtası ile yapılmaktadır. Bu yöntemde istenilen moleküller çözelti halinden yüzeye önceden belirlenen bir düzen içerisinde transfer edilir. 30 ila 50 nm boyutlarında desenler bu yöntemle başarılı bir şekilde transfer edilmişlerdir (Wilson ve ark., 2001). Nano-boyutlarda 3 boyutlu fiziksel desenler ise

silisyum ya da akrilat temelli maddeler üzerine x-ışını girişim (interference) lithografisi (Heyderman ve ark., 2004) ya da e-ışını litografisi (Robinson ve ark., 1999) kullanılarak 30 nm ile 10 nm'ye kadar küçük olacak şekilde üretilir. Daha sonra bu kalıplar nano-desenlere sahip polimerik yüzeylerin hazırlanması için kullanılırlar.

Batılı ülkelerde en başta gelen ölüm sebeplerinden biri küçük ve orta çaplı kan damarlarını etkileyen hastalıklardır. Günümüzde vasküler rekonstrüksiyon için en uygun seçenek otogreftler olmasına rağmen bu greftlerin kullanımlarının sınırlı olmasından dolayı başka seçenekler aranmaya başlanmıştır. Günümüzde vasküler rekonstrüksiyon için en uygun seçenek otogreftler olmasına rağmen bu greftlerin kullanımlarının sınırlı olmasından dolayı başka seçenekler aranmaya başlanmıştır. Doku mühendisliği ile elde edilmiş vasküler greftlerin etkinliği birçok koşula bağlıdır. Bunlardan biri, tromboz ve sonucunda meydana gelen damar tıkanıklığını engellemek amacı ile devamlı bir endotel tabakasına sahip olmasıdır. Diğer çok önemli bir gereklilik de doğal damarlarınkine yaklaşan mekanik özelliklerdir (Mitchell ve Niklason, 2003). Kollajen damar doku mühendisliği uygulamalarında yaygın olarak kullanılmış olmasına karşın başka polimerler de denenmiştir. Otolog hücreler ve biyobozunur poliglikolik asit ve polialkanoatlarla hazırlanmış vasküler greftler koyun pülmoner arteri olarak denenmiş ve sistemik dolaşıma takıldıklarından sonra uygun mekanik kuvvet ve doğal arterinkine yaklaşan kollajen ve DNA içeriği göstermişlerdir (Shum-Tim ve ark., 1999).

Çalışmada doğal ekstraselüler matriksi nano seviyede taklit ederek düz kas hücrelerini ve sonrasında da onlar tarafından salgılanacak olan ekstraselüler matriksi nano-desenler sayesinde doğal damarda olduğu gibi yönlendirmek ve nano-desenlere sahip bir iskele tasarlayıp kullanarak bu alandaki en büyük problemlerden biri olan mekanik kuvvetin arttırılmasını sağlamaktır.

Projeyle İlgili Bilimsel ve Teknik Gelişmeler

1.1 Damar Düz Kas Hücrelerinin Karakterizasyonu

Damar düz kas hücreleri "explant" hücre teknikleri kullanılarak insan toplar damar safeninden izole edilmiştir (Şekil 1).

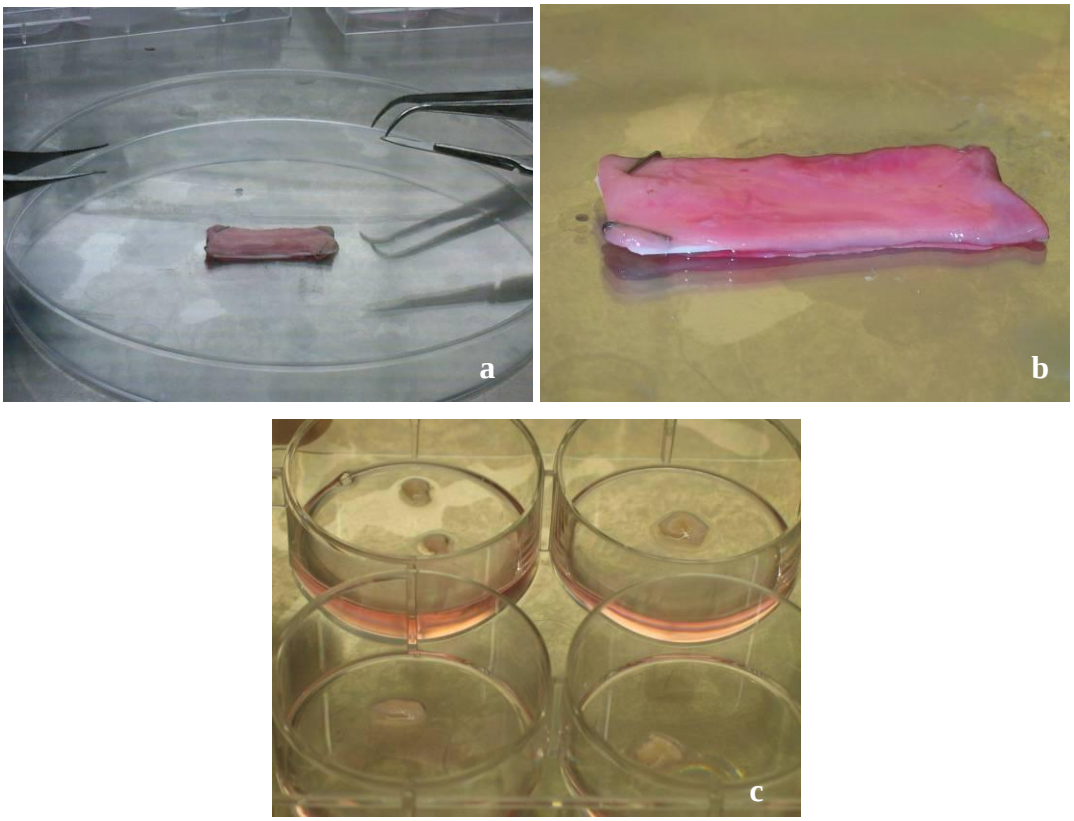

Şekil 1. Damar düz kas hücrelerinin safen toplar damarından izolasyon basamakları. a) Bütün haldeki safen toplardamarının boyuna kesilmesi sonrası görünümü, b) safen toplar damarından en iç (intima) tabakası alındıktan sonra damarın görünümü, c) Eksplant hücre kültüründe kullanılmak üzere orta tabakadan alınan parçaların görünümü

Damar düz kas hücreleri iki hafta içinde, kültür edilmek üzere alınan parçalardan göç etmeye başlamışlardır. Hücreler ışık mikroskobunda incelenip, görüntülenmiştir (Şekil 2).

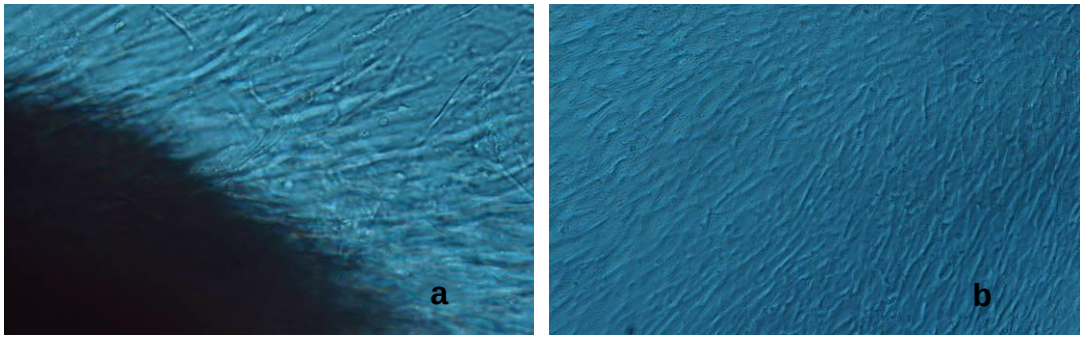

Şekil 2. Damar düz kas hücrelerinin eksplant kültürdeki ışık mikroskobu görüntüleri. a) Damardan alınan doku parçalarına yakın alanlardaki hücrelerin görüntüsü (x 400), b) besiyeri içindeki, parçaların uzak komşuluğundaki hücrelerin görüntüsü (x 100).

Damar düz kas hücreleri bir markör olan "anti-α-smooth muscle actin" ile boyanarak konfokal mikroskobu ile incelenmiştir. Kullanılan markör, hücre iskeletini boyamaktadır. Böylece izole edilen hücrelerin morfolojileri, biçimleri incelenerek fenotipleri doğrulanabilmiştir (Şekil 3).

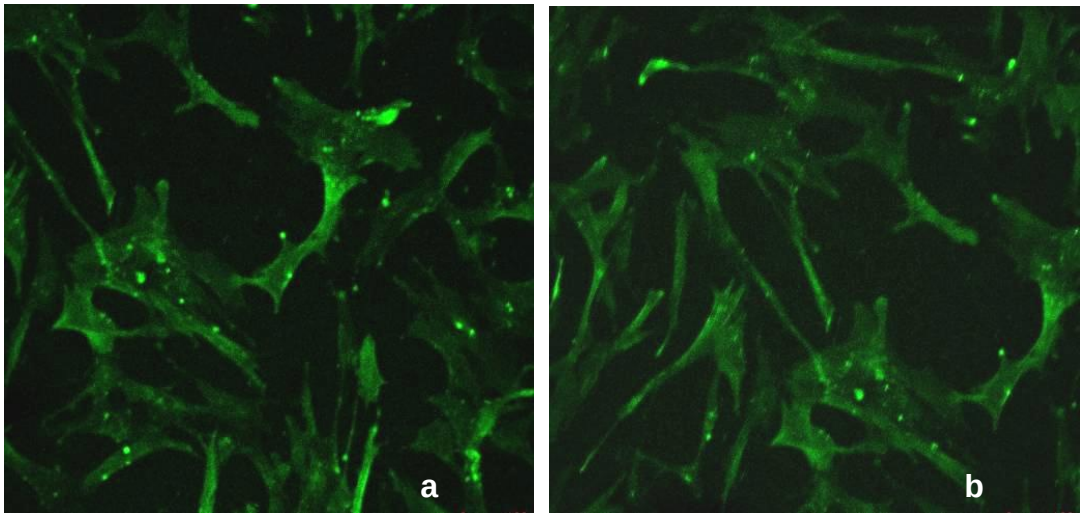

Şekil 3. Anti-α-smooth muscle actin ile boyanmış damar düz kas hücrelerinin konfokal mikroskop görüntüleri (x 200).

6. pasaja kadar çoğaltılan damar düz kas hücrelerinin iskelet ve çekirdekleri boyanarak, hücrelerin izolasyon ve pasajlamalar sonrası ne kadar saf, tek tip oldukları ve özelliklerini kaybederek geri farklılaşma gösterip göstermedikleri araştırılmıştır. Şekil 4 te anti-α-smooth muscle actin ve DAPI ile boyanmış 4 ile 6. pasajlar arası hücreleri gösterilmektedir. Şekil 4'te yalnızca DAPI ile boyanmış, hücre izolasyonundan gelen safsızlığı gösteren veya geriye

farklılaşarak özelliğini kaybeden hücrelere rastlanmamaktadır. Bu sonuçlar hücrelerin 6. pasaja kadar damar düz kas özelliklerini koruduklarını göstermiştir.

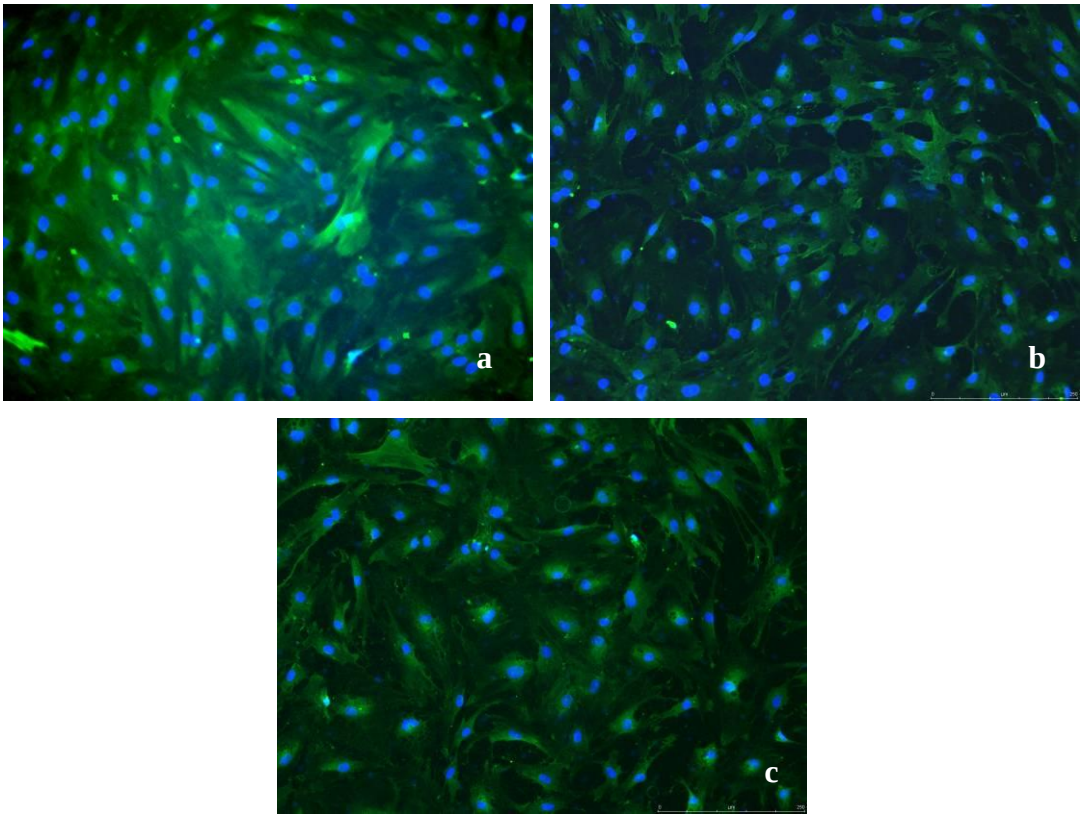

Şekil 4. Anti-α-smooth muscle actin ve DAPI boyalı damar düz kas hücrelerinin floresan mikroskobu görüntüleri. a) 4. Pasaj, b) 5.Pasaj ve c) 6. Pasaj (x 100).

1.2 Silisyum şablonların karakterizasyonu

Duvarları 90^{o} dik olan, nanokanal yapılı silisyum şablonlar AFM (atomic force microscopy) kullanılarak karakterize edilmiştir.

Damar hücrelerinin nano ölçekli topografik özellikleri algılayıp buna göre yönelim gösterip göstermeyeceklerini incelemek üzere tepe ve çukur genişlikleri 332.5 nm (Şekil 5), 500 nm (Şekil 6) ve 650 nm (Şekil 7) olan şablonlar tasarlanmıştır. Bu değerlerin altına inmeye kullanılan yöntemlerin hassasiyeti izin vermemiştir.

Aşağıdaki şekillerde boyut verileri ve şablonların çeşitli görünümleri sunulmuştur. Kanal boyutları ölçüldüğünde tasarlandığı gibi oldukları gözlenmiştir.

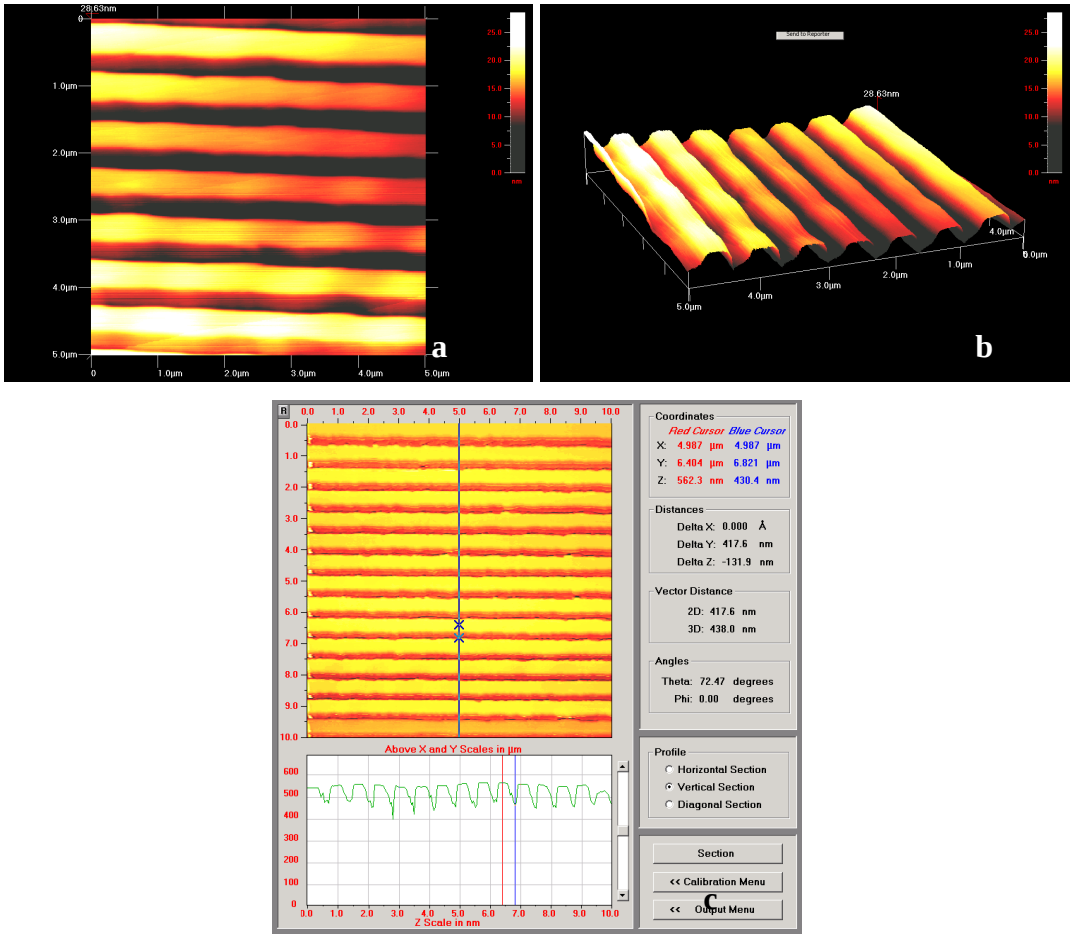

Şekil 5. 332.5 nm kanal genişlikli silisyum şablon.

a) üstten görünüm, b) 3 boyutlu görünüm, c) üstten görünüm ve kanal boyutları verisi.

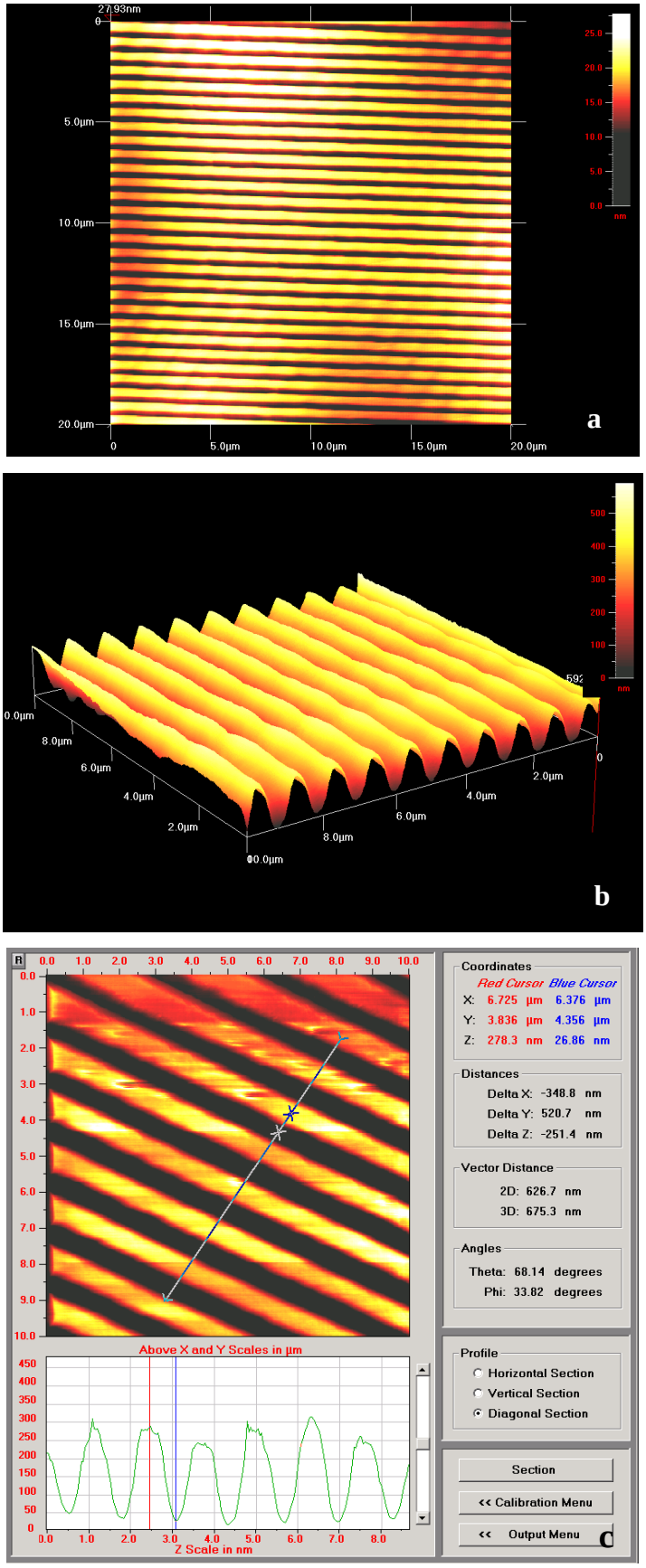

Şekil 6. 500 nm kanal genişlikli silisyum şablon.
a) üstten görünüm, b) 3 boyutlu görünüm, c) üstten görünüm ve kanal boyutları verisi.

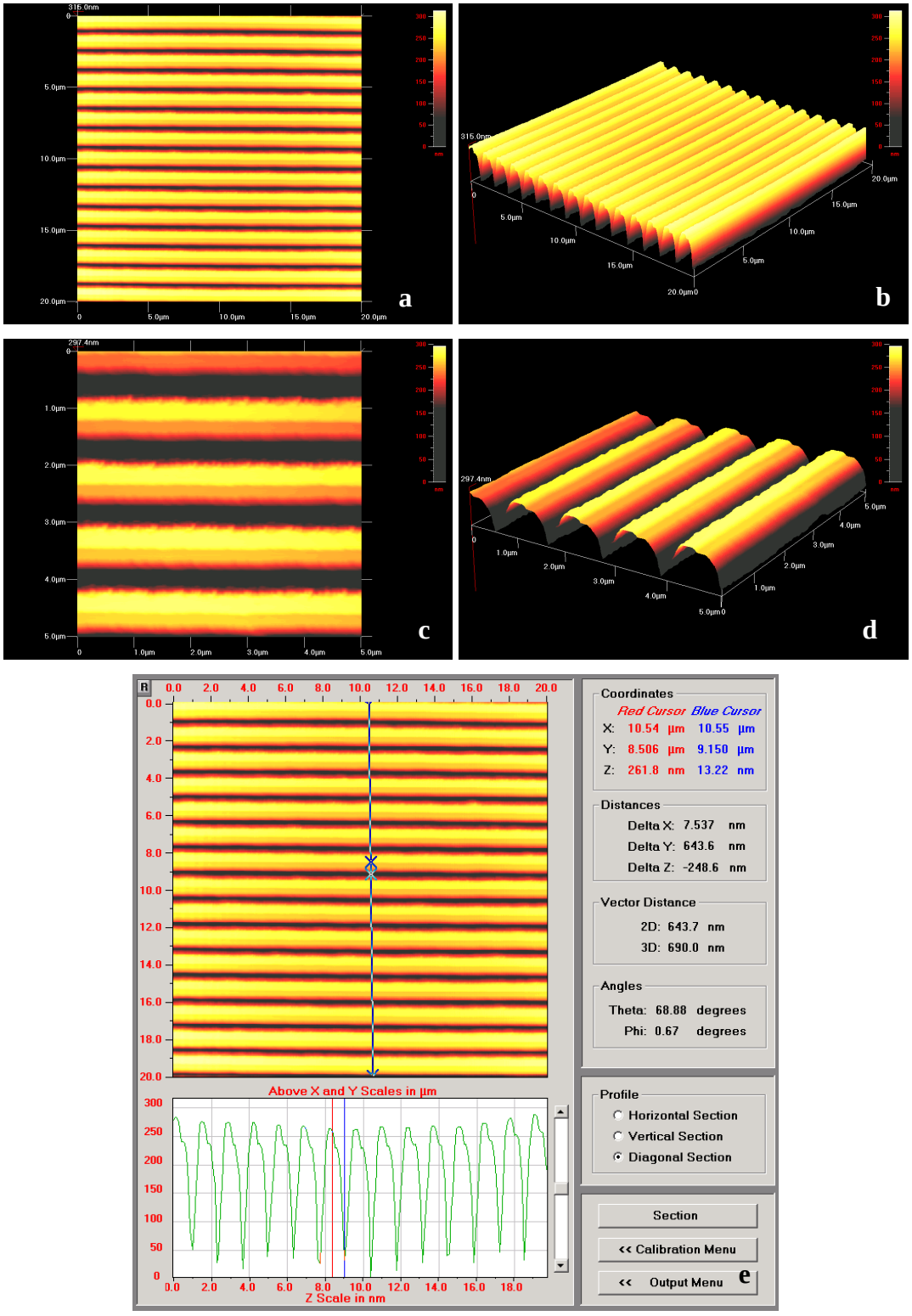

Şekil 7. 650 nm kanal genişlikli silisyum şablon.

a) üstten görünüm, b) 3 boyutlu görünüm, c) büyütülmüş üstten görünüm, d) büyütülmüş 3 boyutlu görünüm, e) üstten görünüm ve kanal boyutları verisi

1.3 Kollajen Yapılı Filmlerin Karakterizasyonu

1.3.1 Izole edilen Tip 1 Kollajen'in SDS-PAGE Analizi

İzole edilen Tip 1 Kollajen'in saflığı SDS-PAGE analiziyle gösterilmiştir (Şekil 8). 1. sütun protein moleküler ağırlık markörlerini göstermektedir. Bantlar yukardan aşağıya 260 kDa, 140 kDa, 100 kDa ve 70 kDa'a karşılık gelmektedir. İzole edilen kollajen (sütun 2 ve sütun 4) ve ticari kollajenden ikişer örnek jelde yürütülmüş, hem ticari hem de izole edilen örneklerden edilen bantların Tip 1 kollajen için belirtilen tipik 115 kDa ve 130 kDa ile 215 ve 235 kDa'a karşılık geldiği görülmüştür. Herhangi bir başka bant olmayışı sıçan kuyruğundan elde edilen kollajenin saflığını göstermektedir.

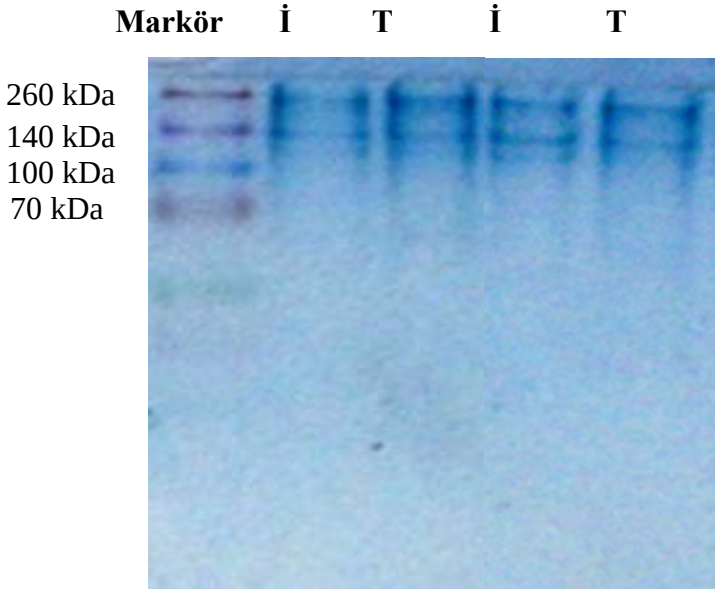

Şekil 8. Sıçan kuyruğundan izole edilen Tip 1 kollajenin SDS-PAGE analizi.
1. sütun protein moleküler ağırlık markörüdür, 2. ve 4. sütunlar izole edilen kollajene aittir. 3. ve 5. sütunlar ticari kökenli, saf, Tip 1 kollajene aittir.

1.3.2 Mikroskopik Karakterizasyon

Silisyum şablonlar üzerinde hazırlanan kollajen filmler SEM ve AFM kullanılarak incelenmiş, kanalların filme aktarılışındaki tasarıma uygunluk ve çapraz bağlama işlemi sonrası yapıların korunduğu bu yolla gösterilmiştir.

Kollajen filmlerin SEM mikrograflarına bakıldığında, 650 nm (Şekil 9a ve 9b) ve 332.5 nm (Şekil 9c ve 9d) genişliğindeki nanokanalların çapraz bağlama öncesinde yüzey özelliklerinin yeterli çözünürlükte ve netlikte oldukları görülmüştür.

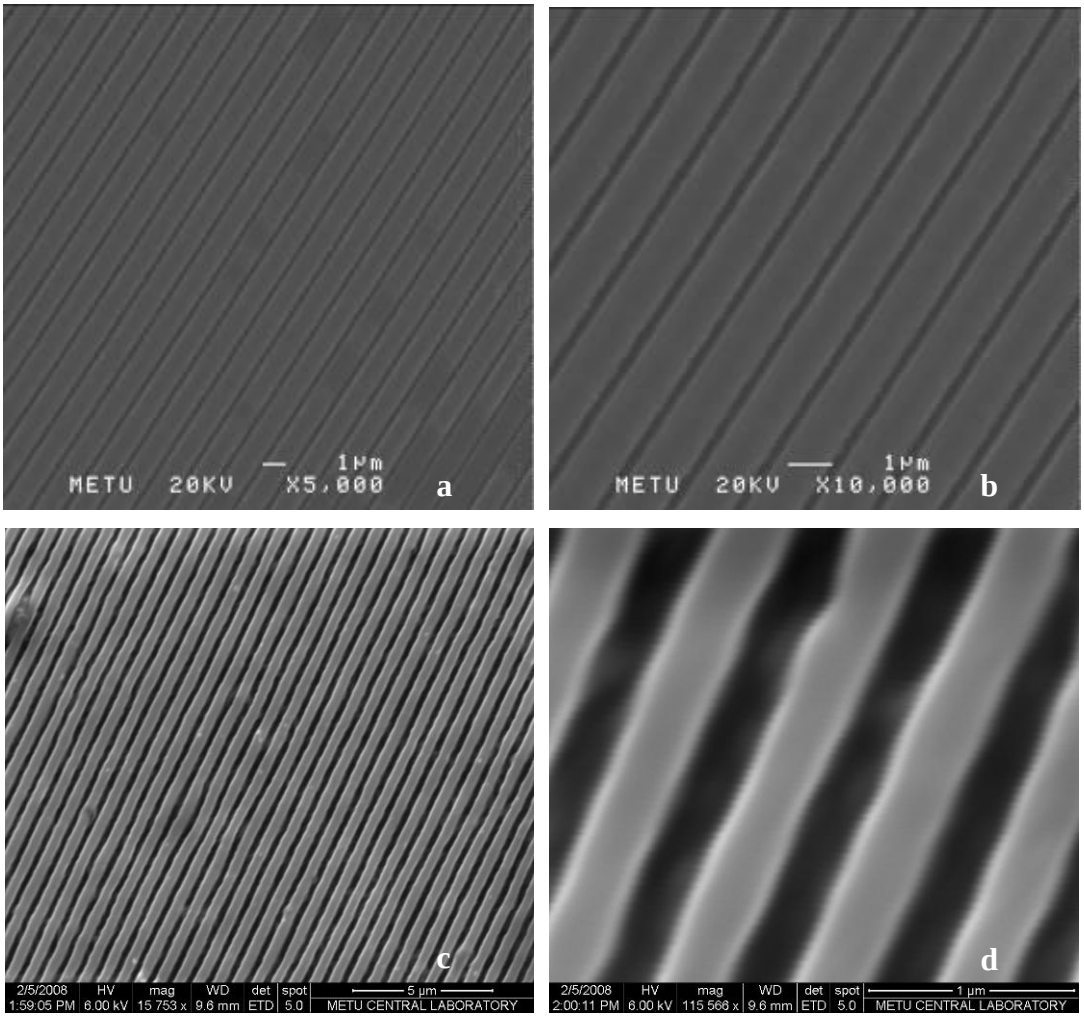

Şekil 9. Çapraz bağlama öncesi nanokanallı kollajen filmlerin SEM görüntüleri.
a) 650 nm genişliğe sahip kanallar (x5000), b) 650 nm genişliğe sahip kanallar (x10000), c) 332.5 nm genişliğe sahip kanallar (x15753), d) 332.5 nm genişliğe sahip kanallar (x115500).

Ancak çapraz bağlama sonrası (filmler silisyum şablonlar üzerindeyken çapraz bağlama yapılmıştır) kanallarda bozulmalar olmuştur (Şekil 10). Filmler, orijinal silisyum şablonun PDMS kopyaları üzerinde hazırlanıp çapraz bağlandığında ilk silisyum şablona benzerlik sağlanmıştır (Şekil 11).

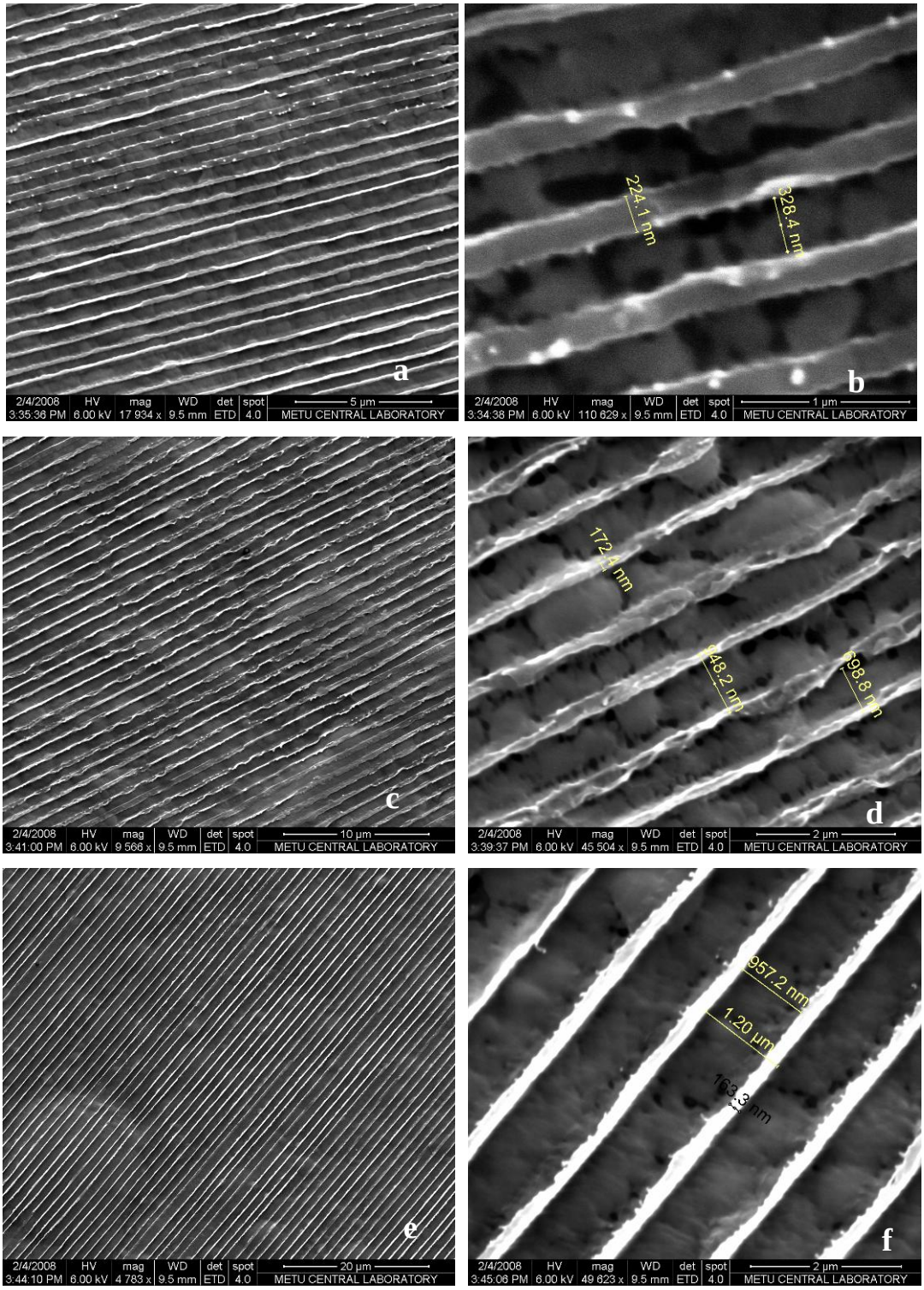

Şekil 10. Silisyum şablonlar üzerindeyken çapraz bağlanan kollajen filmlerin SEM görüntüleri. a) 332.5 nm genişlikli kanal (x17934), b) 332.5 nm genişlikli kanal (x110629), c) 500 nm genişlikli kanal (x9500), d) 500 nm genişlikli kanal (x45504), e) 650 nm genişlikli kanal (x4753), f) 650 nm genişlikli kanal (x40623).

Sonuç olarak, çalışmanın geri kalanında nanokanallı filmlerin yapımında PDMS şablonlar kullanılmıştır (Şekil 7).

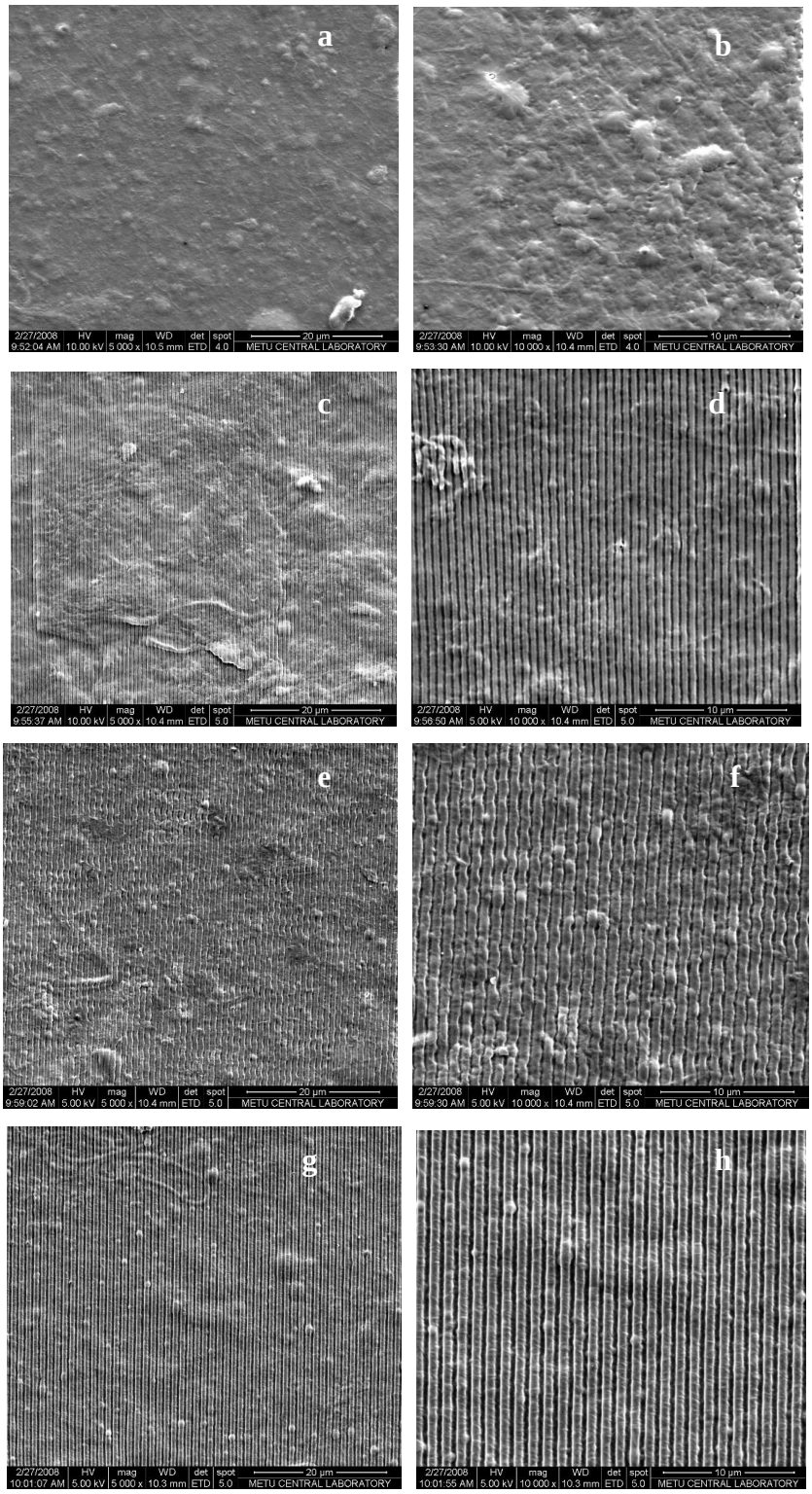

Şekil 11. PDMS kopya üzerinde hazırlanıp çapraz bağlanan kollajen filmin SEM görüntüleri.
a) kanalsız, düz film (x5000), b) kanalsız düz film (x10000), c) 332.5 nm genişlikli kanal (x5000), d) 332.5 nm genişlikli kanal (x10000), e) 500 nm genişlikli kanal (x5000), f) 500 nm genişlikli kanal (x10000), g) 650 nm genişlikli kanal (x5000), h) 650 nm genişlikli kanal (x10000).

650 nm genişlikli kanallı kollajen filmler çapraz bağlama öncesi (Şekil 9a ve 9b) ve sonrası (Şekil 10e ve 10f) AFM ile incelenmiştir. Alınan sonuçlar SEM görüntülerini doğrulamıştır. AFM ile kanalların derinliği de ölçülebilmiştir. AFM ile nanokanallı filmlerin incelenmesinin zorluğundan dolayı burada en geniş (650 nm) kanallı yapıya ait görüntüler verilmiştir. Kollajen filmler üzerindeki kanalların genişliği orijinal silisyum şablonlardaki gibidir. Kanal derinliği orijinal silisyum şablonlara göre biraz daha azdır (300 nm yerine 250 nm). Ancak bu değerler kabul edilebilir olarak değerlerndirilmiş ve filmlerin in vitro testlerde kullanımına karar verilmiştir.

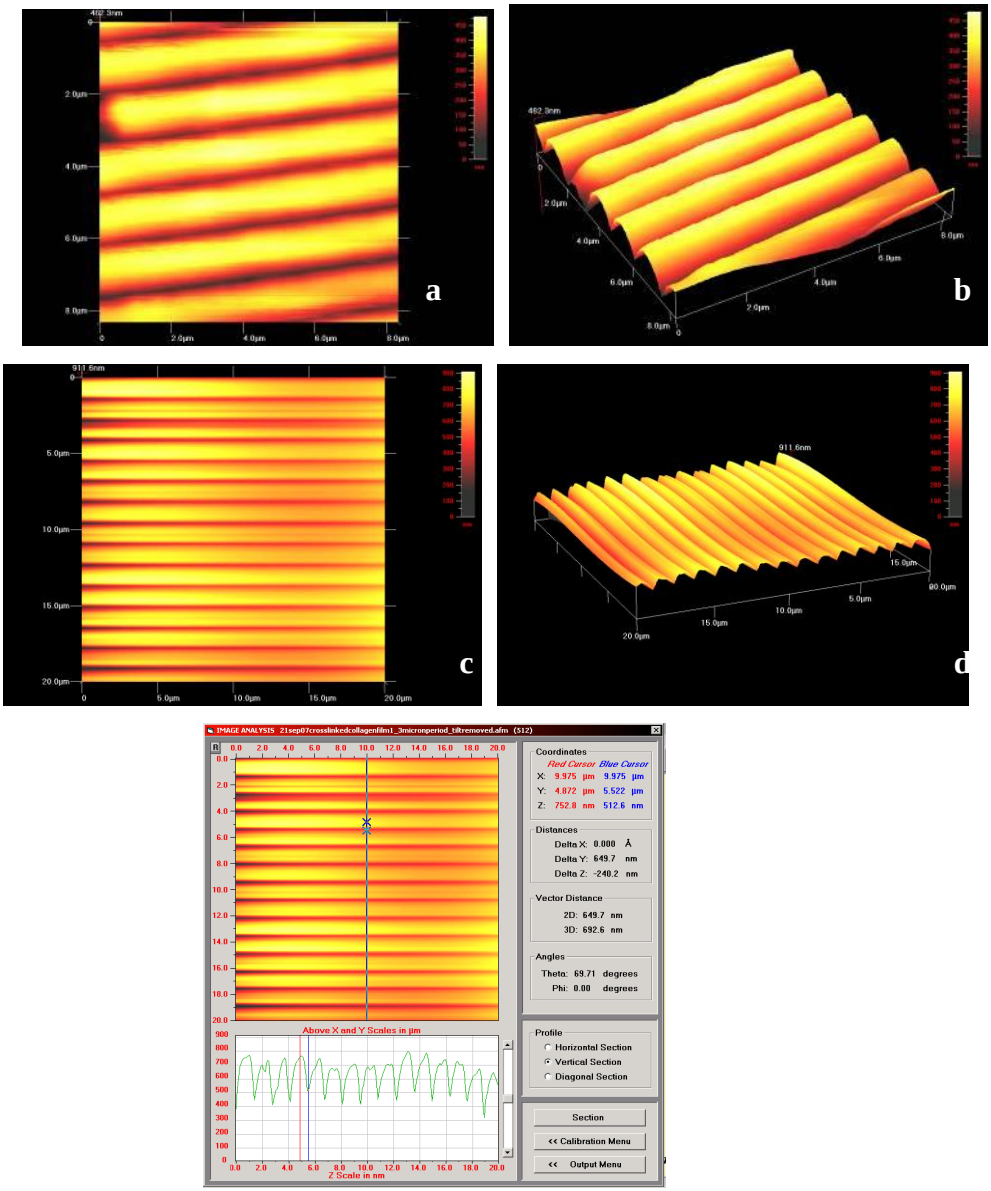

Şekil 12. 650 nm genişlikli kanallar içeren kollajen film in AFM sonuçları. a) üst görünüm, b) 3 boyutlu görünüm. Çapraz bağlı film c) üst görünüm, d) 3 boyutlu görünüş, e) üst görünüm ve boyutların gösterilmesi.

1.4 In Vitro Çalışmalar

1.4.1 Damar Düz Kas Hücrelerinin (VSMC) Kollajen Filmler Üstünde Çoğaltılması

Kollajen filmlerin üstündeki hücre sayısı hesaplanırken Alamar Blue absorpsiyonda "% azalma" esas alınmıştır. Kalibrasyon eğrisi hazırlandıktan sonra % azalma değerleri hücre sayısına dönüştürülmüştür. Alamar Blue testiyle kollajen filmlere ekilmiş düz kas hücrelerinin 1., 7. ve 14. gün sonundaki sayıları belirlenmiştir. Sonuçlar bütün kollajen filmlerin üzerinde hücre çoğalmasının sağlanabildiğini göstermiştir. Hücre yapışması (1. gün) kanal boyutları küçük filmler söz konusu olduğunda daha yüksektir (Şekil 13). Hücre yapışması kanalsız filmlerde ve TCPS (Tissue Culture Polystyrene, referans doku kültür yüzeyi) üzerinde daha azdır. Her ne kadar ilk aşamada kanalsız filmlerdeki hücre yapışması kontrol örneği olan TCPS'den fazla olsa da, iki örnek arasındaki hücre sayısı farkı 21. güne kadar giderek yavaş yavaş azalmıştır. Bunun olası nedeni TCPS'nin daha geniş olan toplam yüzeyinin (2.27 cm^2), kollajen film yüzeyi (1 cm^2) ile karşılaştırıldığında hücrelerin kontakt inhibisyon öncesi daha çok çoğalmasına olanak tanımasıdır. Bütün zamana bakıldığında yine de en yüksek hücre sayısı en küçük boyutlu nano kanallı (335.5 nm) filmlerde bulunmuştur. Daha önce damar düz kas hücrelerinin herhangi bir topografik özelliği olmayan düz kollajen membranlarda çoğaldıkları gösterilmiştir (Elliott ve ark., 2005). Ancak, polimerik yapı iskeleleri ile karşılaştırıldığında nanokanallı kollajen filmler üstündeki VSMC'lerin poly(L-laktid-ko-ε-kaprolakton) kullanılarak elektroeğirme (electrospin) edilmiş hemen hemen aynı boyutlardaki (500 nm) nanofiberlere ekilen koroner damar düz kas hücrelerine göre iki kat fazla çoğalmışlardır (Xu ve ark., 2004).

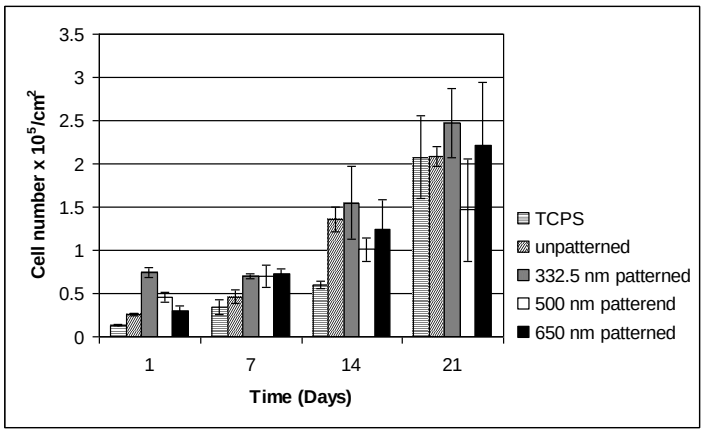

Şekil 13. Damar düz kas hücrelerinin (VSMC) kollajen filmler üstündeki çoğalmaları. Alamar Blue testi. (n=3)

1.4.2 Damar Düz Kas Hücrelerinin (VSMC) Kollajen Filmler Üstündeki Biçimi, Yönlenim ve Fenotip Analizleri

Damar düz kas hücrelerinin (VSMC) fenotiplerinin ve hücre iskeletlerinin nano kanallarca yönlendirilmelerini göstermek amacıyla kanallı ve düz (kanalsız) kollajen filmler üstünde çoğaltılan hücreler 1, 7, 14 ve 21 günlükken "anti-α-smooth muscle actin" ile boyanmıştır. (Şekil 14-17). Kullanılan markör, hücre iskeleti elemanlarını boyadığından görüntülerde hücre iskeletinin nanokanallar tarafından yönlendirildiği gösterilmiştir. Buna ek olarak aynı şekiller deney esnasında hücre fenotipinin korunduğunu göstermiştir.

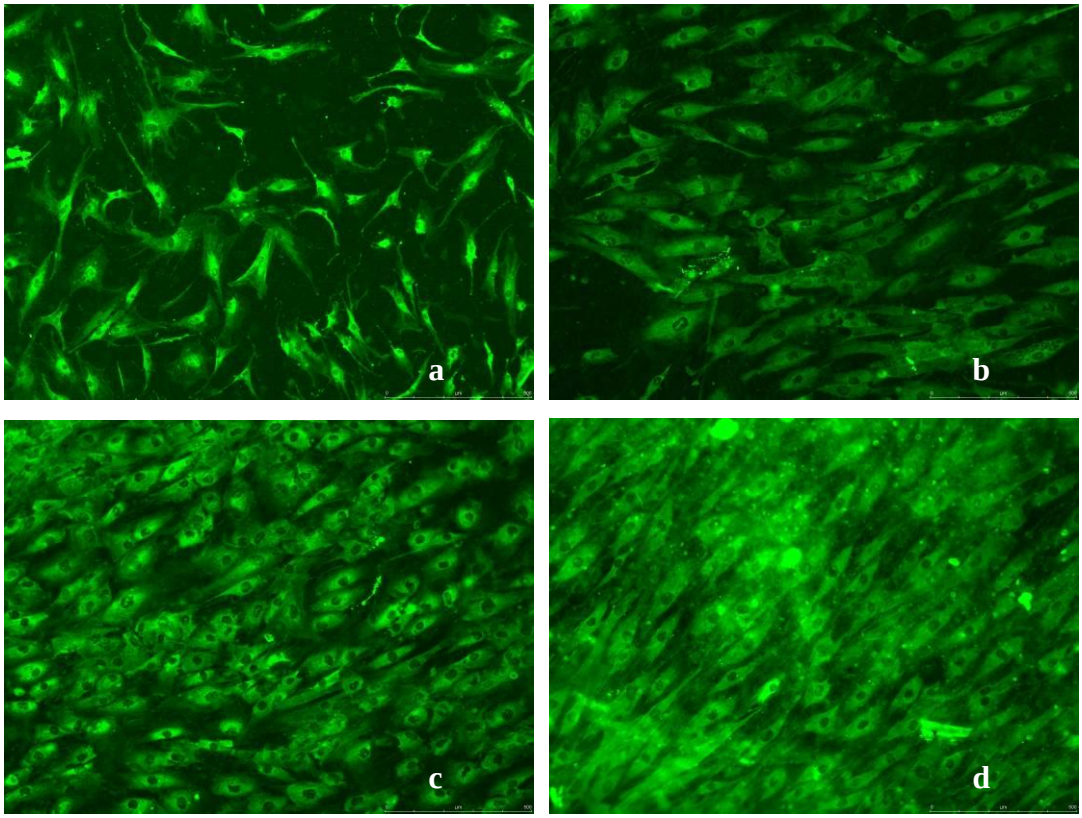

Şekil 14. Kollajen film üstünde damar düz kas hücreleri **(**VSMCs). a) Kanalsız film üstünde, b) 332.5 nm genişlikli kanallar üstünde, c) 500 nm genişlikli kanallar üstünde, d) 650 nm genişlikli kanallar üstünde (x 100). 1. Gün. Boya: "anti-α-smooth muscle actin".

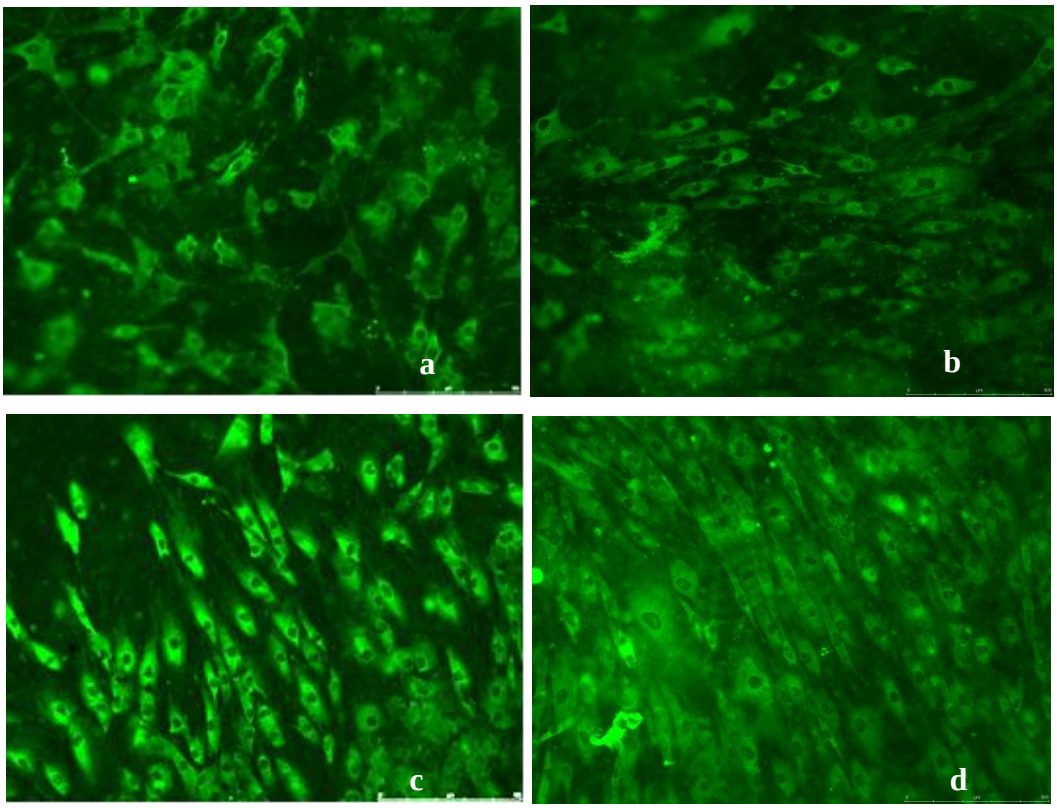

Şekil 15. Kollajen film üstünde damar düz kas hücreleri **(**VSMCs). a) Kanalsız film üstünde, b) 332.5 nm genişlikli kanallar üstünde, c) 500 nm genişlikli kanallar üstünde, d) 650 nm genişlikli kanallar üstünde (x 100). 7. gün, Boya: "anti-α-smooth muscle actin".

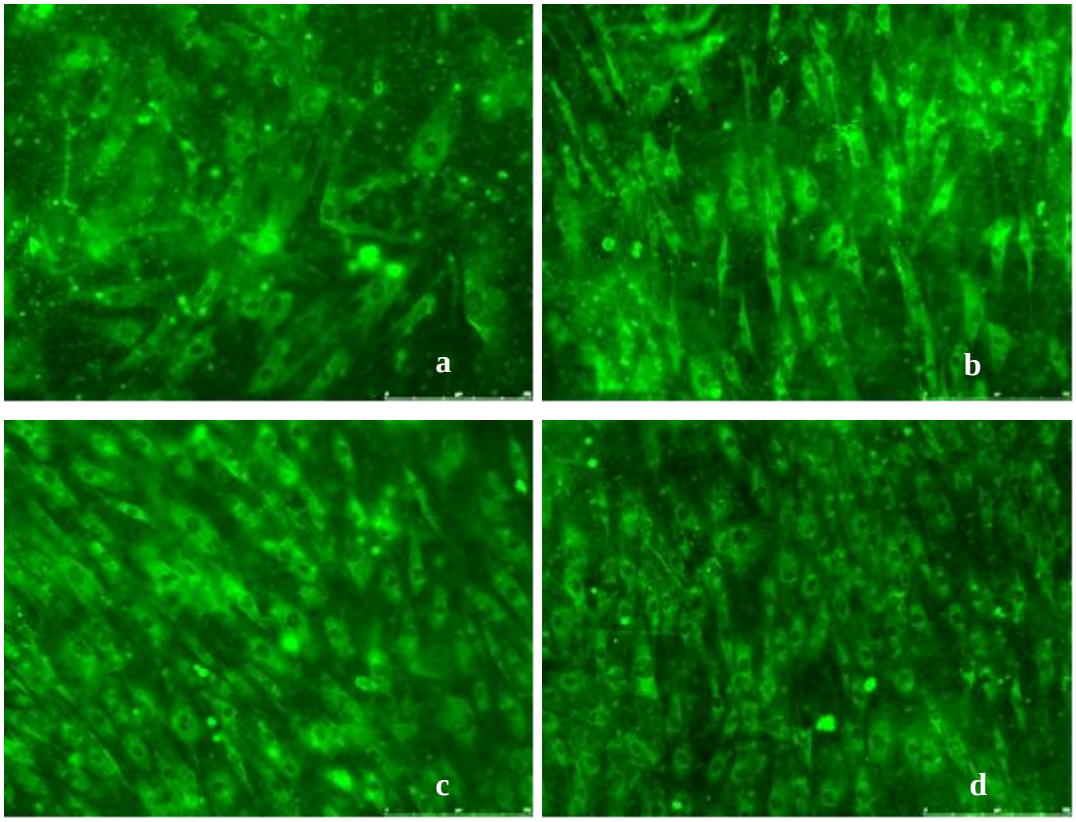

Şekil 16. Kollajen film üstünde damar düz kas hücreleri **(**VSMCs). a) Kanalsız film üstünde, b) 332.5 nm genişlikli kanallar üstünde, c) 500 nm genişlikli kanallar üstünde, d) 650 nm genişlikli kanallar üstünde (x 100). 14. gün, Boya: "anti-α-smooth muscle actin".

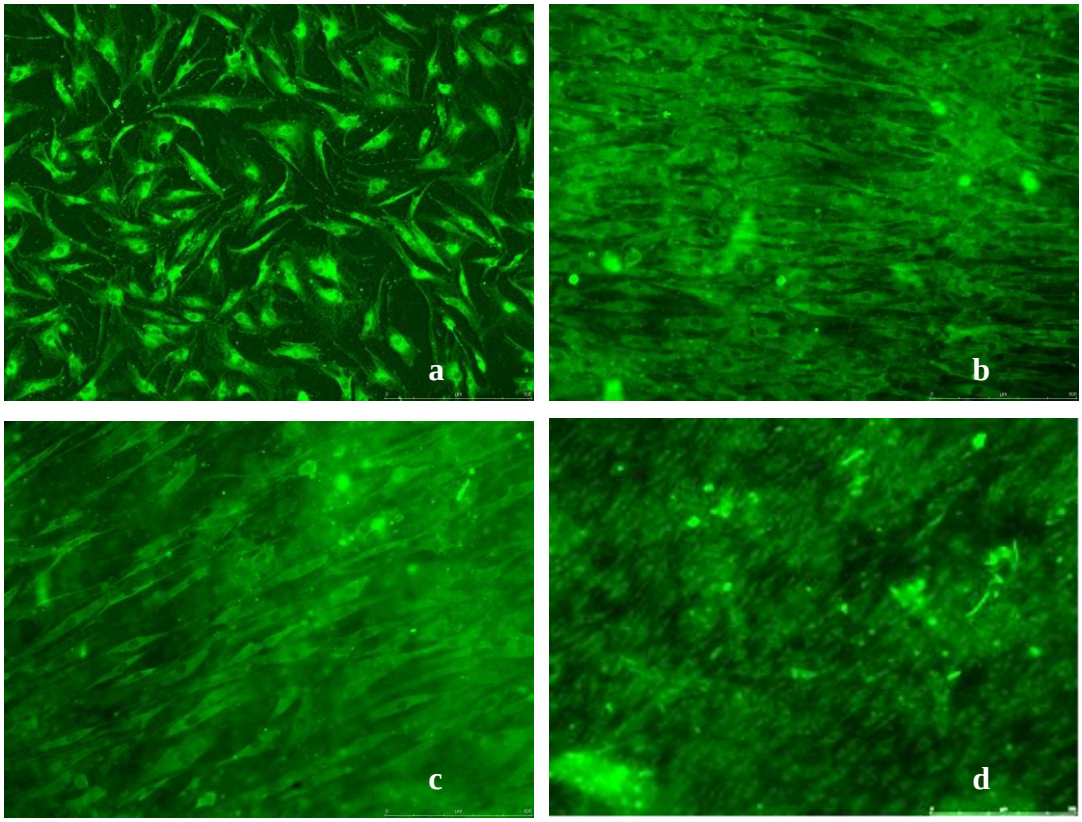

Şekil 17. Kollajen film üstünde damar düz kas hücreleri **(**VSMCs). a) Kanalsız film üstünde, b) 332.5 nm genişlikli kanallar üstünde, c) 500 nm genişlikli kanallar üstünde, d) 650 nm genişlikli kanallar üstünde (x 100). 21. gün, Boya: "anti-α-smooth muscle actin".

Hücre yönelimini belirlemek amacıyla nanokanallı ve düz (kanalsız) filmler üstünde çoğaltılan 1, 7, 14 ve 21 günlük damar düz kas hücreleri filmler üstün de sabitlenerek SEM ile incelenmiştir (Şekil 18-21). Kanalların nano ölçeğindeyken hücrelerin mikron ölçeğinde olmaları, hücre yönelimini ve nanokanalları aynı mikrografi üzerinde görmeye olanak vermemiştir. Bu nedenle, hücrelere yakın film yüzeyini gösteren yüksek büyütmelerdeki görüntüler şekillere katılmıştır.

Her üç tip nanokanallı filmde damar düz kas hücrelerinin yönlendiği ancak hücrelerin kanalsız filmler üzerinde yönlenmediği görülmüştür. Bu sonuç 332.5 nm kadar küçük ölçekli kanalların kendilerinden en az 10 kat büyük hücreleri etkin biçimde yönlendirdiklerini kanıtlamıştır. Benzer sonuçlar kemik iliği kökenli mezenkimal kök hücrelerin 200 nm genişlikli yapılar içeren polimetilakrilat yüzeylerde yöneliminin gerçekleştirildiğini daha önce bildirilmiştir (Engel ve ark., 2008). Mikron ölçekli desenlerde hücrelere göre daha büyük olan ve hücreyi yönelime iten fiziksel sınırlamaların aksine, nanokanallar üzerindeki moleküler

seviyedeki etkileşimler yönelim faktörlerini oluşturmaktadırlar. Daha önce damar düz kas hücrelerinin kollajen membranlar üzerinde mikron ölçekli yüzey özellikleri kullanılarak hizalandıkları gösterilmiştir. Bir başka çalışmada insan göbek bağı atar damar düz kas hücreleri 33, 13 and 7 mikron genişliğinde kanallı kollajen yüzeyler üstünde yönlendirilmiştir (Vernon ve ark., 2005). Buna ek olarak, 40, 80, 120, or 160 mikron ölçekli kanallar içeren sentetik polimerik membranlar ((poli (σ-kaprolakton-r-L-laktit-r-glikolit) diakrilat) üstünde yönelimin olduğu ve yönelimin kanal genişliğinin artışıyla azaldığı bildirilmiştir (Shen ve ark., 2006). Bunun dışında damar düz kas hücrelerinin nano ölçekli yüzeylerdeki yönelimi 500 nm çaplı polimerik fiberler üzerinde gösterilmiştir (Xu ve ark., 2004). Bilindiği kadarıyla sunulan çalışmamız damar düz kas hücrelerinin nano ölçekte desenlenmiş kollajen membranlar üstündeki yönelimini gösteren ilk çalışmadır.

Filmlerin yüksek büyütmedeki SEM görüntülerinde henüz hücre ile örtülmemiş bölgelere bakıldığında hücre kültürü süresince kanalların kalitesinin korunduğu görülmektedir. Özet olarak, kollajen yapılı filmlerdeki nanokanalların hücrelere rehberlik etmekte etkili oldukları ve nanokanalların en azından 21 günlük hücre kültürü koşullarında yapılarını korudukları sonucuna varılmıştır. Bu kararlılık özellikle çapraz bağlamanın bir sonucudur ve nanokanallardaki yönelimin gerçekleşmesini sağlayan anahtar etkenlerden bir tanesidir.

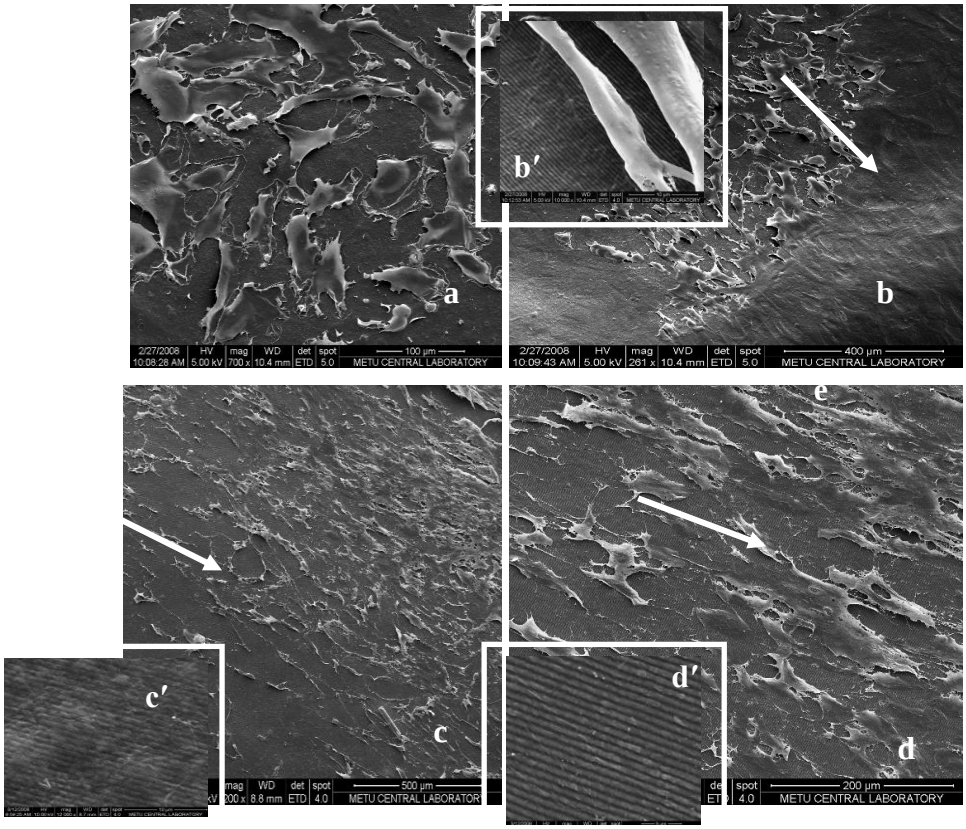

Şekil 18. Kollajen filmler üstündeki damar düz kas hücrelerinin SEM görüntüleri, 1. gün. a) Düz/kanalsız film (x 700), b) 332.5 nm genişlikli kanal (x 261), b′) 332.5 nm genişlikli kanal (aynı örnek üstünde hücreler tarafından kaplanmamış bölge, x10,000), c) 500 nm genişlikli kanal (x 200), c′) 500 nm genişlikli kanal (aynı örnek üstünde hücreler tarafından kaplanmamış bölge, x10,000) d) 650 nm genişlikli kanal (x 600), d′) 650 nm genişlikli kanal (aynı örnek üstünde hücreler tarafından kaplanmamış bölge, x10,000). Beyaz renkli oklar kanalların yönünü göstermektedir.

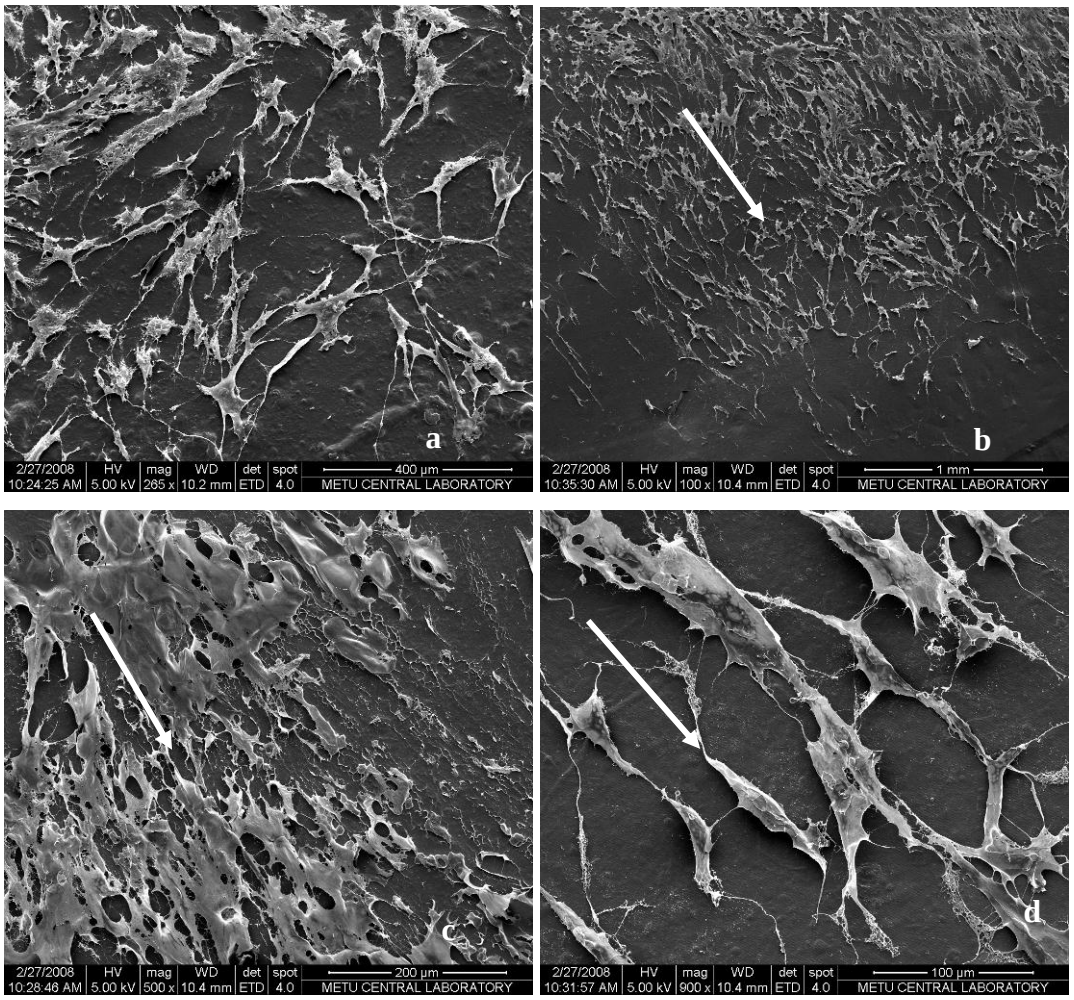

Şekil 19. Kollajen filmler üstündeki damar düz kas hücrelerinin SEM görüntüleri, 7. Gün. a) düz film (kontrol) (x 265), b) 332.5 nm genişlikli kanal (x 100), c) 500 nm genişlikli kanal (x 500), d) 650 nm genişlikli kanal (x 900). Beyaz renkli oklar kanalların yönünü göstermektedir.

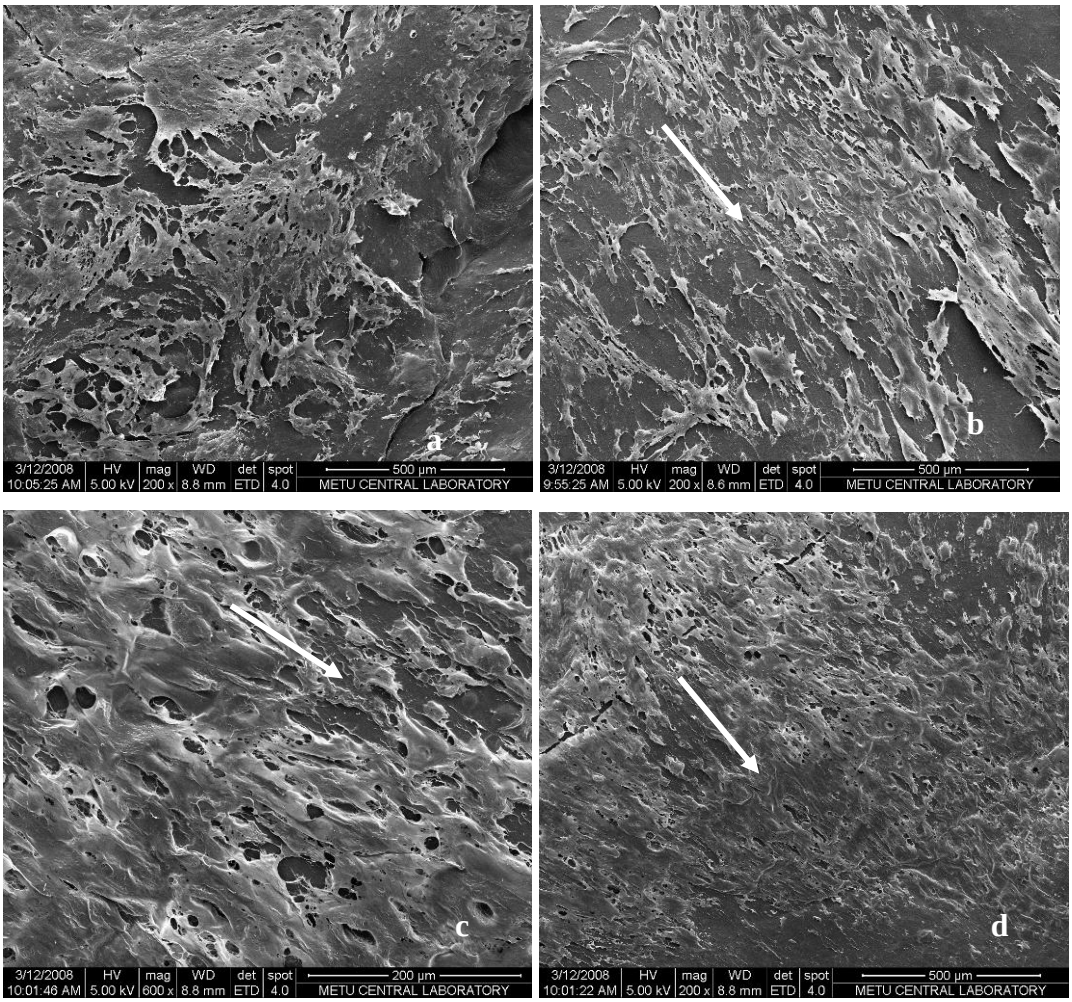

Şekil 20. Kolajen filmler üstündeki damar düz kas hücrelerinin SEM görüntüleri. 14. Gün. a) Kanalsız, düz film (x 200), b) 332.5 nm genişlikli kanal (x 200), c) 500 nm genişlikli kanal (x 600), d) 650 nm genişlikli kanal (x 200). Beyaz renkli oklar kanalların yönünü göstermektedir.

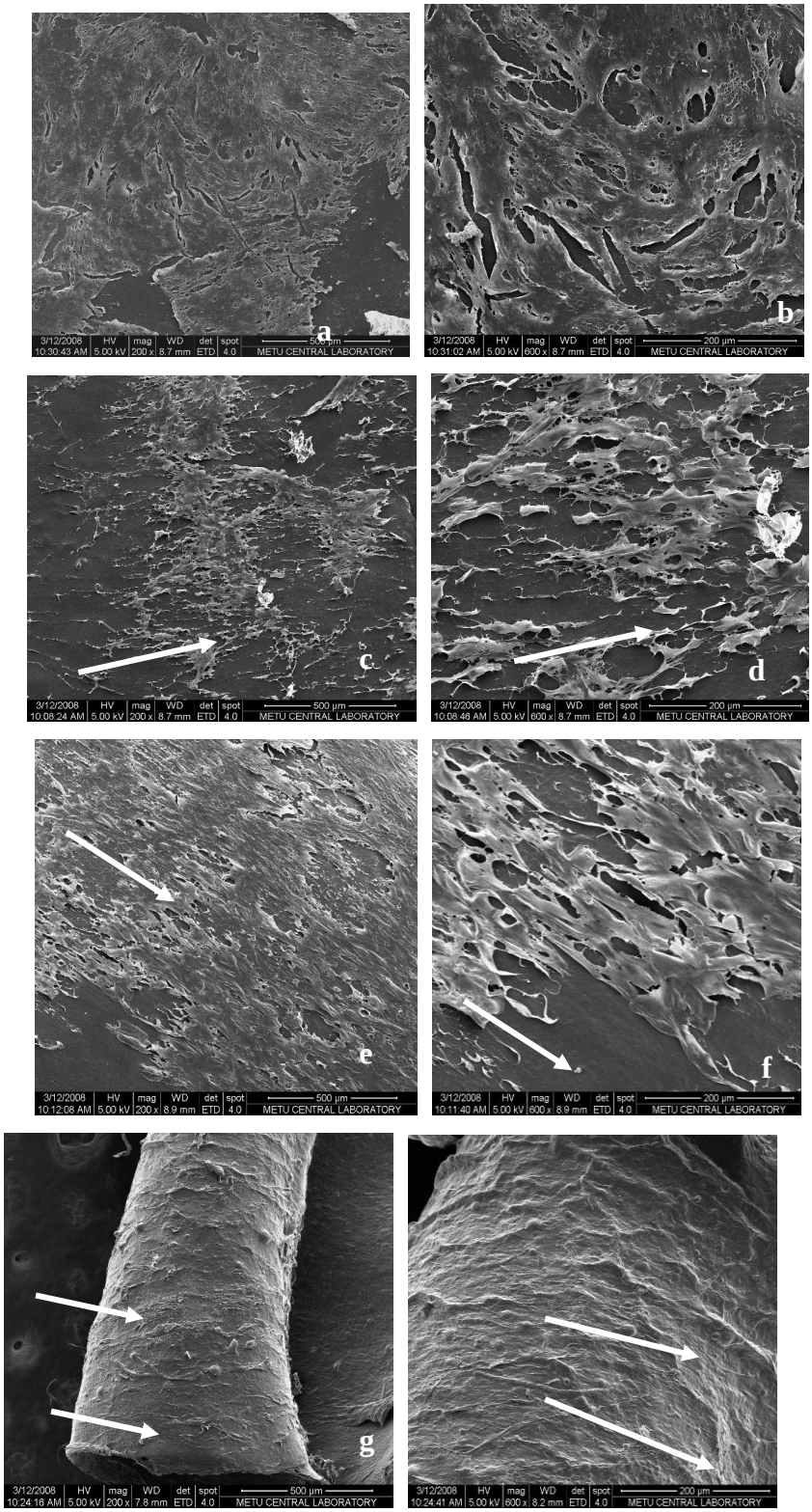

Şekil 21. Kollajen filmler üstündeki damar düz kas hücrelerinin SEM görüntüleri. 21. gün. a) Kanalsız, düz film (x 200), b) kanalsız düz film (x 600) c) 332.5 nm genişlikli kanal (x 200), d) 332.5 genişlikli kanal (x 600) e) 500 nm genişlikli kanal (x 200) f) 500 nm genişlikli kanal (x 600) g) 650 nm genişlikli kanal (yapışan hücrelerin kasılmasıyla rulo haline gelmiş film, x 200), h) 650 nm genişlikli kanal (x 600). Beyaz renkli oklar kanalların yönünü göstermektedir.

1.5 Mekanik Testler

Gerilme testi uygulanarak elde edilen veriler kullanılarak hücresiz, hücreli 45 ve 75 gün kültür ortamında tutulan filmlerin grafikleri çizilmiştir. Şekil 22 hücresiz kollajen filmlerin sonuçlarını ayrı ayrı ve ortalama değer olarak göstermektedir.

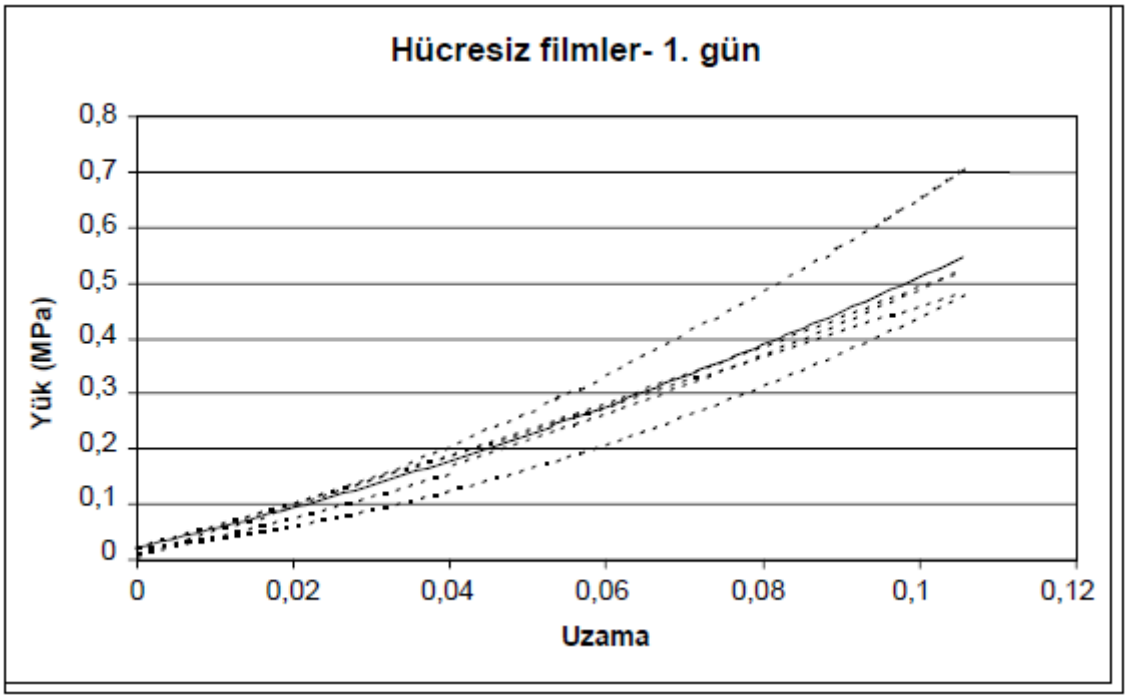

Şekil 22. Hücresiz kollajen filmlerin Yük-Uzama (stress-strain) grafiği. Kesikli çizgiler test tekrarlarını, kesiksiz eğri ise ortalama değeri göstermektedir.

Literatürde damar doku mühendisliği amacıyla tasarlanan yapı iskelelerinin dayanıklılıklarını inceleyen çalışmalar bulunmaktadır. Yang ve arkadaşları (2005), poli(diol sitrat)'tan üretilen bifazik yapı iskelelerinin mekanik özelliklerini ölçmüşler ve doğal damarlara yakın sonuçlar bulmuşlardır. Yapı iskelesinin Young modülü ve en üst yük değerleri UTS 2 MPa civarındadır ve bu çalışmada kullanılan damar düz kas hücresi ekili nanokanallı kollajen filmlerin değerlerine yakındır. Yakın zamanlı bir çalışmada Thomas ve arkadaşları (2007), elektroeğirme yoluyla elde ettikleri tübüler poliglikonat yapı iskelelerinin mekanik açıdan damar doku mühendisliğine uygun olduklarını görmüşlerdir. Yapı iskelelerinin, 2 MPa civarında UTS değerine ve doğal damarlardan 3 kat daha yüksek, 9 MPa civarında Young modüllerine sahip oldukları ölçülmüştür.

Hücre ekili olarak 45 ve 75 gün boyunca in vitro ortamda tutulan filmlerin gerilme test sonuçları Şekil 23'te verilmiştir. Şekil 24 UTS'in zamanla değişimini göstermektedir. Filmlerin sertliklerinin belirlenmesi amacıyla Young modülleri hesaplanmıştır (Şekil 25). Tablo1 bütün UTS ve Youn modül verilerini özetlemektedir.

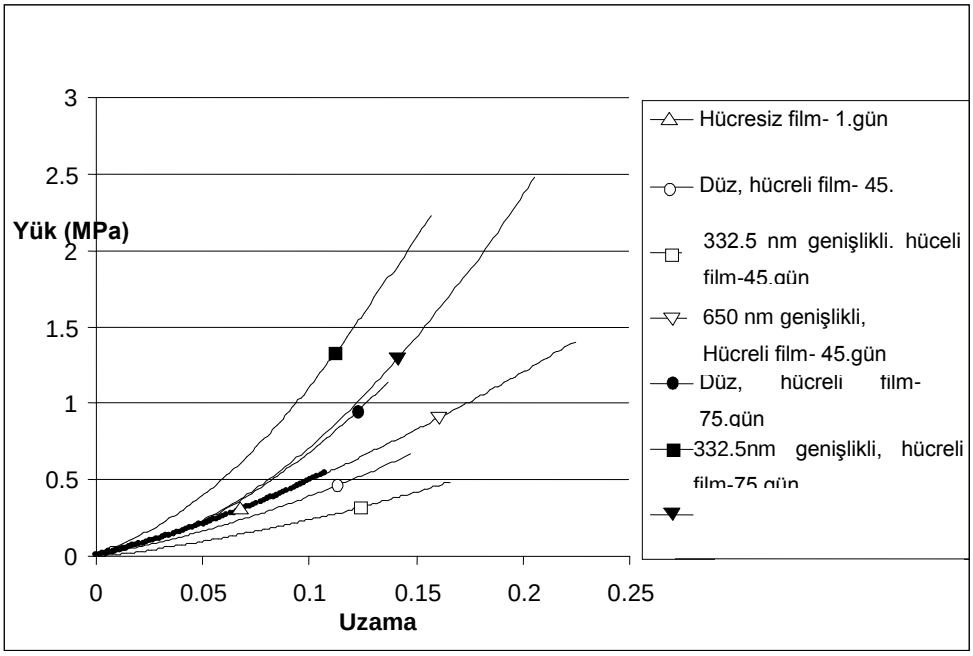

Şekil 23. Hücresiz ve damar düz kas hücre ekilerek hücre kültürü ortamında 45 ve 75 gün tutulan nanokanallı ve düz kollajen filmlerin ortalama Yük-Uzama davranışı *(n=6).*

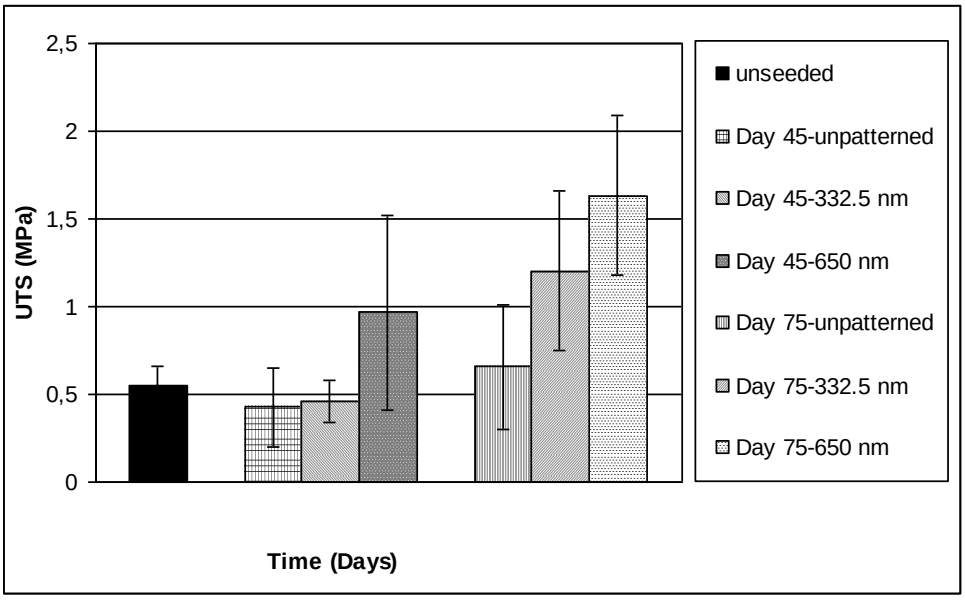

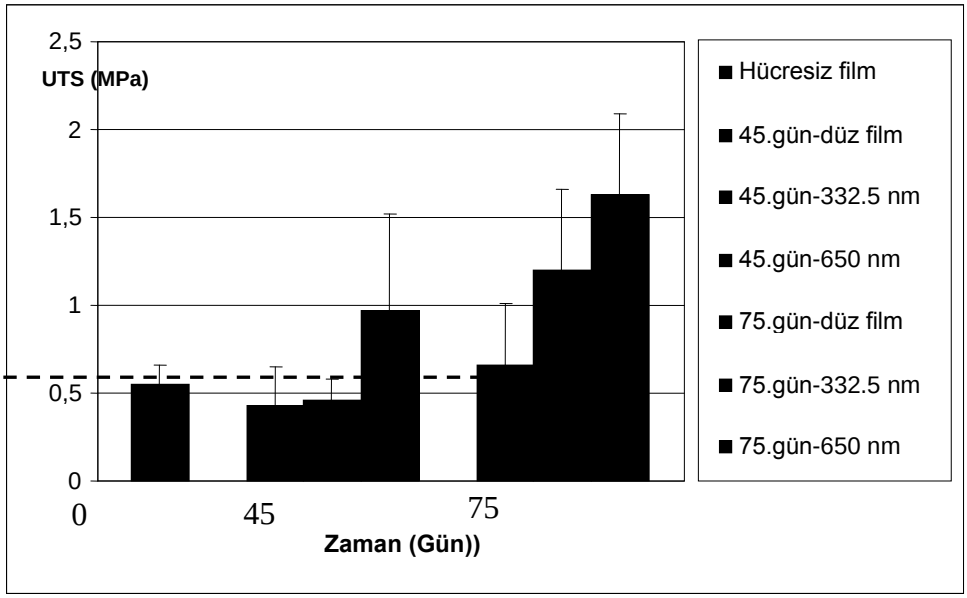

Şekil 24. Damar düz kas hücresi ekili olarak 45 ve 75 gün hücre kültürü ortamında tutulmuş nanokanallı kollajen filmlerin UTS değerleri.

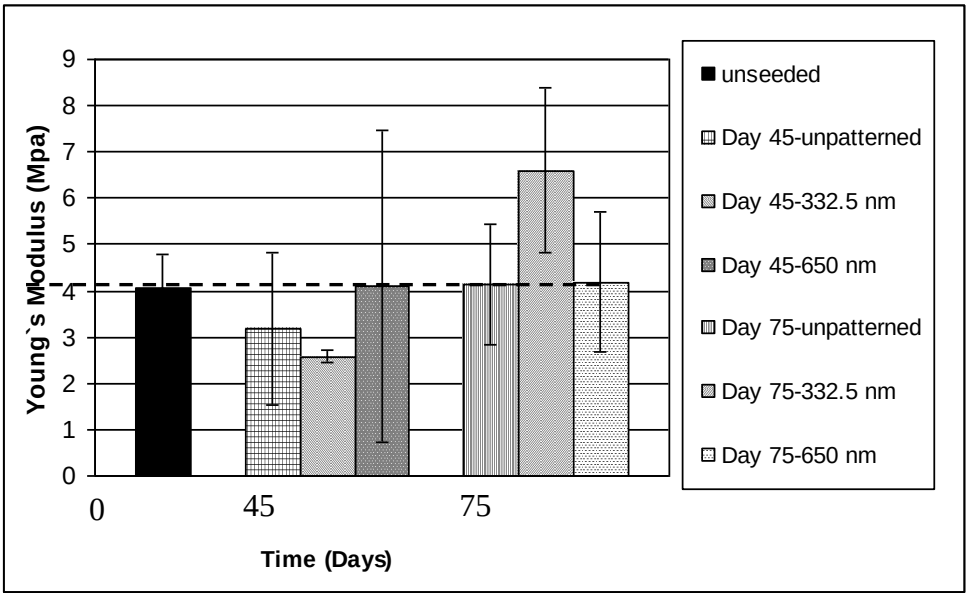

Şekil 25. Damar düz kas hücresi ekilerek 45 ve 75 gün hücre kültürü ortamında tutulan kanallı filmlerin Young Modül değerleri**.**

Tablo 1. Hücreli ve hücresi kollajen filmlerin UTS ve Young Modül değerleri. *(n=6).*

Örnek			UTS (MPa)	Young Modülü (MPa)
Desen (nm)	VSMC	Kültürde bekleme süresi (Gün)		
Düz	-	0	0.55 ± 011	4.05 ± 0.73
Düz	+	45	0.43 ± 0.23	3.16 ± 1.65
332.5	+	45	0.46 ± 0.12	2.59 ± 0.12
650	+	45	0.97 ± 0.55	4.10 ± 3.36
Düz	+	75	0.66 ± 0.35	4.12 ± 1.30
332.5	+	75	1.20 ± 0.46	6.60 ± 1.79
650	+	75	1.63 ± 0.46	4.19 ± 1.52

Hücresiz düz kollajen filmi için UTS değeri 0.55 ± 0.11 MPa olarak hesaplanmıştır. Bu ölçüm EDC/NHS çapraz bağlı kollajen filmler için literarürde yer alan 0.7 MPa civarındaki değer ile uyumludur (Faraj ve ark., 2007). Kanalların derinliği (en çok 200 nm) olmasından dolayı, filmin bütün kalınlığı gözönüne aldığında (kabaca 35 μm), ihmal edilebilir bir büyüklüktedir. Buna ek olarak derinlik yalnızca yüzey söz konusu olduğunda mekanik özellikleri etkilediğinden, kanallı ve düz filmler başlangıç anında (0. Gün) ölçülmemiş, başlangıç değerleri her iki film için de aynı kabul edilmiştir. 332.5 nm genişlikli filmlere hücre ekilerek hücre kültürü ortamında 45 gün tutulduktan sonra UTS değerinin 0.55 MPa'dan, 0.46 MPa'a indiği görülmüştür. Ancak 75. gün sonunda UTS değeri 1.2 MPa olarak ölçülmüş, bu da film yapısının damar düz kas hücreleri tarafından salgılanan ECM ile güçlendiğini düşündürmüştür (Tablo 1). Ayrıca 75 gün sonunda düz filmler ile kanallı filmlerin UTS değerleri arasında önemli bir fark bulunmaktadır. düz filmlerin 0.66 ± 0.35 MPa değerine karşılık 332.5 nm genişlikli kanallı filmlerde 1.20 ± 0.46 MPa, 650 nm genişlikli kanallı içeren filmlerde 1.63 ± 0.46 MPa'dır. Bu sonuç hücre uzanımının ve bunun sonucu oluşan ECM organizasyonun kollajen filmleri güçlendirdiği düşüncesini desteklemektedir. Bu fark 75 gün boyunca hücre kültüründe inkübe edilmiş 650 nm genişlikli kanallı filmlerle düz filmler karşılaştırıdığında oldukça belirgindir. Aynı filmlerin UTS değerleri karşılaştırıldığında düz filmlerde ölçülen 0.66 ± 0.35 MPa değeri, desenli filmlerde ölçülen 1.63 ± 0.46 MPa değerinin yaklaşık üçte biri kadardır. Bu sonuçlar daha önce literatürde sunulan uzanım gösteren MC3T3 hücrelerinin ECM olarak kollajen tip üretiklerini gösteren çalışmayı destekler niteliktedir (Wang ve ark.,

2003). Düz kas hücresi ekili, kollajen kullanılarak üretilen yapı iskeleleri periyodik gerilim uygulandığında da benzer sonuçlar alınmıştır. (Isenberg ve ark., 2003). İlk 2 hafta içinde gerek hücrelerin varlığı gerekse periyodik gerilimin herhangi bir etkisi görülmemiş ancak 5 hafta sonra UTS değeri 1.6 kat artarak 0.4 MPa'a ulaşmıştır (bu değer hala damar doku mühendisliği uygulamaları için yeterince yüksek değildir). Bu çalışmada, hücresiz veya hücre ekilmiş düz filmlerin UTS değerleri bir atardamarın düz kısmının UTS değerinden, yaklaşık 1.3 MPa, daha düşüktür (Yamada, 1970). Sonuçta, kanallı filmlerdeki hücreler filmin mekanik gücünü 1.76 MPa'dan 2.64 MPa'a artırmış neredeyse boyun arteri değerine vardırmıştır (Kurane ve ark., 2007).

Farklı grupların Young modülleri arasında önemli bir fark görülmemiştir. Bütün test gruplarının değerleri 4 MPa civarındadır (Tablo1). Bütün örneklerde zamanla sertleşmeyi gösteren küçük artışlar gözlenmiştir. 4 MPa Young modül değeri bir toplar damarınkinden çok az büyük (3.11±0.65 MPa), bir atar damarınkinden (1.54±0.33 MPa) ise oldukça büyüktür (Pukacki ve ark., 2000).

Bizim çalışmamıza benzer biçimde, Greiner ve ark. uzanım gösteren fibroblastlara uygulanan statik gerilimin hücre katmanının, uzanım göstermeyenlere karşılık mekanik özelliklerinde 7 kata yakın bir artışa neden olduğunu gözlemişlerdir. Yakın zamanda yapılan bir çalışma damar düz kas hücrelerinin yönleniminde etkili olan mekanik uyarıları ve topografik ipuçlarını karşılaştırmış, hücrelerin mekanik uyarılardan çok topografik ipuçları ışığında mikrokanallarda uzandıklarını göstermiştir (Houtchens ve ark., 2008). Damar düz kas hücrelerinin yönelimin topografik ipuçlarıyla aynı gözlemleri mekanik uyaranlarla güçlendirildiği mikrotopografik bilginin hücrenin yönelimini değiştirdiği belirlenmiştir. Wang ve ark. (2005) aynı şeyleri fibroblastlarda da yapmıştır. Çalışmamızda her ne kadar mikrokanallar yerine nanokanallar kullanıldıysa da topografik bilginin kollajen filmlerin dayanıklığını artırdıkları açıktır.

1.6 Nanoçıkıntılı Polimerik Yüzeylerin Damar Düz Kas Hücrelerini Yönlendirmedeki Etkilerinin Araştırılması

Damar doku mühendisliği biyoteknolojinin oldukça yoğun çalışılan ve hızla gelişen bir araştırma alanı konumundadır. Ancak var olan biyofabrikasyon işlemleri oldukça zor, pahalı, zaman alan ve otomatize olmayan biyoreaktör temelli uygulamalar olarak karşımıza çıkmaktadır. Mikro ve nanoteknolojideki gelişmeler damar yapı iskelelerine ek fonksiyonel özellikler katmakta, damar iç yüzeyinin topografisinin kontrolüne olanak tanımakta hatta kök hücrelerin damar hücresi fenotipine farklılaşmalarını kontrol edebilmektedir. Damar dokusunun biyofabrikasyon metotlarındaki mikro ve nanoteknolojiye dayalı gelişmler biyoreaktöre bağlı üretim gereğini ortadan kaldırmaktadır.

Bu bakış açısıyla çalışmamızda kullandığımız nanokanallı yapılara ek olarak damar düz kas hücrelerinin yönlenmesini daha detaylı incelemek için mikro ve nanoçıkıntılı polimerik yüzeyler çalışmaya dahil edilmiştir.

İlk olarak silisyum çipler üstüne e-ışını litografisi ve reaktif iyon kazıma (etching) yöntemi kullanılarak nano ölçekli desenler işlenmiştir ve onların damar hücrelerini VSMC yönlendirmedeki etkileri de incelenmiştir. Burada boyları 650 nm ile 1.5 μm arasında değişen çıkıntılar üretilmiş ve bunların polidimetilsiloksan kopyaları hazırlanarak nanoyapıların negatifleri elde edilmiştir.
PDMS kopyalar ikinci bir taslak görevi görmüş ve bunlar kullanılarak 2 boyutlu polimerik film kopyalar hazırlanmıştır. Işık mikroskopu, elektron tarama mikroskopu (SEM) ve Atomik Kuvvet Mikroskopu (AFM) yoluyla yapılan incelemelerle çalışmanın başarısı ve tekrarlanabilirliği incelenmiştir (Şekil 26-28). Yüzey özelliklerinin boyutları kopyalama hassasiyetini etkilememiştir. İşlemin temel kısıtlayıcılığı PLLA polimerinin tipik bir inorganic yapıya oranla yumuşak oluşu olmuştur. Bu özellik filmler PDMS kalıplardan çıkarılırken şekil bozulmalarına neden olabilmektedir.

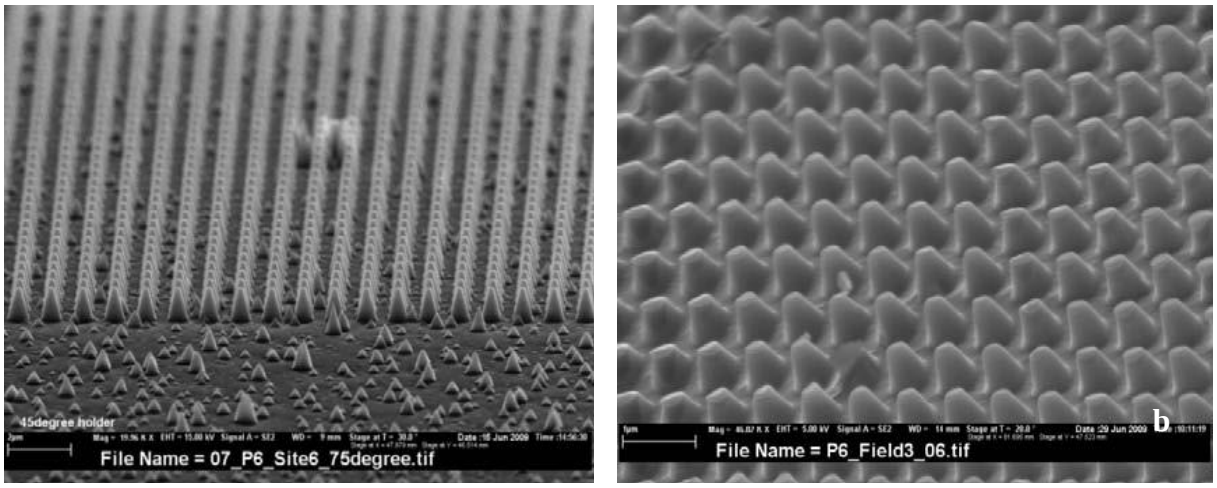

Şekil 26. 800-950 nm boyundaki çıkıntıların SEM görüntüleri. a) Orijinal silisyum yüzey, b) PLLA kopya film yüzeyi.

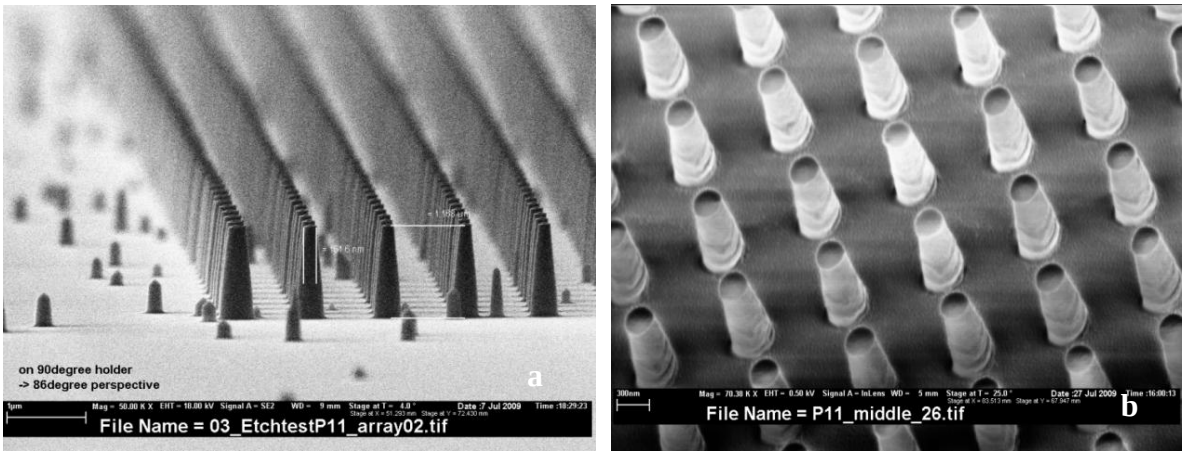

Şekil 27. a) 1.5 µm boyundaki çıkıntıların SEM görüntüleri. a) Orijinal silisyum yüzeyindeki çıkıntılar, b) PLLA kopya film yüzeyi.

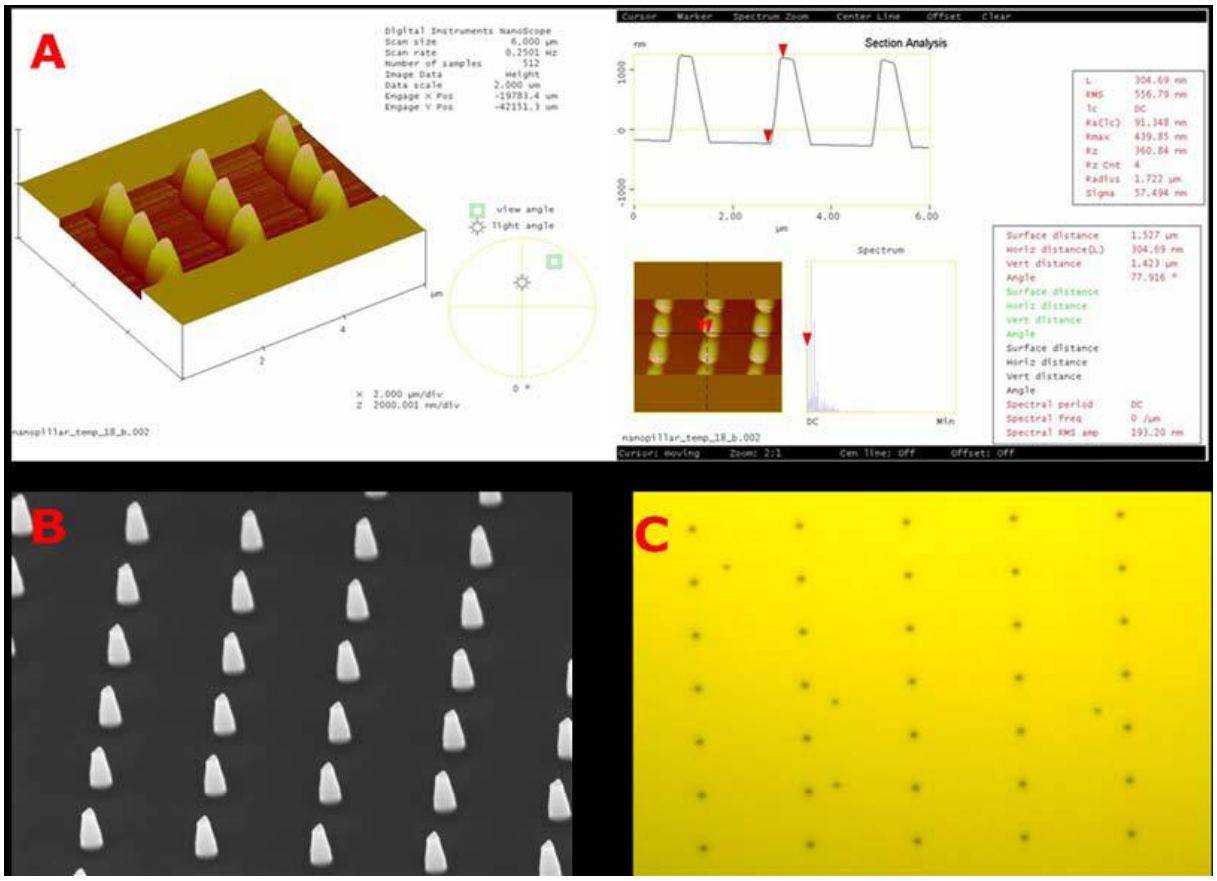

Şekil 28. E-ışın litografisi yoluyla üretilen 1.5 µm'lik orijinal silisyum yüzey görüntüleri A) AFM, B) SEM. (C) PLLA filme kopyalanan yapıların ışık mikroskopu görüntüsü.

SEM, AFM ve ışık mikroskopuyla elde edilen görüntülerde neredeyse hatasız kopyaların üretildiği görülmektedir. İki basamaklı kopyalama yöntemi izlenerek nanoçıkıntılı PLLA filmler hazırlanmış, kopyalamanın başarısı AFM yoluyla incelenmiştir. Çalışmada 900 nm boyundaki çıkıntılar başarıyla kopyalanmıştır. Kullanılan silisyum şablonda çıkıntıların birbirine uzaklığı 1 ile 10 µm arasında değişmektedir.

Bu yüzeylerde damar düz kas hücrelerinin yüzeye yapışma davranışları, yönelimleri, mekanik özellikleri araştırılmıştır. Damar düz kas hücreleri 20.000 hücre/film yoğunluğunda ekilerek 2 gün sonunda hücreler DAPI ve Phalloidin ile boyanmıştır. Kullanılan floresan boyalardan DAPI hücre DNA'sını boyarken Phalloidin hücre iskeleti elemanlarından aktini boyamaktadır. Hücrelerin yönelim davranışları floresan mikroskobu yoluyla incelenmiştir (Şekil 29). Damar düz kas hücreleri nanoçıkıntılı yüzeylerde herhangi bir yönelim davranışı göstermemişlerdir. Bunun nedeni olarak hücrelerin çıkıntılar arası boşluklara sığamayacak

kadar büyük olmaları gösterilebilir. Hücrelerde toplu ve belirgin bir uzanım davranışı görülmese de tek tek bakıldığında hücrelerin çıkıntılar üzerinde yayılıp, hücre iskeletlerinin uzantılar meydana getirdikleri görülmektedir (Şekil 30). Buna ek olarak aynı şekiller deney esnasında hücre fenotipinin korunduğunu göstermiştir.

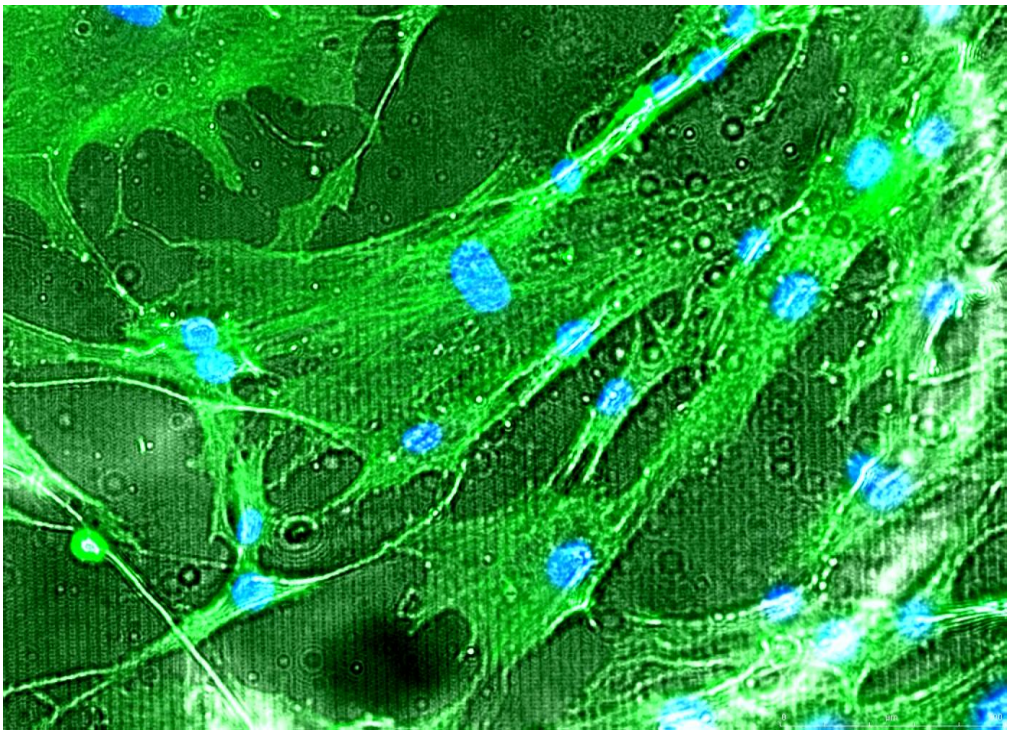

Şekil 29. Nanoçıkıntılı yüzeylerde çoğaltılan Phalloidin-DAPI boyalı damar düz kas hücrelerinin floresan mikroskobu görüntüsü (2. Gün, x 20)

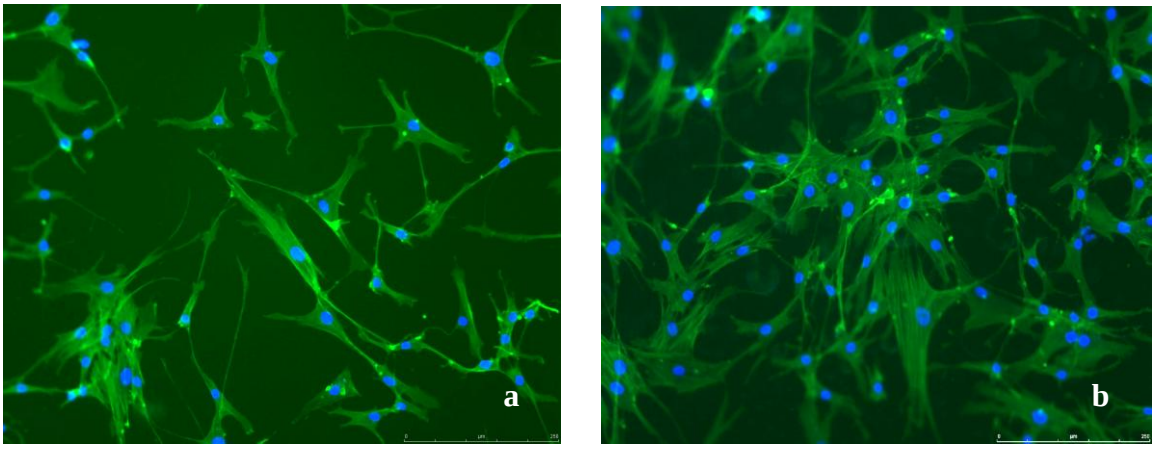

Şekil 30. Nanoçıkıntılı yüzeylerde çoğaltılan Phalloidin-DAPI boyalı damar düz kas hücrelerinin floresan mikroskobu görüntüsü. (2. gün, x 20).

1.7 Mikroçıkıntılı Polimerik Yüzeylerin Damar Düz Kas Hücrelerini Yönlendirmedeki Etkilerinin Araştırılması

Damar düz kas hücrelerinin bu yanıtından sonra çalışmaya mikrodüzeyli ve yine çıkıntı biçiminde olan ve özellikle hücre çekirdeklerini etkilediği için önem taşıyan şablonlarla devam edilmiştir. Bu basamakta kullanılan şablonlar fotolitografi yöntemiyle üretilerek yukarda söz edilen ve nano ölçekli çıkıntıların polimerik kopyalarını hazırlamakta kullanılan 2 basamaklı yöntem başarıyla uygulanmıştır. Polimerik filmler SEM kullanılarak karakterize edilmiştir (Şekil 31). **A tipi** kare yüzeyli çıkıntılar simetrik dağılımlıdır. Çıkıntılar arası uzaklık x ve y eksenleri boyunca 7 µm'dur. **B tipi** yüzey ise asimetrik olarak dağılım gösteren çıkıntılardan oluşmaktadır. Çıkıntılar arası uzaklık eksenler boyunca 12 ve 24 µm'dir. Çıkıntıların boyları 4-5 µm civarındadır. Çıkıntıların dağılımı göz önünde bulundurulduğunda A tipi çıkıntılar damar düz kas hücrelerinin tutunma davranışlarını, B tipi çıkıntılar ise hücrelerin yönelim/uzanım davranışlarını incelemeye olanak sağlamıştır. Damar düz kas hücreleri 20.000 hücre/film yoğunluğunda ekilerek 2 gün sonunda hücreler DAPI ve Phalloidin ile boyanmıştır. Hücrelerin tutunma ve uzanım davranışları floresan mikroskobuyla incelenmiştir (Şekil 32).

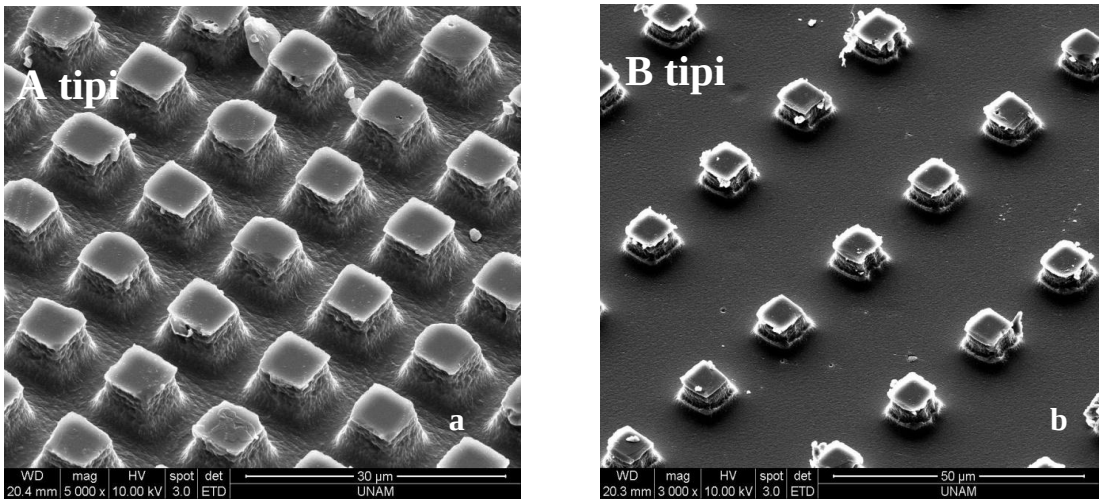

Şekil 31. PLLA film kopyalarındaki mikro çıkıntılı yüzey özelliklerin SEM görüntüleri.

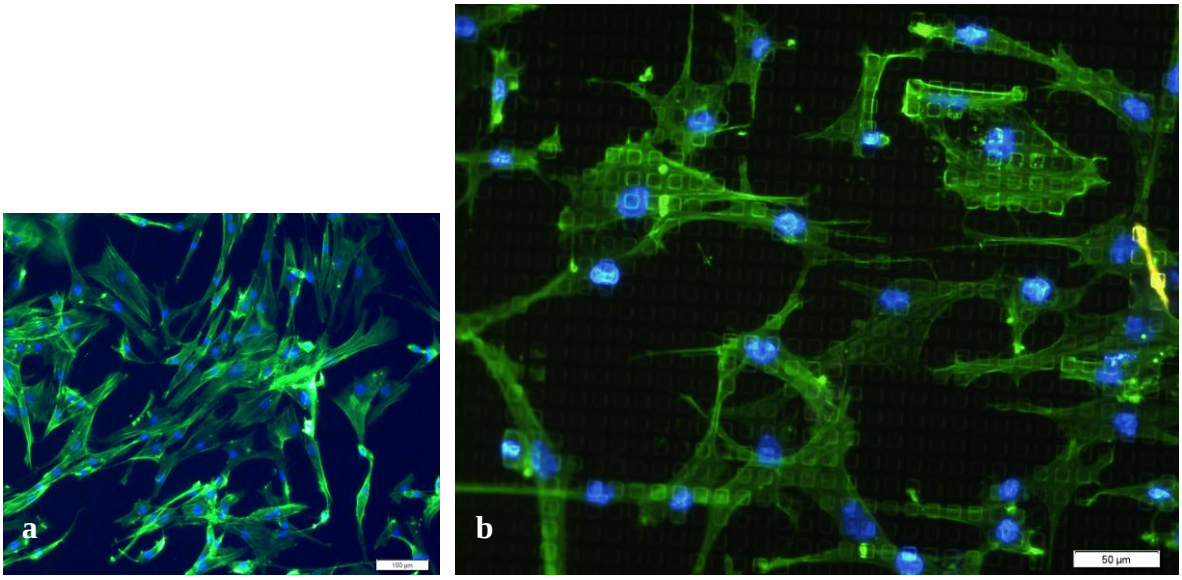

Şekil 32. DAPI ve Phalloidin boyalı damar düz kas hücrelerinin floresan mikroskobu görüntüleri. (a) düz (desensiz) polimerik yüzey üzerindeki (b) A tipi çıkıntılar (x 20)

Düz polimerik yüzeyde çoğaltılan kontrol örneklerinde damar düz kas hücrelerinin tipik, tek çekirdekli, ince-uzun yapıları görülmektedir (Şekil 32 (a). Ancak simetrik dağılım göstern A tipi çıkıntılı yüzeydeki hücrelere bakıldığında bunların çıkıntılar üzerine yayıldıkları gözlenmiştir (Şekil 32 (b)). Çıkıntılar arası uzaklık hücrelerin araya girmesini engelleyecek boyutlarda olduğundan bu şaşırtıcı olmamıştır.

Çalışmada kullandığımız B tipi mikro çıkıntılar gösterdikleri dağılım açısından hücrelerin yönlenimin olanak tanır niteliktedir. Çıkıntılar arası uzaklığın 24 µm olduğu hat göreceli ve dolaylı olarak bir kanal niteliğindedir. Aktin filamenleri Phalloidin ile boyandığı zaman damar düz kas hücrelerinin bu düşüncemizi doğrular biçimde yönelim göstermiştir. A tipi çıkıntılardan farklı olarak, hücrelerin çıkıntıların üstüne yayılmak yerine daha çok oluşan suni kanallar içinde, tipik ince-uzun düz kas morfolojisini sergilemişlerdir (Şekil 34).

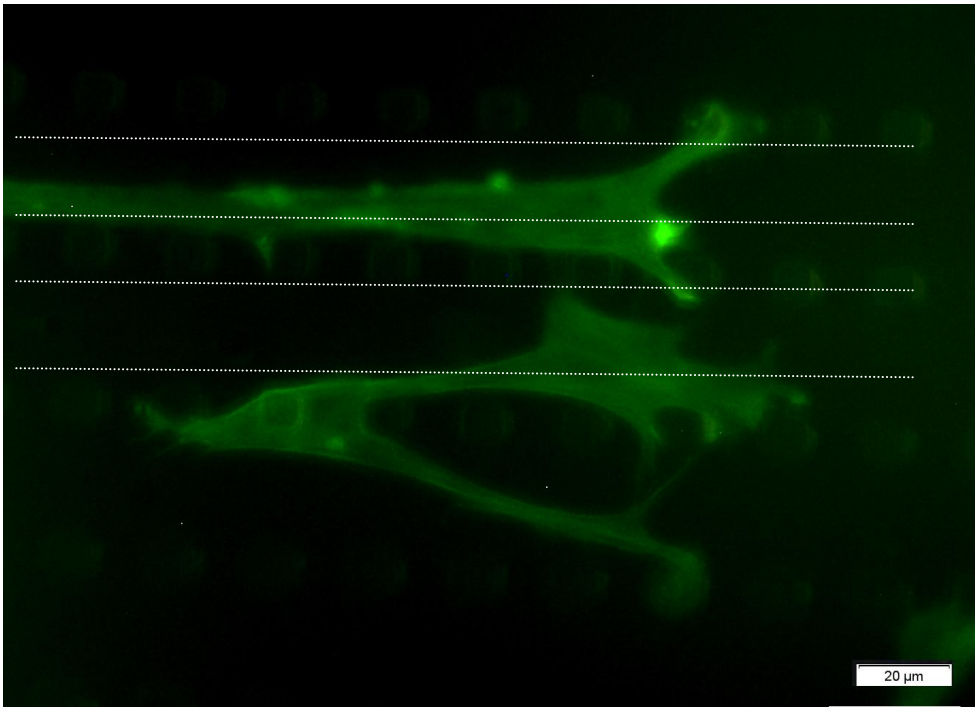

Şekil 34. B tipi asimetrik dağılımlı mikro çıkıntılı polimerik yüzeylerde çoğaltılan ve Phalloidin boyalı hücrelerin floresan mikroskop görüntüleri (x 40)

Sonuç

Damar düz kas hücreleriyle yapılan hücre kültürü çalışmaları nanokanallı kollajen filmlerin hücre tutunması ve çoğalması için uygun sübstratlar olduklarını göstermiştir. Hücreler her üç farklı genişlikli film üstünde fenotiplerini korumuşlar ve kanallar yönünde uzanmışlardır. Damar düz kas hücrelerinin tıpkı doğal damar yapısındaki gibi yönlenmelerinin tasarımın mekanik özelliklerinin iyileştirilmesinde kullanılabileceği öngörülmektedir. Bu çalışma 21 gün sonunda yönlenmenin hücre çoğalmasını etkilemese de yapı iskelesinin mekanik özelliklerini artırdığını göstermiştir.

Nano kanallı kollajen filmlerle yapılan çalışmalar topografinin hücre yönlenmesinde oldukça etkin bir rol oynadığını göstermiştir. Buradan hareketle, damar düz kas hücrelerinin yönlenme davranışları ve biyomekanik özellikleri hakkında ek bilgiler edinmek ve yeni tasarımlarımızı bu bilgiler ışığında geliştirmek amacıyla çalışmaya nano ve mikro çıkıntılı yüzeyler dahil edilmiştir. Damar düz kas hücreleri nano ölçekli çıkıntıların boyutları ve gösterdikleri dağılıma göre oldukça büyük olduğundan belirgin bir uzanım gözlenmemiştir. Mikro çıkıntılı polimerik filmlerle yapılan çalışmalar ise simetrik dağılım gösteren A tipi çıkıntılar damar düz kas hücrelerinin uzanımlarından çok morfolojilerini etkilemiş, düz yüzeylerde tipik ince

uzun yapılı olan hücreler bu çıkıntıların üzerine yayılarak geniş alanlı hücrelere dönüşmüşlerdir. Nanokanallı tasarımlardaki kadar olmasa bile asimetrik dağılım gösteren B tipi çıkıntılı yüzeylerde hücre yönlenmesi görülmüştür.

Şu andaki yaklaşımla, kollajenin iyi biyolojik özellikleri ve hücre rehberliği ile elde edilen mekanik özellikler birleştirilerek damar doku mühendisliğinde kullanmak üzere başarılı yapı iskeleleri üretilebileceği görülmektedir.

TEŞEKKÜR

Mikro ve naoçıkıntılı orjinal silisyum şablonları sağlayan Dr. Celestino Padeste'ye (PSI-İsviçre) teşekkür ederiz.

REFERANSLAR

Dalton B.A., Evans M.D.M., McFarland G.A., Steele J.G. Modulation of corneal epithelial stratification by polymer surface topography J Biomed Mater Res. 1999; 45(4): 384-94

Elliott J.T., Woodward J.T., Langenbach K.J., Tona A., Jones P.L., Plant A.L., Vascular smooth muscle cell response on thin films of collagen. Matrix Biol 2005; 24: 489-502

Engel E., Michiardi A., Navarro M., Lacroix D., Planell J.A. Nanotechnology in regenerative medicine: the materials side. Trends Biotechnol 2008; 26: 39-47

Faraj KA, van Kuppevelt TH, Daamen WF. Construction of Collagen Scaffolds That Mimic the Three-Dimensional Architecture of Specific Tissues. Tissue Eng 2007; 13 (10): 2387-94

Freyman T.M., Yannas I.V., Gibson L.J. Cellular materials as porous scaffolds for tissue engineering *Progress in Material Science* 2001; 46: 273-282

Grenier G., Rémy-Zolghadri M., Larouche D., Gauvin R., Baker K., Bergeron F., Dupuis D., Langelier E., Rancourt D., Auger F.A., Germain L. Tissue reorganization in response to mechanical load increases functionality. Tissue Eng 2005; 11: 90-100

Hasirci V., Vrana E., Zorlutuna P., Ndreu A., Yilgor P., Basmanav F.B., Aydin E. Nanobiomaterials: a review of the existing science and technology, and new approaches J Biomater Sci Polym Ed. 2006; 17(11): 1241-68

Houtchens G.R., Foster M.D., Desai T.A., Morgan E.F., Wong J.Y. Combined effects of microtopography and cyclic strain on vascular smooth muscle cell orientation. J Biomech 2008; 41: 762-9

Heyderman L.J., Solak H.H., David C., Atkinson D., Cowburn R.P., Nolting F. Arrays of nanoscale magnetic dots: Fabrication by x-ray interference lithography and characterization Appl Phys Lett 2004; 85(21): 4989-91.

Isenberg B.C. and Tranquillo R.T. Long-term cyclic distention enhances the mechanical properties of collagen-based media-equivalents. Ann Biomed Eng 2003; 31: 937-49.

Kenar H., Kose G.T., Hasirci V. Tissue engineering of bone on micropatterned biodegradable polyester films Biomaterials 2006; 27(6): 885-95.

Kurane A., Simionescu D.T., Vyavahare N.R. In vivo cellular repopulation of tubular elastin scaffolds mediated by basic fibroblast growth factor. Biomaterials 2007; 28: 2830–38

Langer R. and Vacanti J. P. Tissue engineering *Science* 1993; 260: 920-926

Lee C.H., Singla A., Lee Y. Biomedical applications of collagen *Int J Pharm* 2001; 221(1-2): 1-22

Mitchell S.L. and Niklason L.E. Requirements for growing tissue-engineered vascular grafts. *Cardiovasc Pathol* 2003;12(2):59-64

Pins G.D., Toner M. and Morgan J.D. Microfabrication of an analog of the basal lamina: biocompatible membranes with complex topographies The FABES Journal 2000; 14: 593-602

Pukacki F., Jankowski T., Gabriel M., Oszkinis G., Krasinski Z., Zapalski S. The Mechanical Properties of Fresh and Cryopreserved Arterial Homografts. Eur J Vasc Endovasc Surg 2000; 20: 21–4

Quirk R.A., France R.M., Shakesheff K.M., Howdle S.M. Supercritical fluid technologies and tissue engineering scaffolds *Current Opinion in Solid State and Materials Science* 2004; 8 (3-4): 313-21.

Robinson A.P.G., Palmer R.E., Tada T., Kanayama T., Allen M.T., Preece J.A. Harris K.D.M. 10 nm scale electron beam lithography using a triphenylene derivative as a negative/positive tone resist *J Phys D Appl Phys* 1999; 32(16): 75-8

Schmalenberg K.E., Buettner H.M., Uhrich K.E. Microcontact printing of proteins on oxygen plasma-activated poly(methyl methacrylate) Biomaterials 2004; 25: 1851-57

Shen J.Y., Chan-Park M.B., He B., Zhu A.P., Zhu X., Beuerman R.W., Yang E.B., Chen W., Chan V. Three-dimensional microchannels in biodegradable polymeric films for control orientation and phenotype of vascular smooth muscle cells. Tissue Eng 2006, 12 (8): 2229-40

Shen J.Y., Chan-Park M.B., Feng Z.Q., Chan V., Feng Z.W. UV-embossed microchannel in biocompatible polymeric film: application to control of cell shape and orientation of muscle cells. J Biomed Mater Res B 2006; 77: 423-30

Shi C., Zhu Y., Ran X., Wang M., Su Y., Cheng T. Therapeutic potential of chitosan and its derivatives in regenerative medicine *J Surg Res* 2006; 133(2):185-92

Shum-Tim D., Stock U., Hrkach J., Shinoka T., Lien J., Moses M.A., Stamp A., Taylor G., Moran A.M., Landis W., Langer R., Vacanti J.P., Mayer J.E. Jr. Tissue engineering of autologous aorta using a new biodegradable polymer. Ann Thorac Surg 1999;68(6):2298-304

Thomas V., Zhang X., Catledge S.A., Vohra Y.K. Functionally graded electrospun scaffolds with tunable mechanical properties for vascular tissue regeneration. Biomed Mater 2007; 2: 224–32

Xu C.Y., Inai R., Kotaki M., Ramakrishna S. Aligned biodegradable nanofibrous structure: a potential scaffold for blood vessel engineering. Biomaterials 2004, 25: 877–86

Vernon RB., Gooden M.D., Lara S.L., Wight T.N. Microgrooved fibrillar collagen membranes as scaffolds for cell support and alignment. Biomaterials 2005; 26: 3131–40

Vladimir M. Vladimir K. and Roger R. M. Nanotechnology in vascular tissue engineering: from nanoscaffolding towards rapid vessel biofabrication, Trends in Biotechnology 2008; 26: 338-344.

Wang J.H.C., Jia F., Gilbert T.W., Woo S.L.Y. Cell orientation determines the alignment of cell-produced collagenous matrix. J of Biomech 2003; 36: 97–102

Wang J.H., Yang G., Li Z. Controlling cell responses to cyclic mechanical stretching. Ann Biomed Eng 2005; 33: 337-42

Wilson D.L., Martin R., Hong S., Cronin-Golomb M., Mirkin C.A., Kaplan D.L. Surface organization and nanopatterning of collagen by dip-pen nanolithography Proc Natl Acad Sci USA 2001; 98(24): 13660-4

Yang J., Motlagh D., Webb A.R., Ameer G.A. Novel Biphasic Elastomeric Scaffold for Small-Diameter Blood Vessel Tissue Engineering. Tissue Eng 2005; 11 (11-12): 1876-86

Yamada H. Strength of Biological Materials. p. 114-130. Williams & Wilkins, Baltimore (1970)

2. İdari Gelişmeler

Pınar Zorlutuna'nın ayrılması nedeniyle projeye ODTÜ Fen Bilimleri Enstitüsü Biyoloji ABD Doktora öğrencisi Hayriye Özçelik TBAG Grubunun onayıyla katılmıştır.

3. Projenin Çalışma Takvimine Uygun ilerlemesi

Proje çalışma takvimine uygun yürümüştür.

4. Proje Harcamalarına İlişkin Açıklamalar

Projede önemli düzeyde kimyasalın yanında, Floresan mikroskop kamerası ataçmanları, yazılımı ve bunlarla uyumlu bilgisayar, Multiskan Spektrum ve Cole Parmer Vakum Fırını ile Vakum Pompası alınıp yerleştirilmiş, cihazlar aktif kullanıma sokulmuştur. Bölüm payı ile ise bir FTIR alımı gerçekleştirilmiştir.

5. Proje Konusunda Yapılan Yayınlar ve Bildiriler

Yayınlar

P.Zorlutuna, Z.Rong, P.Vadgama, V.Hasirci, Influence of Nanopatterns on Endothelial Cell Adhesion: Enhanced Cell Retention under Shear Stress, Acta Biomater 5(7), 2451-2459, 2009.

P.Zorlutuna, P.Yilgor, F.B.Basmanav, V.Hasirci, Biomaterials and tissue engineering research in Turkey: The METU Biomat Center experience, Biotechnology Journal 4(7), 965-980, 2009.

P.Zorlutuna, A.Elsheikh, V.Hasirci, Nanopatterning of Collagen Scaffolds Improve the Mechanical Properties of Tissue Engineered Vascular Grafts, Biomacromolecules 10(4), 814-821, 2009.

Bildiriler

5. Ulusal Nanobilim ve Nanoteknoloji Kongresi, Eskişehir Anadolu Üniversitesi, Patterned surfaces modify cell behavior and/or deform cells and organelles, V. Hasırcı, H. Ozcelik, P. Zorlutuna, 8-12 Haziran 2009 (Sözlü bildiri).

ESB2009, 22th European Symposium on Biomaterials, Lozan, İsviçre, Nanopatterned Collagen Scaffolds Improve the Mechanical Properties of Tissue Engineered Vascular Grafts, P. Zorlutuna, A. Elsheikh , V. Hasirci, 7-11 Eylül 2009 (Sözlü bildiri)

Nanobio 2010, Third International NanoBio Conference Zurich, İsviçre, Replication of nano-pillar array structures for tissue engineering applications, H. Özçelik, C. Padeste, J. Ziegler, A. Schleunitz, M. Bednarzik, V. Hasırcı, 24-27 Ağustos, 2010 (Poster)

NanoTR6, 2010, Nanobilim ve Nanoteknoloji Konferansı, İzmir, Türkiye, The Effect of Surface Nanotopography on Neural Stem Cell Alignment, Hayriye Özçelik , Deniz Yücel, Celestino Padeste, Vasıf Hasırcı, 15-18 Haziran 2010 (Poster)

ESB 2010, 23th European Symposium on Biomaterials, Tampere, Finlandiya, The Role of Nanopillars on Adhesion and Orientation of Saos-2 and Bone Marrow Stem Cells, H. Özçelik, J. Ziegler, A. Schleunitz, M. Bednarzik, C. Padeste, V. Hasırcı (Sözlü Bildiri)

10th Anniversary BioMACROMOLECULES

Article

Nanopatterning of Collagen Scaffolds Improve the Mechanical Properties of Tissue Engineered Vascular Grafts

P. Zorlutuna, A. Elsheikh, and V. Hasirci

Biomacromolecules, **2009**, 10 (4), 814-821• DOI: 10.1021/bm801307y • Publication Date (Web): 18 February 2009

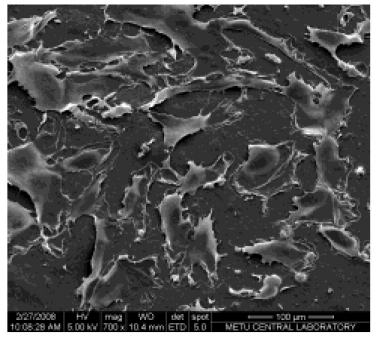

VSMC on smooth collagen surface

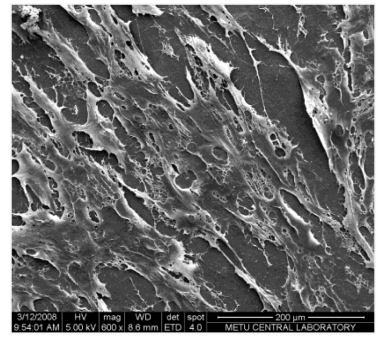

VSMC on nanopatterned collagen surface

More About This Article

Additional resources and features associated with this article are available within the HTML version:

- Supporting Information
- Access to high resolution figures
- Links to articles and content related to this article
- Copyright permission to reproduce figures and/or text from this article

View the Full Text HTML

Biomacromolecules is published by the American Chemical Society. 1155 Sixteenth Street N.W., Washington, DC 20036

Nanopatterning of Collagen Scaffolds Improve the Mechanical Properties of Tissue Engineered Vascular Grafts

P. Zorlutuna,[†] A. Elsheikh,[‡] and V. Hasirci*[,†,§]

METU, BIOMAT, Departments of Biological Sciences and Biomedical Engineering and Biotechnology, Biotechnology Research Unit, Ankara, Turkey, and Division of Civil Engineering, University of Dundee, Dundee DD1 4HN, United Kingdom

Received November 12, 2008; Revised Manuscript Received January 19, 2009

Tissue engineered constructs with cells growing in an organized manner have been shown to have improved mechanical properties. This can be especially important when constructing tissues that need to perform under load, such as cardiac and vascular tissue. Enhancement of mechanical properties of tissue engineered vascular grafts via orientation of smooth muscle cells by the help of topographical cues have not been reported yet. In the present study, collagen scaffolds with 650, 500, and 332.5 nm wide nanochannels and ridges were designed and seeded with smooth muscle cells isolated from the human saphenous vein. Cell alignment on the construct was shown by SEM and fluorescence microscopy. The ultimate tensile strength (UTS) and Young's modulus of the scaffolds were determined after 45 and 75 days. Alamar Blue assay was used to determine the number of viable cells on surfaces with different dimensioned patterns. Presence of nanopatterns increased the UTS from 0.55 ± 0.11 to as much as 1.63 ± 0.46 MPa, a value within the range of natural arteries and veins. Similarly, Young's modulus values were found to be around 4 MPa, again in the range of natural vessels. The study thus showed that nanopatterns as small as 332.5 nm could align the smooth muscle cells and that alignment significantly improved mechanical properties, indicating that nanopatterned collagen scaffolds have the potential for use in the tissue engineering of small diameter blood vessels.

1. Introduction

In the developed countries, cardiovascular diseases are among the major causes of death. According to the Department of Health and Human Services of the United States Center for Chronic Disease Prevention, it is the predominant cause of death, killing more people than cancer every year.[1] Arterial autografts have many invaluable properties such as viability, proportional growth when used in children, and appropriate mechanical properties including flexibility at joints,[2] but their limited availability is a major drawback. When autografts are not available, synthetic grafts made from Dacron,[3] expanded poly(tetrafluoroethylene) (ePTFE),[4] or polyurethane[5] are used. Synthetic vascular grafts are freely available but clogging, compliance mismatch, and fibrous tissue formation are major problems leading in some cases to graft failure.[6] Different approaches including antithrombogenic coatings,[7] endothelial cell seeding,[8,9] and modification of pore size and surface texture have been tried to solve them.[10−12] Even though these approaches improved the performance of the synthetic grafts, they were still limited to the treatment of large arteries (>6 mm inner diameter).

Tissue engineering may offer a solution to the problem of replacement for smaller diameter vessels.[13] The general approach in vascular tissue engineering is to produce tubular constructs of a degradable material and autologous vascular cells[14] that have an appropriate mechanical strength and a viable, continuous lining of endothelial cells.[15] Stiff materials have compliance mismatch that leads to neointimal hyperplasia and atherosclerosis and materials with low ultimate tensile strength (UTS) rupture under blood pressure.[16] Many different materials including collagen,[17,18] elastin,[19] poly(ε-caprolactone),[20] polyglyconate,[21] polyester,[22] and silk fibroin[23] were tested as films or tubes. An extreme case is cell sheets rolled around mandrels (without any scaffold material), which were found to possess good mechanical strength (burst strength of 2000 mmHg) and suturability but limited patency after 3 to 4 weeks of transplantation.[24]

As a scaffold material, collagen type I has a special place because it is the predominant protein in the natural extracellular matrix (ECM) of the blood vessels. It is secreted by vascular smooth muscle cells (VSMCs) and is essential for mechanically strong vessels.[25] Collagen type I is hemocompatible; it does not enhance blood coagulation or modify the viscoelastic properties of the blood or cause excessive platelet adhesion and aggregation.[26] However, engineered vascular grafts from reconstituted collagen possess lower mechanical properties than the natural vessels.[18]

Even though the artificial blood vessels consist mainly of collagen as the natural blood vessel this low mechanical property could be related with the fibrillar nature and high organization in the natural vessels and its absence in the scaffolds from reconstituted collagen. It was also suggested that circumferential orientation of natural smooth muscle cells could be the reason for the observed mechanical property, so mimicking this could increase the mechanical strength of the engineered vessels.[27] Mimicking of natural tissues was attempted by cell guidance using physical cues.[28−31] In this approach, surface topography is modified to improve attachment, orientation, and morphology of the cells. Because it is known that orientation of cells affects the morphology and this in return affects their function, achieving an organization similar to that in their natural

* To whom correspondence should be addressed. Tel.: 90.312.210L180. Fax: 90.312.2101L42. E-mail: vhasirci@metu.edu.tr.
[†] Department of Biotechnology.
[‡] University of Dundee.
[§] Departments of Biological Sciences and Biomedical Engineering.

10.1021/bm801307y CCC: $40.75
Published on Web 02/18/2009

environment is important.[32] A proof of this was obtained when alignment of VSMCs with the help of microchannels in a pattern similar to their natural organization resulted in cells with the "contractile phenotype", which is necessary for functional blood vessels, rather than the "synthetic phenotype".[33] Patterns created on the surfaces for this purpose were at micron-scale because the cells were of micron dimension and also the techniques used to create the desired patterns had micron scale resolution. Nanoscale modification of cell carriers was possible recently through the help of nanotechnology, and thus, the natural ECM can be mimicked at the molecular level.[34,35] The microlevel depths on a micropatterned membrane weakened the scaffold mechanically due to the presence of thinner regions (bottoms of the channels), whereas nanoscale patterns on similar thickness membranes did not adversely affect the mechanical properties of the scaffold. The question here is "can nano-patterns guide cells"? Previously, guidance of VSMCs was accomplished by using electrospun poly(L-lactide-*co*-ε-caprolactone) (75:25) nanofibrous two-dimensional (2D) scaffolds with 500 nm fiber diameter.[36] This alignment was suggested for probable mechanical property enhancement, but the correlation of cell guidance and mechanical properties was not studied experimentally.

Effect of cells on mechanical properties of tissue engineered constructs has been studied from different angles. Presence of fibroblasts in collagen gels increased the mechanical properties starting with day 3 of culture up to a few weeks by contracting the collagen fibers in the gel, an effect that decreased as the culture period increased.[37] Also, human dermal fibroblasts showed improvement of mechanical properties of collagen gels supported by a cross-linked collagen sleeve with respect to uncrosslinked and support-free constructs even though the cells were not oriented.[38] Presence of cells could affect the mechanical properties of the tissue engineering scaffolds through interfering with their metabolism as well. In a study it was shown that addition of fibronectin on collagen gels seeded with fibronectin-null myofibroblasts resulted in polymerization of fibronectin into ECM and increase in mechanical strength.[39] Mechanical stimulus was also used to enhance the mechanical properties of cell seeded scaffolds. Although it was not effective at 2 weeks, cyclic distention was shown to increase the mechanical properties of SMC seeded collagen-based scaffolds after 5 weeks of incubation.[40] Alignment of fibroblasts by static mechanical stimuli was also shown to increase the mechanical properties of cell sheets.[41] Earlier studies by our group on cell guidance for corneal tissue engineering had shown that seeding with keratocytes enhanced the mechanical properties of micropatterned polymeric films but seeding with epithelial cells did not, suggesting that the presence of the cells was not enough, rather, the ECM secreted by the guided cells was needed to enhance the mechanical properties of the scaffold.[42,43] Thus, increase of mechanical strength due to guidance of cells was only possible if that cell type secreted its own ECM.

The cell source for tissue engineered vascular grafts is an important issue. Common autografts used in the clinics is the vein; it is more available in adequate length, easily harvested, and adapts well to placement in arterial circulation.[44] The saphenous vein is the first choice of the surgeons because of its appropriate diameter, relatively thick walls and providing sufficient length (due to being the longest vein in the body). Therefore, the cells harvested by a small biopsy sample from the saphenous vein is a suitable cell source for vascular tissue engineering both because of these properties and also since the cells can be isolated with high efficiency and can be proliferated and passaged without dedifferentiation.

Effect of VSMC alignment with the help of topographical cues on the mechanical properties of engineered vascular grafts has not been reported yet. The aim of this study was to achieve the alignment of the VSMCs on 2D nanopatterned scaffolds and investigate the influence of this cell growth and alignment on the mechanical properties of these collagen scaffolds. The hypothesis is that cells aligned on the biodegradable films will strengthen them mechanically as a result of the metabolic products and the ECM secreted by them. Nanopatterned collagen films were prepared to observe and test this effect knowing that these 2D films can be effectively converted into tubes after rolling and cross-linking while in tubular form and align VSMCs as was reported as a preliminary study in our recent publication.[45] In the current study, alignment of VSMCs on three different nanosized patterns and the effect of the pattern dimension on cell attachment, cell proliferation, and mechanical properties was examined. Mechanical test results showed that aligning VSMCs, and probably the ECM that was secreted by them, just as in the natural ECM of the vessels, indeed improved the mechanical properties, bringing them to the range of the natural vessels. Therefore, this study showed that cell guidance can be used to enhance the mechanical properties of engineered vessels as proposed several times in the literature and overcome one of the two most important challenges in vascular tissue engineering; the adequate mechanical properties.

2. Materials and Methods

2.1. Template Preparation. X-ray interference lithography (Bilkent University, Physics Department, Ankara, Turkey) was used to create three different templates with nanochannels. Briefly, a silicon wafer with a photoresist (AZ 5214) of 500 nm thick was exposed to a laser ($\lambda = 325$ nm) for 10 min and developed. Later, patterns were transferred to silicon by using an epoxy replica. The patterns obtained were parallel channels of equal groove and ridge widths of 650 nm with 300 nm depth, 500 nm with 250 nm depth, and 332.5 nm with 200 nm depth. The templates were characterized with Atomic Force Microscopy (AFM, Ambios Technology Inc., U.S.A.) in noncontact mode. Poly(dimethylsiloxane) (PDMS) replicas of these silicon templates were prepared by using PDMS and the curing agent (Sylgard 184 Elastomer Kit, Dow Corning, U.S.A.) 10 to 1 (w/w) ratio and curing at 65 °C for 3 h.

2.2. Collagen Film Preparation. Collagen films (1 cm^2) were prepared by solvent casting from a 10 mg/mL solution of collagen type I isolated from Sprague−Dawley rat tails (250 $\mu L/cm^2$, 0.5 M, in acetic acid) on nanopatterned and unpatterned PDMS templates. After overnight drying at room temperature, films were cross-linked using 1-ethyl-3-[3-dimethylaminopropyl]carbodiimide hydrochloride (EDC, Pierce, U.S.A.) and *N*-hydroxysulfosuccinimide (NHS, Sigma Chem. Co., U.S.A.).[46] Collagen films were incubated in 170 mM EDC and 217 mM NHS in 50 mM NaH_2PO_4 solution (pH 5.5). After 2 h at room temperature, films were washed with 0.1 M Na_2HPO_4 (pH 9.1) for 1 h, with 1 M NaCl for 2 h, 2 M NaCl for 1 day, and finally with distilled water. After drying at room temperature, the films were peeled off the surface and stored in a desiccator. The thickness of the films was 35 ± 1.4 μm. Pattern fidelity was confirmed with AFM in noncontact mode.

2.3. VSMC Isolation. Human saphenous vein section was obtained from bypass surgery patients at Bayindir Hospital (Ankara, Turkey) in compliance with the rules of their Ethical Committee. The section (ca. 2 cm long) was put into the transport medium (DMEM (Gibco, U.S.A.)/HamF12 (Gibco, U.S.A.), 1:3 supplemented with 10% FCS (Hyclone, U.S.A.) and 10 μL/mL penicillin-streptomycin (10000 units, Sigma Chem. Co., U.S.A.)) and stored at room temperature (not more than 3 h). In the laboratory, the vein was washed with PBS (pH: 7.4, 10 mM), cut longitudinally, and the endothelial cells were scraped off with a #15 scalpel blade. Vein was then scrubbed with a sterile gauze soaked

in PBS to remove any remaining endothelial cells. Then the de-endothelialized vein was cut into smaller pieces (ca. 4 mm^2) and placed with the luminal surface facing down into 35 mm Petri dishes, which were precoated with gelatin (Sigma Chem. Co., USA). To improve the adhesion of explants onto the gelatin coated Petri surface, a small amount (500−700 μL) of DMEM-HamF12 (3:1) supplemented with 30% FCS, 75 μL/mL ECGS (Sigma Chem. Co., U.S.A.), and 10 μL/mL penicillin−streptomycin was added and the CO_2 concentration of the incubator was increased to 8% until the cells migrated out of the biopsy samples. Extreme care was taken in the manipulation of dishes to keep the explants attached to the surface.[47] Within 2 weeks, cells started to migrate out of the biopsy samples.

2.4. Culturing of the Isolated Cells. When the explant cultures reached subconfluency (90%), they were trypsinized with 0.25% Trypsin EDTA solution (Sigma, U.S.A.) by incubating for 1 min and counted with NucleoCounter (ChemoMetec A/S, Denmark). Cells (5000 cells/cm^2) were seeded on poly(L-lysine) coated coverslips for immunostaining, and the rest of the cells were transferred into T75 tissue culture flasks and incubated in the standard medium (3:1-DMEM:HAM F12 supplemented with 10% FCS and penicillin−streptomycin). At subconfluency, cells were passaged until passage 6 or they were frozen at lower passage numbers for future use. In freezing the cells with 10% DMSO, the standard medium was used.

2.5. Characterization of Isolated Cells. VSMCs at passages 4, 5, and 6 were immunostained to show that the cells did not dedifferentiate during cell culture and passaging. Cells were seeded on the coated coverslips and stained for α-smooth muscle actin (Sigma Chem. Co., U.S.A.) using Alexa 488 (Sigma Chem. Co., U.S.A.) as the secondary antibody to show the cells with VSMC phenotype and with DAPI (Sigma Chem. Co., U.S.A.) to show all the cell nuclei regardless of phenotype. After fixing the cells with paraformaldehyde (4%, Sigma Chem. Co., U.S.A.) for 30 min at room temperature, cells were permeabilized with Triton X-100 (Sigma Chem. Co., U.S.A.; 1%) for 5 min and washed three times with PBS. Then they were incubated in blocking solution (0.5% BSA, 0.1% Tween 20, 0.1% FCS, 0.1% sodium azide in PBS) for 30 min at room temperature and in primary antibody solution (anti-α-smooth muscle actin diluted in blocking solution to achieve a concentration of 10 μg/mL for 2 h at 37 °C). After washing three times with PBS, cells were incubated 1 h in the secondary antibody solution (Alexa 488 diluted 1:400 in blocking solution), which also contained DAPI (1:5000 diluted) at 37 °C. After a final three times with PBS, coverslips were placed on them, and cells were examined with a fluorescence microscope (Olympus IX70, Japan).

2.6. Proliferation of VSMC on Collagen Films. Collagen films were sterilized in EtOH (70%, 2 h) and washed with PBS. VSMCs were seeded at a density of 5000 cells/film, and the films were placed into tissue culture wells after placing a Teflon sheet at the bottom of the well to prevent the cells from migrating to the bottom of the wells and proliferating there. Tissue culture polystyrene (TCPS) was used as control. On days 1, 7, 14, and 21, Alamar Blue assay was performed to assess cell number on the films ($n = 3$). Briefly, cells were incubated in 10% Alamar Blue (BD Biosciences, U.S.A.) in colorless DMEM (Gibco, U.S.A.) for 1 h, and optical density was measured at 570 and 595 nm with a kinetic microplate reader (Maxline Vmax, Molecular Devices, U.S.A.). From these optical density values, % reduction was calculated and converted to cell numbers by using a calibration curve.

2.7. Microscopic Examination of VSMCs on Collagen Films. On days 1 and 21, cells on the films were fixed with 4% paraformaldehyde and immunostaining was carried out as before. Also on day 14, cells on the films were cross-linked with glutaraldehyde (2.5% in cacodylate buffer 0.1 M, pH 7.4) for 2 h at room temperature and examined with SEM (Quanta 400F Field Emission SEM, FEI Company, U.S.A.) after coating with gold under vacuum.

2.8. Tensile Testing of VSMCs on Collagen Films. Test samples were patterned (650 and 332.5 nm), and unpatterned films that were seeded with VSMCs. They were tested on days 45 and 75 after seeding. The control was pristine unseeded wet films (day 0). The time points were chosen to allow the cells to secrete their own ECM and also to give time for the collagen scaffold to degrade. All test groups had 6 samples per time point ($n = 6$). Patterned films (500 nm) were not included in the mechanical test groups; only two extreme dimensions at hand were examined to see the effect of guidance on mechanical properties since all three patterns were shown to guide the cells. None of the tested samples was fixed. The test samples were about 10 × 4 mm rectangles. Samples were secured with special clamps designed for testing such small specimens with the patterns along the tension direction. Testing was performed at room temperature (21 °C) in wet state with an Instron 3366 (50 N load cell, Instron Engineering Corporation, U.S.A.). The specimens were subjected to uniaxial tension with an elongation rate of 0.4 mm/min (corresponds to a strain rate of 10%/min). Testing continued until failure.

3. Results and Discussion

3.1. Characterization of Templates and Films. The silicon templates with three different nanopattern dimensions were characterized with AFM (Figure 1a−c). The reason for using nanochannels with three different channel dimensions was to examine whether the cells can orient themselves with the nanolevel topographical features and the range was dictated by the systems capability. Smaller features would have been tested if possible.

The patterns on one of the collagen films (650 nm) were examined with AFM to show the quality of the pattern transfer (Figure 1d). The resolution of the patterns on the silicon templates and the collagen film were found to be satisfactory. Due to the difficulty of examining the nanopatterned collagen surfaces with AFM, only the AFM of the film with the largest pattern is presented in the Figure 1. The pattern on the collagen film was more shallow (200 instead of 300 nm) and more irregular than that on the silicon wafer (Figure 1c), but was still satisfactory as was observed in the in vitro tests. The other films were examined with SEM and the pattern fidelity was verified (data not shown).

3.2. Characterization of VSMC. Isolated VSMCs were stained for α-smooth muscle actin and cell nuclei through passages 4 to 6 to study the purity of the culture and the extent of dedifferentiation during cell culture and passaging. Figure 2 shows that the cells in all three passages were stained with both anti-α-smooth muscle actin and DAPI. α-Smooth muscle actin is a marker for VSMC phenotype and can be used for distinguishing fibroblasts from smooth muscle cells. There were no cells stained only with DAPI; this would have indicated impurities from cell isolation or dedifferentiated cells. As a result, it was shown that the cells maintained their VSMC character through passage 6.

3.3. VSMC Proliferation on Collagen Films. Alamar Blue assay performed on days 1, 7, 14, and 21 on VSMC seeded samples. Results showed that all the collagen films supported cell growth and the cell adhesion was higher when the pattern dimension was smaller, as the day 1 results imply (Figure 3). Meanwhile, unpatterned film and TCPS showed lower cell adhesion. Although initially the number of cells attached on the nanopatterned films was higher than the TCPS control, the difference in the cell numbers gradually decreased until day 21, when there was no appreciable difference. This leveling off is probably due to overall higher surface area of the TCPS (2.27 cm^2) compared to collagen films (1 cm^2), which allowed the cells on TCPS to proliferate in higher numbers before they were contact inhibited because of confluency. Still, throughout the whole duration, the highest number of cells was always found on the nanopatterned film with the smallest pattern dimension

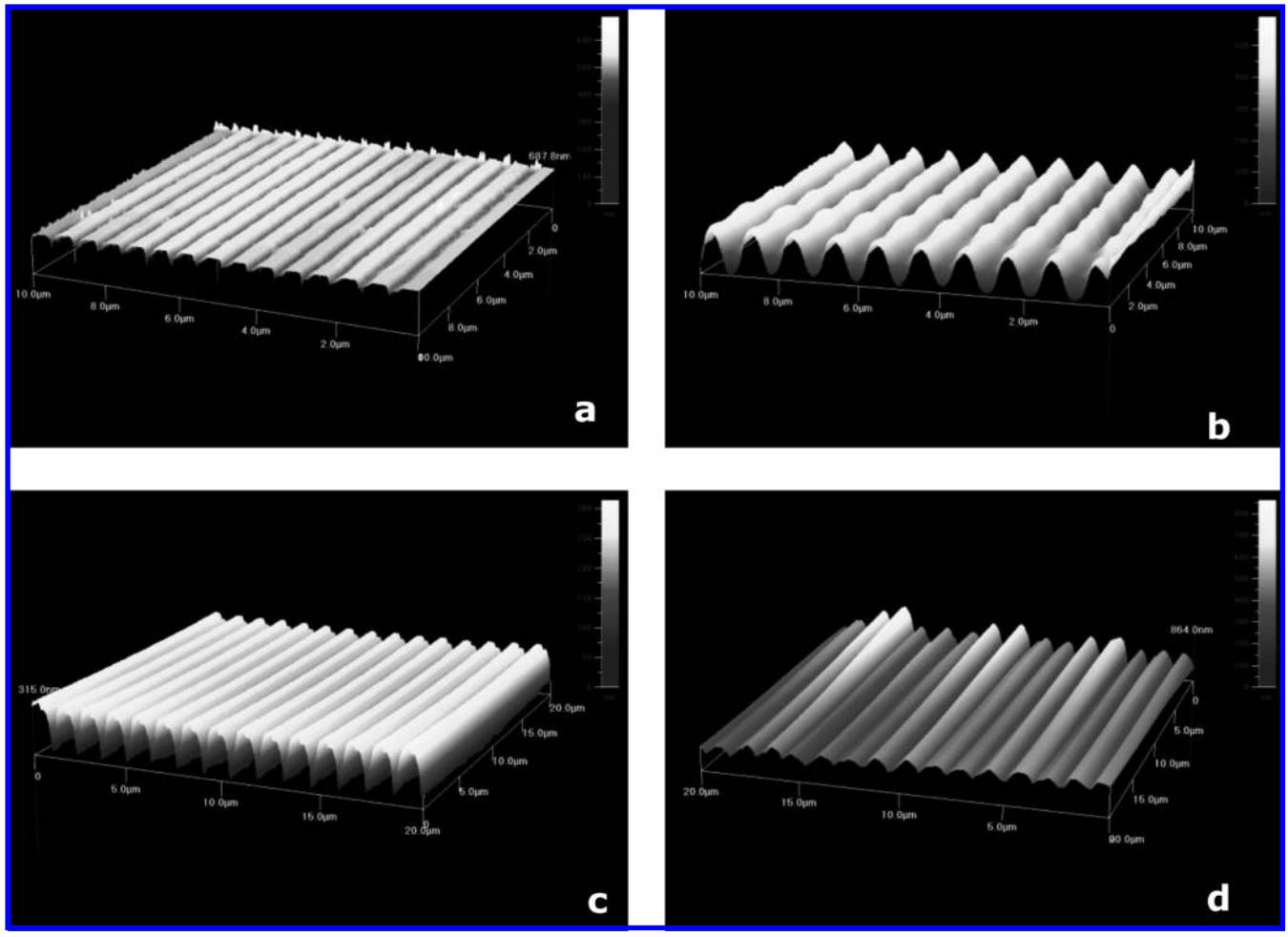

Figure 1. AFM images of silicon templates and collagen film: (a) 332.5 nm silicon template, (b) 500 nm silicon template, (c) 650 nm silicon template, and (d) 650 nm nanopatterned collagen film.

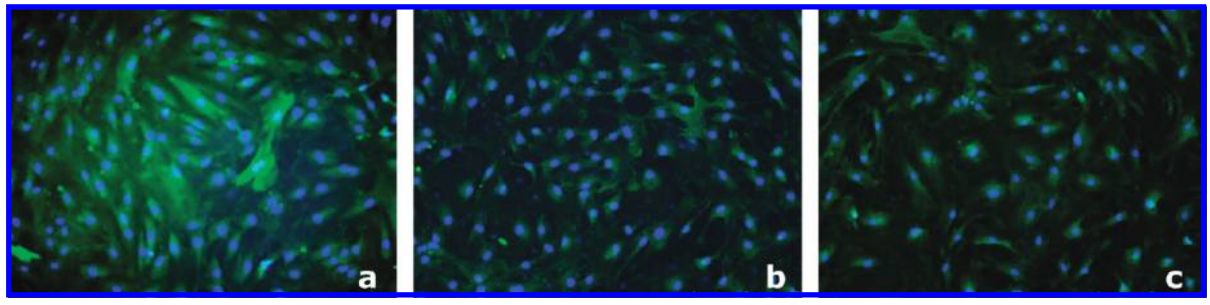

Figure 2. Fluorescence micrographs of VSMCs stained with anti-α-smooth muscle actin (green) and DAPI (blue): (a) passage 4, (b) passage 5, (c) passage 6 (×100).

(332.5 nm). Vascular smooth muscle cells were previously shown to proliferate properly on collagen membranes without any topographical modifications.[48] On the other hand, when compared to synthetic polymeric scaffolds, VSMCs on nanopatterned collagen films proliferated twice as much as the human coronary artery smooth muscle cells on the poly(L-lactid-*co*-ε-caprolactone) nanofibrous electrospun scaffolds, which had similar nanoscale guidance (500 nm diameter fibers).[36]

3.4. VSMC Orientation on Collagen Films. On day 14, VSMCs on the nanopatterned and unpatterned films were fixed and examined with SEM to assess cell orientation (Figure 4). The images on the 2 nd column of Figure 4 show the film surfaces near the cells at a higher magnification to show the presence of the nanopatterns (Figure 4b, d, f, and h). It is not possible to see both the alignment of the cells and the

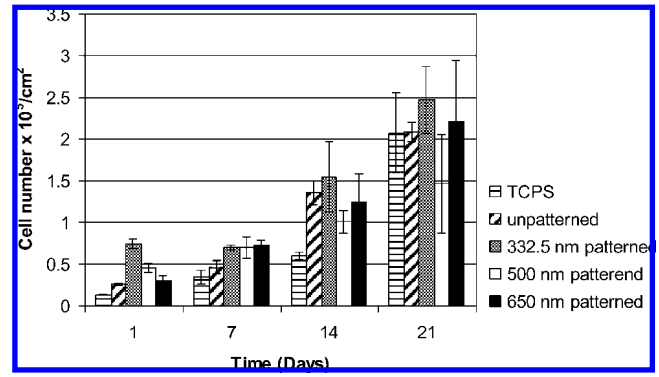

Figure 3. Cell proliferation was determined on collagen films and TCPS with Alamar Blue assay for 21 days ($n = 3$).

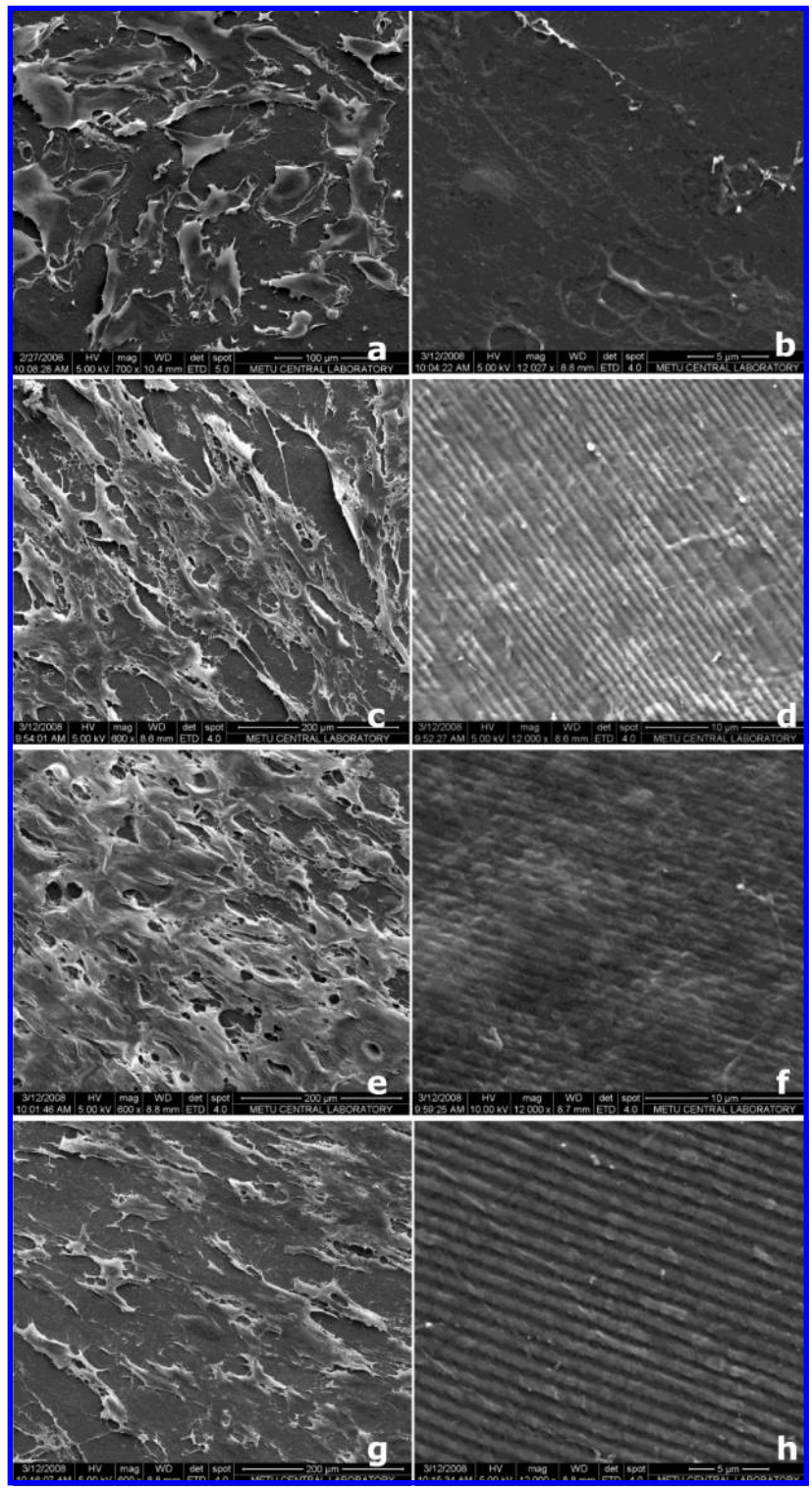

Figure 4. SEM micrographs of VSMCs on day 14: (a) unpatterned film (×700), (b) unpatterned film, region of the sample not occupied by the cells (×12000), (c) 332.5 nm patterned film (×600), (d) 332.5 nm patterned film, region of the sample not occupied by the cells (×12000), (e) 500 nm patterned film (×600), (f) 500 nm patterned film, region of the sample not occupied by the cells (×12000), (g) 650 nm patterned film (×600), and (h) 650 nm patterned, film region of the sample not occupied by the cells (×12000).

nanopatterns in a single micrograph because the patterns are in nanometer range, while the cells are in the micron range. Cell alignment could be seen on all three types of the nanopatterned films, whereas cells were randomly oriented on the unpatterned films. This proves that patterns as small as 332.5 nm can effectively align cells that are at least 10-fold larger. Similar results were previously reported for bone marrow derived mesenchymal stem cells, where the cell alignment was achived by using nanopatterns of 200 nm wide channels on polymethylmethacrylate (PMMA).[49] So, unlike micropatterns where physical restrictions larger than the cells lead to aligning, on the nanochannels molecular level interactions are the aligning factors. Alignment of vascular smooth muscle cells by using micron-range surface features on collagen membranes was previously shown. Human umbilical artery smooth muscle cells were oriented by using surfaces with 33, 13, and 7 μm wide

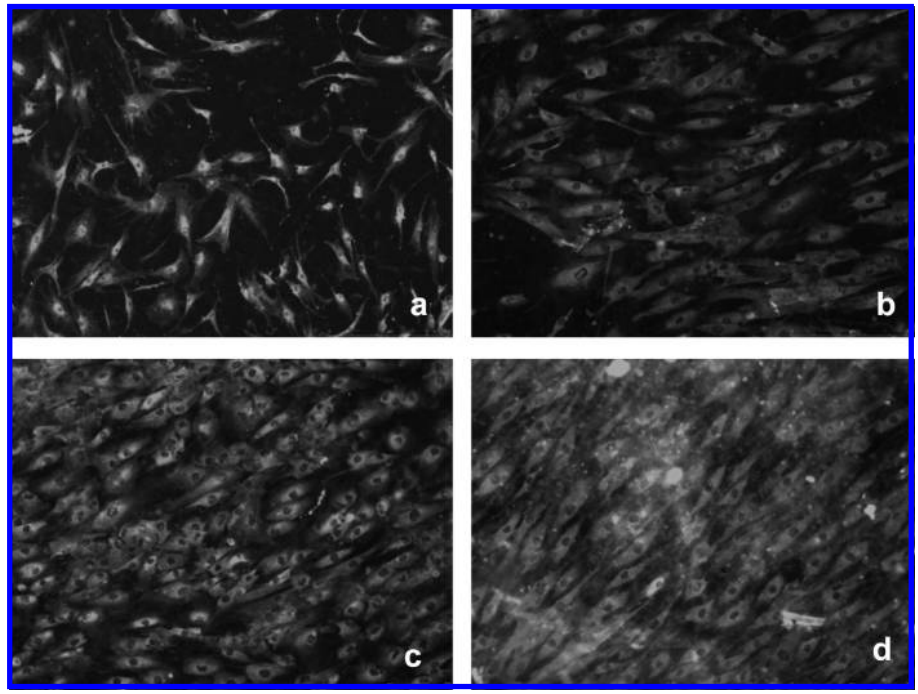

Figure 5. Anti-α-smooth muscle actin staining of VSMC on day 1: (a) unpatterned, (b) 332.5 nm, (c) 500 nm, and (d) 650 nm (×100).

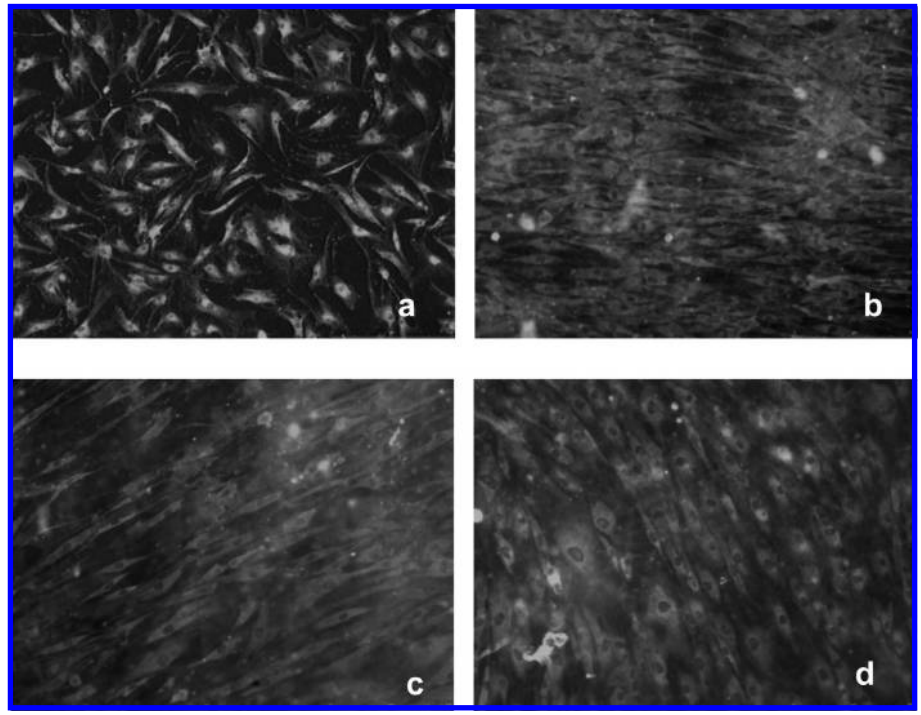

Figure 6. Anti-α-smooth muscle actin staining of VSMC on day 21: (a) unpatterned, (b) 332.5 nm, (c) 500 nm, and (d) 650 nm (×100).

channels.[50] Alignment on synthetic membranes with 40, 80, 120, or 160 μm channels was also achieved; orientation decreased with increased channel width.[51] Alignment on nanoscale topography was shown on synthetic polymeric fibers with 500 nm diameter.[36] As far as we know, the present study is the first that shows alignment of vascular smooth muscle cells on nanoscale patterned collagen membrane.

The second SEM in each row showed a region of the film not yet covered with cells and clearly reveal good quality patterns maintained after 2 weeks. It can be concluded that collagen nanopatterns are effective in cell guidance and nanopatterns are quite stable in the growth medium under cell culture conditions for at least 14 days. This stability is specifically a result of cross-linking.

Cell orientation was also confirmed by staining VSMCs on collagen films with anti-α-smooth muscle actin on days 1 (Figure 5) and 21 (Figure 6). Figures show the alignment of cell cytoskeleton by the nanopatterns since the marker used stains the cytoskeletal elements. The figures also show that the cell phenotype was maintained through out the experiment.

3.5. Mechanical Testing. In the literature there are studies reporting the mechanical adequacy of scaffolds designed for vascular tissue engineering purposes. Yang et al. (2005) tested mechanical properties of biphasic scaffolds that were fabricated

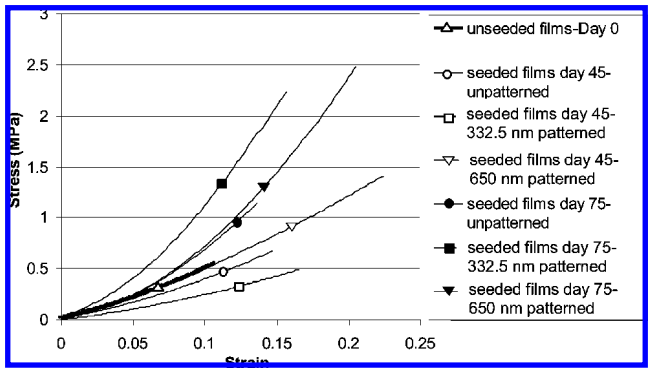

Figure 7. Stress−strain graph of average curves of unseeded and VSMC seeded nanopatterned and unpatterned collagen films after 45 and 75 days of incubation ($n = 6$).

Table 1. UTS and Young's Modulus of the Seeded and Unseeded Collagen Films ($n = 6$)

specimen type	UTS (MPa)	Young's modulus (MPa)
unseeded film, day 0	0.55 ± 011	4.05 ± 0.73
seeded film, day 45, unpatterned	0.43 ± 0.23	3.16 ± 1.65
seeded film, day 45, 332.5 nm	0.46 ± 0.12	2.59 ± 0.12
seeded film, day 45, 650 nm	0.97 ± 0.55	4.10 ± 3.36
seeded film, day 75, unpatterned	0.66 ± 0.35	4.12 ± 1.30
seeded film, day 75, 332.5 nm	1.20 ± 0.46	6.60 ± 1.79
seeded film, day 75, 650 nm	1.63 ± 0.46	4.19 ± 1.52

from poly(diolcitrate) and found them to be similar to native vessels.[52] The scaffold's Young's modulus and UTS values were both around 2 MPa, close to those of our VSMC seeded nanopatterned collagen films used in this study. In a recent work, Thomas et al. (2007) reported their electrospun polyglyconate tubular scaffolds as mechanically suitable for vascular tissue engineering which had UTS values around 2 MPa with a higher Young's modulus of 9 MPa, which is about three times higher and, therefore, stiffer than the natural veins.[21]

Tensile test results of the unseeded and cell seeded films incubated for 45 and 75 days are presented in Figure 7, which compares stress−strain curves, and Table 1 shows the UTS and Young's modulus values calculated from this graph. UTS of cell-free, pristine collagen film was 0.55 ± 0.11 MPa. This value is consistent with the literature value which is around 0.7 MPa for EDC/NHS cross-linked collagen.[53] Upon cell seeding and incubation in the culture medium for 45 days the UTS decreases from 0.55 to 0.46 MPa for the 332.5 nm patterned film. However, after 75 days, the UTS is measured as 1.2 MPa, indicating a substantial gain in the strength due to ECM secretion by the VSMCs (Table 1). Also, by day 75, there was a significant difference between the UTS of unpatterned and nanopatterned films (0.66 ± 0.35 MPa vs 1.20 ± 0.46 for 332.5 nm and 1.63 ± 0.46 for 650 nm), suggesting that cell alignment and resultant ECM organization along with the cells increased the strength of the collagen films. This difference was particularly distinct when the results of 650 nm patterned samples for day 75 were compared with unpatterned films. In this case, UTS value was 1.63 ± 0.46 MPa when cells were seeded on nanopatterned films, whereas the value for the unpatterned film at same time point was nearly one-third; 0.66 ± 0.35 MPa. Support for this is found in the literature, where it was previously shown that aligned MC3T3 cells produce aligned collagen type I as ECM.[54] Consistent results were reported when smooth muscle cell-seeded collagen based scaffolds were mechanically stimulated using cyclic distension.[40] In the first two weeks of incubation, there was no effect of cell presence or cyclic distension, but after five weeks, the UTS had increased by 1.6-fold to around 0.4 MPa, which was still not high enough for vascular tissue engineering applications. The UTS values of cell free, pristine, or cell seeded unpatterned films in the current study were lower than the average UTS of a straight portion of an artery (around 1.3 MPa).[55] Thus, aligning cells on nanopatterned films improved the mechanical strength to the level of the UTS of fresh carotid arteries (1.76−2.64 MPa).[19]

There was no significant difference between the Young's modulus' of different groups; all the test groups had values around 4 MPa (Table 1), and with time, a slight increase was observed in all the sample types, indicating some stiffening. The value of 4 MPa is somewhat higher than the Young's modulus of veins (3.11 ± 0.65 MPa) and is significantly higher than that of the arteries (1.54 ± 0.33 MPa).[56]

Similar to our case, Grenier and co-workers showed mechanical stimuli applied by static stretching aligned fibroblasts, and this resulted in improved mechanical properties of cell sheets by about 7-fold when compared to randomly oriented cell sheets.[41] A recent study comparing orientation of VSMCs by mechanical stimuli and by topographical cues showed that cells tend to orient themselves in the direction of the topographical cues (microgrooves) rather than in the direction of the mechanical stimulus. However, orientation with mechanical stimuli was enhanced in the presence of topographical cues which implies that microtopographical cues modulate the orientation response of VSMCs to mechanical stimuli.[57] Wang et al. also observed the same with fibroblasts.[58] Although the present study uses nanochannels instead of microchannels, effectiveness of topographical cues in cell orientation is evident.

The nanopatterned scaffolds designed in this study, when seeded with VSMCs that align on them, showed both UTS and Young's modulus values quite close to that of the native vessels and is therefore appropriate for further testing. Coculture of VSMCs with endothelial cells on the tubular forms of these nanopatterned collagen scaffolds are currently being conducted to study the potential to serve as small diameter vascular grafts.

4. Conclusion

Cell culture studies with VSMCs showed that nanopatterned collagen films are good substrates for cell attachment and cell proliferation. The cells retained their phenotype and were aligned by the nanopatterns on all 3 nanopattern dimensions. It has been suggested that aligning VSMCs in the same way as they are in the natural tissue might be used to improve the mechanical properties. This study showed that this indeed is true, although alignment did not affect cell proliferation at the end of day 21, it increased the mechanical properties of the scaffolds. With the current approach, the good biological properties of collagen could be combined with the adequate mechanical properties obtained through cell guidance to create scaffolds for use in vascular tissue engineering.

Acknowledgment. We acknowledge Prof. Atilla Aydinli and Askin Kocabas of Bilkent University (Ankara, Turkey) for providing the patterned templates and Prof. Yaman Zorlutuna of Baylndlr Hospital (Ankara, Turkey) for providing the biological specimens. We also gratefully acknowledge the support of State Planning Organization of Turkey (DPT) through the Project BAP 01.08.DPT.2003K120920-20, METU through project BAP2007-01-08-02, and The Scientific and Technical Research Council of Turkey (TUBITAK) grant to P.Z. through METUNANOBIOMAT.

References and Notes

(1) National Center for Chronic Disease Prevention and Health Promotion, Chronic Disease Overview, United States Government, 2008. Available from URL http://www.cdc.gov/nccdphp/overview_text.htm.
(2) Ferrari, E. R.; von Segesser, L. K. *Curr. Opin. Cardiol.* **2006**, *21*, 584–588.
(3) Kannan, R. Y.; Salacinski, H. J.; Butler, P. E.; Hamilton, G.; Seifalian, A. M. *J. Biomed. Mater. Res., Part B* **2005**, *74*, 570–581.
(4) Zdrahala, R. J. *J. Biomater. Appl.* **1996**, *10*, 309–329.
(5) Zhang, Z.; Marois, Y.; Guidoin, R. G.; Bull, P.; Marois, M.; How, T.; Laroche, G.; King, M. W. *Biomaterials* **1997**, *18*, 113–124.
(6) Henze, U.; Kaufmann, M.; Klein, B.; Handt, S.; Klosterhalfen, B. *Biomed. Pharmacother.* **1996**, *50*, 388.
(7) Rhee, R. Y.; Gloviezki, P.; Camria, R. A.; Miller, V. M. *Cardiovasc. Surg.* **1996**, *4*, 746–752.
(8) Thompson, M. M.; Budd, J. S.; Bell, P. R. F. *Surgery* **1994**, *100*, 392–399.
(9) Sarkar, S. J.; Sales, K. M.; Hamilton, G.; Seifalian, A. M. *J. Biomed. Mater. Res., Part B* **2007**, *82*, 100–108.
(10) Hellener, G.; Cohn, D.; Marom, G. *Biomaterials* **1994**, *15*, 1115–1121.
(11) Sandusky, G. E.; Lantz, G. C.; Badylak, S. F. *J. Surg. Res.* **1995**, *58*, 415–422.
(12) Marois, Y.; Paris, E.; Zhang, Z.; Doillon, C. J.; King, M. W.; Guidoin, R. G. *Biomaterials* **1996**, *17*, 1289–1300.
(13) Ratcliffe, A. *Matrix Biol.* **2000**, *19*, 353–357.
(14) Boccafoschi, F.; Rajan, N.; Habermehl, J.; Mantovani, D. *Macromol. Biosci.* **2007**, *25*, 719–726.
(15) Greenwald, S. E.; Berry, C. L. *J. Pathol.* **2000**, *190*, 292–299.
(16) Salacinski, H. J.; Goldner, S.; Giudiceandrea, A.; Hamilton, G.; Seifalian, A. M. *J. Biomater. Appl.* **2001**, *15*, 241–276.
(17) Takei, T.; Yamaguchi, S.; Sakai, S.; Ijima, H.; Kawakami, K. *J. Biosci. Bioeng.* **2007**, *104*, 435–438.
(18) Berglund, J. D.; Mohseni, M. M.; Nerem, R. M.; Sambanis, A. *Biomaterials* **2003**, *24*, 1241–1254.
(19) Kurane, A.; Simionescu, D. T.; Vyavahare, N. R. *Biomaterials* **2007**, *28*, 2830–2838.
(20) Chong, M. S. K.; Lee, C. N.; Teoh, S. H. *Mater. Sci. Eng., C* **2007**, *27*, 309–312.
(21) Thomas, V.; Zhang, X.; Catledge, S. A.; Vohra, Y. K. *Biomed. Mater.* **2007**, *2*, 224–232.
(22) Rohman, G.; Pettit, J. J.; Isaure, F.; Cameron, N. R.; Southgate, J. *Biomaterials* **2007**, *28*, 2264–2274.
(23) Zhang, X.; Baughman, C. B.; Kaplan, D. L. *Biomaterials* **2008**, *29*, 2217–2227.
(24) L'Heureux, N.; Paquet, S.; Lacoe, R.; Germain, L.; Auger, F. A. *FASEB J.* **1998**, *12*, 47–56.
(25) Mitchell, S. L.; Niklason, L. E. *Cardiovasc. Pathol.* **2003**, *12*, 59–64.
(26) Boccafoschi, F.; Habermehl, J.; Vesentini, S.; Mantovani, D. *Biomaterials* **2005**, *26*, 7410–7417.
(27) Tranquillo, R. T.; Girton, T. S.; Bromberek, B. A.; Triebes, T. G.; Mooradian, D. L. *Biomaterials* **1996**, *17*, 349–353.
(28) Dalton, B. A.; Evans, M. D. M.; McFarland, G. A.; Steele, J. G. *J. Biomed. Mater. Res.* **1999**, *45*, 384–394.
(29) Pins, G. D.; Toner, M.; Morgan, J. D. *FASEB J.* **2000**, *14*, 593–602.
(30) Kenar, H.; Kose, G. T.; Hasirci, V. *Biomaterials* **2006**, *27*, 885–895.
(31) Zorlutuna, P.; Tezcaner, A.; Kiyat, I.; Aydinli, A.; Hasirci, V. *J. Biomed. Mater. Res., Part A* **2006**, *79*, 104–113.
(32) Walboomers, X. F.; Jansen, J. A. *Odontology* **2001**, *89*, 2–11.
(33) Shen, J. Y.; Chan-Park, M. B.; He, B.; Zhu, A. P.; Zhu, X.; Beuerman, R. W.; Yang, E. B.; Chen, W.; Chan, V. *Tissue Eng.* **2006**, *12*, 2229–2240.
(34) Craighead, H. G.; James, C. D.; Turner, A. M. P. *Curr. Opin. Solid State Mater. Sci.* **2001**, *5*, 177–184.
(35) Diehl, K. A.; Foley, J. D.; Nealey, P. F.; Murphy, C. J. *J. Biomed. Mater. Res., Part A* **2005**, *75*, 603–611.
(36) Xu, C. Y.; Inai, R.; Kotaki, M.; Ramakrishna, S. *Biomaterials* **2004**, *25*, 877–886.
(37) Feng, Z.; Yamato, M.; Akutsu, T.; Nakamura, T.; Okano, T.; Umezu, M. *Artif. Organs* **2003**, *27*, 84–91.
(38) Berglund, J. D.; Mohseni, M. M.; Nerem, R. M.; Sambanis, A. *Biomaterials* **2003**, *24*, 1241–54.
(39) Gildner, C. D.; Lerner, A. L.; Hocking, D. C. *Am. J. Physiol.* **2004**, *287*, 46–53.
(40) Isenberg, B. C.; Tranquillo, R. T. *Ann. Biomed. Eng.* **2003**, *31*, 937–49.
(41) Grenier, G.; Rémy-Zolghadri, M.; Larouche, D.; Gauvin, R.; Baker, K.; Bergeron, F.; Dupuis, D.; Langelier, E.; Rancourt, D.; Auger, F. A.; Germain, L. *Tissue Eng.* **2005**, *11*, 90–100.
(42) Zorlutuna, P.; Builles, N.; Damour, O.; Elsheikh, A.; Hasirci, V. *Biomaterials* **2007**, *28*, 3489–3496.
(43) Vrana, N. E.; Elsheikh, A.; Builles, N.; Damour, O.; Hasirci, V. *Biomaterials* **2007**, *28*, 4303–4310.
(44) Farsak, B.; Tokmakoglu, H.; Kandemir, O.; Gunaydin, S.; Aydin, H.; Yorgancioglu, C.; Suzer, K.; Zorlutuna, Y. *J. Cardiovasc. Surg.* **2003**, *18*, 524–531.
(45) Zorlutuna, P.; Hasirci, N.; Hasirci, V. *J. Tissue Eng. Regener. Med.* **2008**, *2*, 373–377.
(46) Staros, J. V.; Wright, R. W.; Swingle, D. M. *Anal. Biochem.* **1986**, *156*, 220–222.
(47) Grenier, G.; Remy-Zolghadri, M.; Guignard, R.; Bergeron, F.; Labbe, R.; Auger, F. A.; Germain, L. *In Vitro Cell. Dev. Biol.: Anim.* **2003**, *39*, 131–139.
(48) Elliott, J. T.; Woodward, J. T.; Langenbach, K. J.; Tona, A.; Jones, P. L.; Plant, A. L. *Matrix Biol.* **2005**, *24*, 489–502.
(49) Engel, E.; Michiardi, A.; Navarro, M.; Lacroix, D.; Planell, J. A. *Trends Biotechnol.* **2008**, *26*, 39–47.
(50) Vernon, R. B.; Gooden, M. D.; Lara, S. L.; Wight, T. N. *Biomaterials* **2005**, *26*, 3131–3140.
(51) Shen, J. Y.; Chan-Park, M. B.; Feng, Z. Q.; Chan, V.; Feng, Z. W. *J. Biomed. Mater. Res., Part B* **2006**, *77*, 423–30.
(52) Yang, J.; Motlagh, D.; Webb, A. R.; Ameer, G. A. *Tissue Eng.* **2005**, *11*, 1876–1886.
(53) Faraj, K. A.; van Kuppevelt, T. H.; Daamen, W. F. *Tissue Eng.* **2007**, *13*, 2387–2394.
(54) Wang, J. H. C.; Jia, F.; Gilbert, T. W.; Woo, S. L. Y. *J. Biomech.* **2003**, *36*, 97–102.
(55) Yamada, H. In *Strength of Biological Materials*; Williams & Wilkins: Baltimore, 1970; pp 114−130.
(56) Pukacki, F.; Jankowski, T.; Gabriel, M.; Oszkinis, G.; Krasinski, Z.; Zapalski, S. *Eur. J. Vasc. Endovasc. Surg.* **2000**, *20*, 21–24.
(57) Houtchens, G. R.; Foster, M. D.; Desai, T. A.; Morgan, E. F.; Wong, J. Y. *J. Biomech.* **2008**, *41*, 762–9.
(58) Wang, J. H.; Yang, G.; Li, Z. *Ann. Biomed. Eng.* **2005**, *33*, 337–42.

BM801307Y

Available online at www.sciencedirect.com
ScienceDirect
Acta Biomaterialia 5 (2009) 2451–2459
Acta BIOMATERIALIA
www.elsevier.com/locate/actabiomat

Influence of nanopatterns on endothelial cell adhesion: Enhanced cell retention under shear stress

P. Zorlutuna [a,*], Z. Rong [b], P. Vadgama [b], V. Hasirci [a,c]

[a] METU, BIOMAT, Department of Biological Sciences, Biotechnology Research Unit, Ankara, Turkey
[b] IRC in Biomedical Materials, Queen Mary University of London, Mile End Road, London E1 4NS, UK
[c] METU, BIOMAT, Department of Biomedical Engineering, Ankara, Turkey

Received 4 December 2008; received in revised form 16 February 2009; accepted 24 March 2009
Available online 31 March 2009

Abstract

In this study, nanopatterned crosslinked films of collagen Type I were seeded with human microvascular endothelial cells and tested for their suitability for vascular tissue engineering. Since the films will be rolled into tubes with concentric layers of collagen, nutrient transfer through the collagen films is quite crucial. Molecular diffusivity through the collagen films, cell viability, cell proliferation and cell retention following shear stress were studied. Cells were seeded onto linearly nanogrooved films (groove widths of 332.5, 500 and 650 nm), with the grooves aligned in the direction of flow. The nanopatterns did not affect cell proliferation or initial cell alignment; however, they significantly affected cell retention under fluid flow. While cell retention on unpatterned films was $35 \pm 10\%$, it was $75 \pm 4\%$ on 332.5 nm patterned films and even higher, $91 \pm 5\%$, on 650 nm patterned films. The films were found to have diffusion coefficients of *ca.* 10^{-6} cm^2 s^{-1} for O_2 and 4-acetaminophenol, which is comparable to that observed in natural tissues. This constitutes another positive asset of these films for consideration as a scaffold material for vascular tissue engineering.

Keywords: Shear stress; HMEC; Collagen; Nanopattern; Vascular tissue engineering

1. Introduction

Cardiovascular diseases are the leading cause of death in developed countries, and the most common cause is atherosclerosis, a chronic pathological process associated with a raised focal plaque within large vessel intima. Typically, this plaque consists of a lipid core surrounded by an extracellular matrix (ECM) and smooth muscle cells, and is covered by a fibrous cap [1]. In time, the lesion increases in size, restricts blood flow and eventually blocks the vessel. The solution offered at this stage is generally the removal of the diseased vessel segment and implantation of a homograft or a synthetic graft. Homografts are obviously the best choice, but their availability is limited and many factors, including multiple bypass surgery, repeat procedures and age of the patient, decrease their suitability [2]. An alternative to homografts are synthetic grafts [3–6]. Synthetic grafts generally have a lower level of patency because practically all materials are somewhat thrombogenic and clogging of implanted grafts is a common problem [7]. To solve this problem, many different approaches, including a variety of anti-thrombogenic coatings [6,8] and endothelial cell seeding [9,10], have been tried. These treatments have improved the performance of synthetic grafts to a certain extent but they could only be used to replace larger arteries (>6 mm inner diameter). A functional, tissue engineered vessel would be the ultimate solution to vascular reconstruction of smaller diameter vessels [11].

Patency of an engineered vascular graft depends on several parameters. Most importantly, it should have a continuous layer of endothelium to prevent thrombosis and consequent clogging [12]. There are many studies that show that endothelial cells adhere to and proliferate well on many different materials, including polyesters [13,14], and

* Corresponding author. Tel.: +90 312 2105168; fax: +90 312 2101452.
E-mail address: pinarzorlutuna@yahoo.com (P. Zorlutuna).

1742-7061/$ - see front matter © 2009 Acta Materialia Inc. Published by Elsevier Ltd. All rights reserved.
doi:10.1016/j.actbio.2009.03.027

natural polymers like silk fibroin [15] and collagen [16]. However, a major concern is that similar cell behaviour is required under the hemodynamic conditions of the natural blood vessel [17]. More specifically, the endothelial cells need to be retained on a supporting scaffold during exposure to flow and the resultant physiological shear.

In an attempt to mimic a natural tissue environment and thereby to improve attachment and alignment, patterned surfaces have been used. There are studies showing that endothelial cells are aligned by micropatterns [16,18]; however, this is also reported to result in apoptosis due to cell anisotropy and resultant inadequate cell attachment to the surface [19,20]. Nanoscale topographies have also been tried, mainly to increase cell adhesion on synthetic surfaces. PLGA surfaces having nanoscale controlled roughness rather than patterns were tested for improved endothelial cell adhesion, but this resulted in lower cell adhesion than on unmodified planar surfaces [14]. On the other hand, nanoscale modification of alternative vascular graft materials, including polyurethane derivatives [21] and titanium [22], was also tried, and did succeed in increasing endothelial cell attachment and proliferation, apparently through increased surface area.

Another complication to obtaining a continuous layer of functional endothelial cells is biomaterial-induced toxicity. Kader and Yoder have recently shown that synthetic biomaterials cause endothelial cell death due to anoikis, a form of apoptosis caused by an inflammatory reaction due to an inappropriate interaction of cells with the surface [23]. They proposed that endothelial cells on synthetic biomaterials like polytetrafluoroethylene, polyethyleneteraphthalate, polyester and polyethylene produce increased amounts of superoxides and other reactive oxygen species which, in turn, induce a local inflammatory response and cell death. Collagen is a part of the natural ECM and has the required molecular motifs for proper cell attachment, making it a good candidate for a scaffold material [24]. When tested as a scaffold material for vascular tissue engineering, acid soluble type I collagen was found not to enhance blood coagulation, did not interfere with the viscoelasticity of the blood and did not induce excessive platelet adhesion or aggregation, and as such its suitability for vascular tissue engineering has been highlighted [25].

When a tissue-engineered vascular graft is designed, one of the requirements in addition to fluid and nutrient flow through the lumen is adequate graft permeability to oxygen, glucose and other metabolites. This is especially needed when an engineered vessel consists of a tubular scaffold with smooth muscle cells seeded on the periphery and endothelial cells seeded subluminally, where diffusion of nutrients through the scaffold for the endothelial cells would be a major issue. In previous studies, these collagen films were tested with vascular smooth muscle cells and developed into tubular form by crosslinking for vascular tissue engineering [26].

In this study collagen type I films nanopatterned with various dimensions were seeded with human microvascular endothelial cells (HMECs) and tested for vascular tissue engineering purposes. Small molecule diffusivity through the collagen films was measured with or without seeding with the endothelial cells. The molecules selected (oxygen and 4-acetaminophenol) were readily detectable electrochemically and their diffusion to a polarized electrode surface readily tracked [27]. Furthermore, cell viability, cell proliferation and cell adhesion strength during shear stress caused by medium laminar flow over the films was determined.

2. Materials and methods

2.1. Template preparation

Three different templates with nanochannels were created by X-ray interference lithography at the facilities of Bilkent University Physics Department (Ankara, Turkey). Briefly, first a photoresist (AZ 5214) was coated on a silicon wafer (500 nm thickness), exposed to a laser ($\lambda = 325$ nm) for 10 min and developed, then the patterns were transferred to silicon by using an epoxy replica. Subsequent poly(dimethylsiloxane) (PDMS) replicas of the modified silicon templates prepared by applying mixed PDMS and curing agent (in a 10:1 wt./wt. ratio; Sylgard 184 Elastomer Kit, Dow Corning, USA) and curing at 65 °C for 3 h for use in patterned collagen film preparation. The templates prepared had patterns of parallel channels with groove and ridge widths of 650 nm with 300 nm depth, 500 nm with 250 nm depth and 332.5 nm with 200 nm depth.

2.2. Collagen film preparation

Collagen films (1 cm^2) were prepared by solvent casting collagen solution on nanopatterned and unpatterned PDMS templates with overnight drying at room temperature (RT). Collagen type I was isolated from Sprague–Dawley rat tails and used at a concentration of 10 mg ml^{-1} solution (250 μl cm^{-2}, 0.5 M, in acetic acid). Films were stabilized by chemical crosslinking for 2 h at RT using 1-ethyl-3-[3-dimethylaminopropyl]carbodiimide hydrochloride (EDC, Pierce, USA) and *N*-hydroxysulfosuccinimide (NHS, Sigma Chemical Co., USA). The concentrations used were 170 mM EDC and 217 mM NHS in 50 mM NaH_2PO_4 solution (pH 5.5). After crosslinking, films were washed with 0.1 M Na_2HPO_4 (pH 9.1) for 1 h, with 1 M NaCl for 2 h and with 2 M NaCl for 1 day, each with a minimum of five solution changes [28]. Later, films were washed several times with distilled water and peeled off the surface with forceps after drying at RT. Films were examined after crosslinking using scanning electron microscopy (SEM) for pattern fidelity.

2.3. Cell culture studies

HMECs (CDC of USA, CDC Reference Number: E-036-91/0, passage 15) were cultured in MCDB 131 Medium (Gibco, USA) supplemented with 5% fetal calf serum (Gib-

co, USA), 200 mM L-glutamine (Sigma, USA) and 1% streptomycin–penicillin (Gibco, USA), and used for seeding the films at subconfluency. Collagen films were sterilized by incubating in EtOH (70%) for 2 h and washing with phosphate buffered saline (PBS, 10 mM, pH: 7.4). HMECs were seeded at three different seeding densities: 2×10^4, 5×10^4 and 1×10^5 cells per film; for each, tissue culture polystyrene (TCPS) was used as the control.

To check cell viability, 2×10^4 cell seeded samples were double stained at 24 h with calcein AM (Molecular Probes, USA) for live cells and ethidium homodimer-2 (Molecular Probes, USA) for dead cells.

At 48 h, cell numbers on films and TCPS controls were determined with Alamar Blue assay for three different seeding densities. Briefly, cells were incubated in 5 vol.% Alamar Blue (Biosource, USA) in complete medium for 4 h and fluorescence was measured at an excitation wavelength of 544 nm and emission wavelength of 590 nm. Also at 48 h, after dehydration in a graded series of EtOH, films with different seeding densities were examined with SEM after coating with carbon. To examine cell alignment on the nanopatterns, cells on the films, which were seeded with 2×10^4 cells, were fixed after 24 h with 4 vol.% formaldehyde and stained for cell nuclei with 4′-6-diamidino-2-phenylindole (DAPI; Sigma, USA).

2.4. Diffusivity of collagen films

The diffusivity of collagen films to oxygen and 4-acetaminophenol (Sigma, Dorset, UK) was measured in order to assess oxygenation and microsolute transport through the films. 4-Acetaminophenol (mol. wt. 151) was selected because it is similar in size to glucose (mol. wt. 180). Collagen films were placed over a 2 mm diameter platinum working electrode of an electrochemical cell (Rank Brothers Ltd, UK). Additionally, a platinum wire (MW-1032, Bioanalytical System Inc., UK) of 0.5 mm diameter and 75 mm length was used as the counter electrode and the reference electrode was Ag/AgCl (MF-2052, Bioanalytical System Inc., UK). A microAutolab potentiostat instrument (Eco Chemie, Netherlands) was used for the amperometric measurements.

Diffusion for a solute of concentration C through a film follows Fick's second law:

$$\frac{\partial C}{\partial t} = D\frac{\partial^2 C}{\partial x^2} \tag{1}$$

where D is the diffusion coefficient for the solute in the film and t is time. By solving Eq. (1) under the experimental condition of a time dependent sensor response to a step change in concentration, current response, I, is given by [27]:

$$I = \frac{2}{\sqrt{\pi T}} \exp\left(\frac{-1}{4T}\right) \quad \text{for } T \leqslant 0.237 \tag{2a}$$

$$I = 1 - 2\exp(-\pi^2 T) \quad \text{for } T \geqslant 0.237 \tag{2b}$$

where dimensionless time $T = Dt/L^2$ is used for convenience. Diffusion coefficients were calculated by a best-fit procedure, fitting the simulated amperometric current to experimental data.

Experimentally, for 4-acetaminophenol measurements, 5 ml of PBS (pH 7.4) was placed in the Rank cell and stirred with a magnetic stirrer. After application of a polarizing voltage of +0.65 V vs. Ag/AgCl, 4-acetaminophenol was injected into the buffer in the Rank cell to give a final concentration of 1 mM. Test groups for 4-acetaminophenol measurements (in triplicate, $n = 3$) included unseeded films, cell-seeded films, cell-seeded and fixed films, and unseeded and fixed films. Diffusivity of the collagen films to oxygen (mol. wt. 32) was also determined. Here, 2.5 ml of PBS (pH 7.4) was deoxygenated by bubbling argon gas, placed in the Rank cell and stirred. Then 2.5 ml fully oxygenated PBS was added at a pre-stabilized electrode after application of polarizing voltage. Test groups for oxygen included unseeded and unfixed films, unseeded and fixed films and cell-seeded and fixed films ($n = 3$). Cell fixation was done with formaldehyde, which could further crosslink collagen films. Unseeded and fixed films were included in both tests to demonstrate the effect of further crosslinking of the films during cell fixation and the effect of cell presence on the films.

2.5. Flow-shear studies

Flow-shear studies were performed by using a custom flow chamber and a pump (Watson Marlow Pumps, model 205U). Cells were seeded at a density of 5×10^4 cells per film onto 332.5 and 650 nm patterned films as well as unpatterned controls, and were subjected to flow-shear stress after an initial 48 h of incubation. Mean shear stress values on a flat section of an artery are reported to vary between 10 and 20 dynes cm^{-2} [29], so this was used as the guide in this study. Films were placed in a custom-made flow chamber and the flow rate was set to 0.72 ml min^{-1} of complete medium to exert a flow-shear stress of 12 dynes cm^{-2} on the film surface according to following equations:

$$V_m = \frac{Q}{A} \tag{3}$$

$$V = 2V_m\left[1 - \left(\frac{y}{a}\right)^2\right] \tag{4}$$

$$\tau_\omega = -\mu\left.\frac{\partial V}{\partial y}\right|_{y=a} = \mu 2V_m\left.\frac{2y}{a^2}\right|_{y=a} = \frac{4\mu V_m}{a} \tag{5}$$

$$Q = \frac{\tau_\omega A a}{4\mu} \tag{6}$$

where V_m the maximum velocity in the channel (mm s^{-1}), Q is the flow rate (ml min^{-1}), A is the cross-sectional area (mm^2), $2a$ is the depth of the channel (mm), y is displacement coordinate (depth), τ_ω is the flow-shear stress (dynes cm^{-2}) and μ is the viscosity (cp).

After 1 h of flow stress in an incubator at 37 °C and 5% CO_2, cells were fixed with 4 vol.% formaldehyde, permeabilized with Triton X-100 and stained with DAPI for microscopy ($n = 3$). The cell number on films exposed to shear as

well as the control films (seeded at the same time with the same cell density but not subjected to shear stress) were quantified by taking images with a fluorescence microscope (Leica Microsystems, Germany) at 100× magnification from six random areas (each area was calculated to be $\sim 2\ mm^2$) of the film and counting the stained cell nuclei with Image J (NIH).

2.6. Statistical analysis

Data from flow-shear experiments were analyzed for their statistical significance by values defined as $p < 0.05$ based on one-way analysis of variance followed by Tukey's test to determine the significance of any differences between groups ($p \leqslant 0.05$).

3. Results and discussion

3.1. Characterization of collagen films

The preservation of the nanopatterns after processing was essential for this study. SEM images showed that nanopatterns were transferred to collagen in high fidelity for all three nanopattern dimensions (Fig. 1). Since these micrographs were those of crosslinked samples, they also prove that crosslinking does not disrupt the patterns.

3.2. HMEC viability on collagen films

Cell viability was investigated qualitatively by staining with calcein AM (for live cells) and ethidium homodimer-2 (for dead cells) without any fixation. Fig. 2a shows the live cells on the control, TCPS. There was a similarly high number of live cells (Fig. 2b) and very few dead cells (Fig. 2c) on the collagen film, indicating the suitability of the collagen films for in vitro use.

3.3. HMEC proliferation on collagen films

Alamar Blue results showed that the numbers of cells on all the collagen films and the TCPS were similar, regardless of the nanopattern dimensions (Fig. 3). This suggests that, while processed collagen films were suitable for microvascular endothelial cell growth, the presence of the nanopatterns or their dimensions appeared to have no effect on cell proliferation or viability.

3.4. HMEC alignment on collagen films

At 24 h, the cells on the unpatterned and nanopatterned films, which had each been seeded with 2×10^4 cells, were fixed by using 4% formaldehyde and stained with DAPI

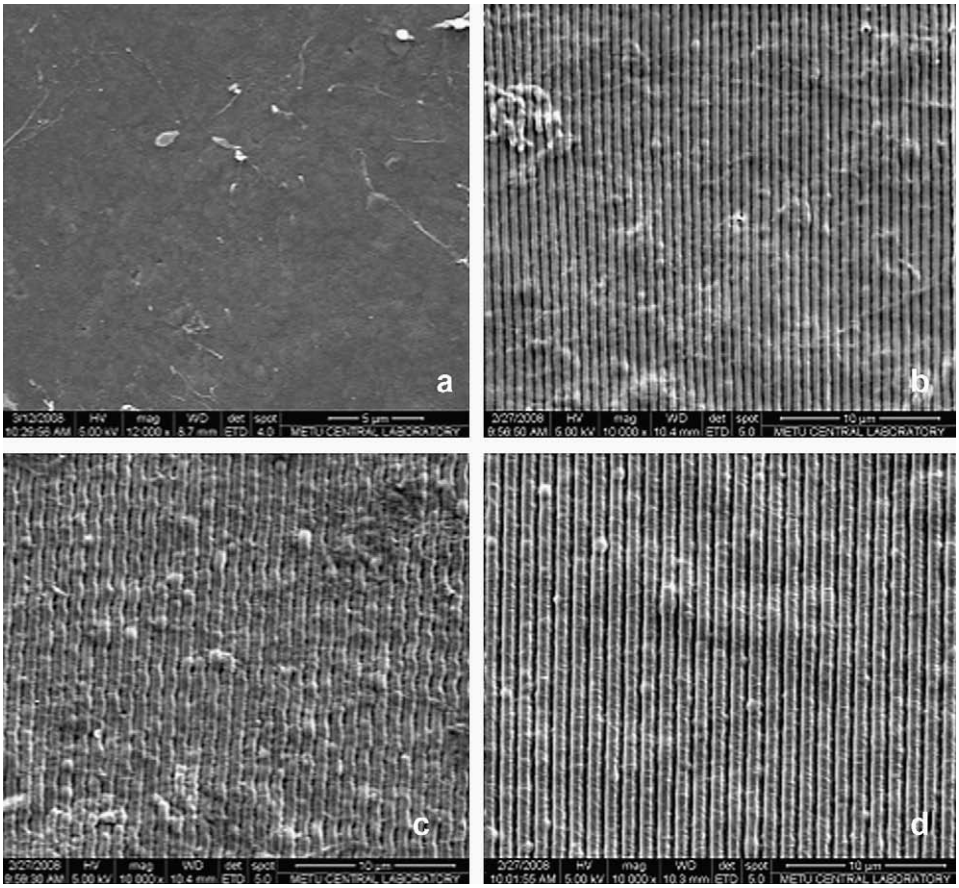

Fig. 1. SEM images of crosslinked collagen films prepared on PDMS replicas of original silicon wafers. (a) Unpatterned film (×12,000); (b) 332.5 nm patterned film (×10,000); (c) 500 nm patterned film (×10,000); (d) 650 nm patterned film (×10,000).

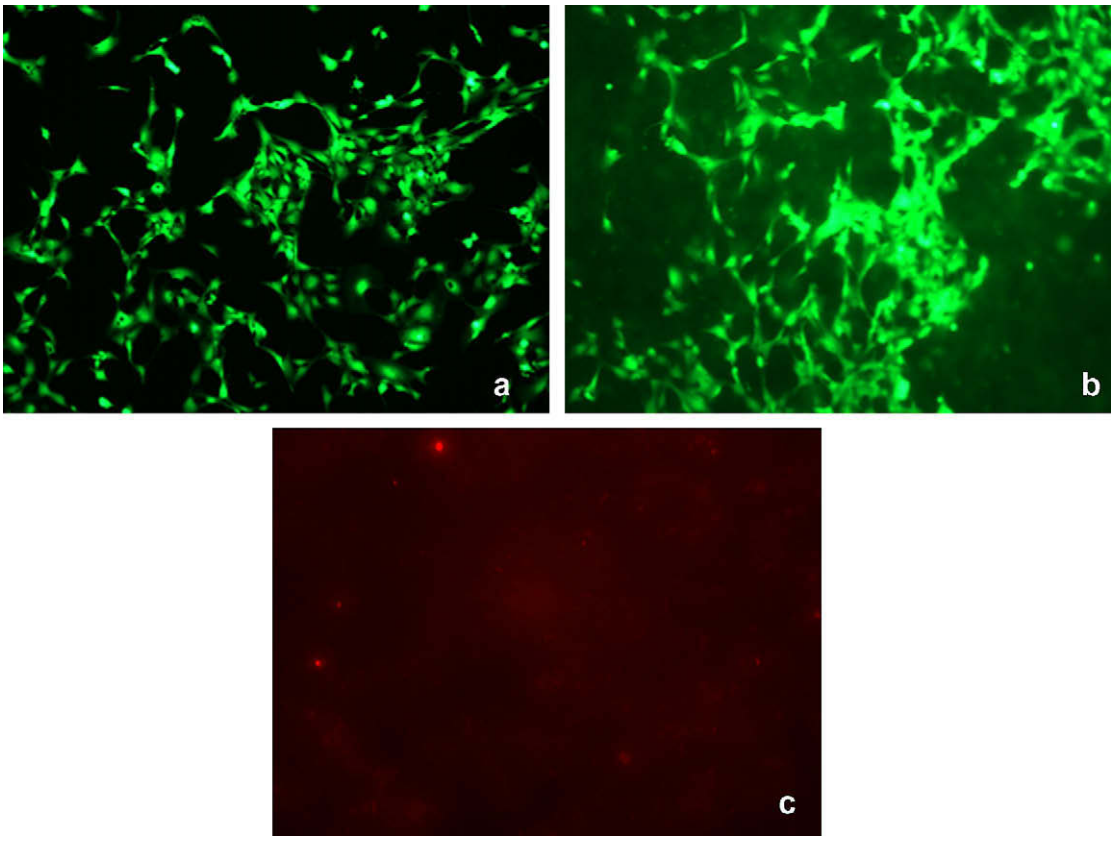

Fig. 2. Calcein AM-ethidium homodimer-2 double staining of HMECs on (a) TCPS at the excitation wavelength for Calcein (488 nm), showing live cells, (b) nanopatterned collagen film at the excitation wavelength for Calcein, showing live cells, and (c) on the films at the excitation wavelength for ethidium homodimer-2 (590 nm), showing dead cells.

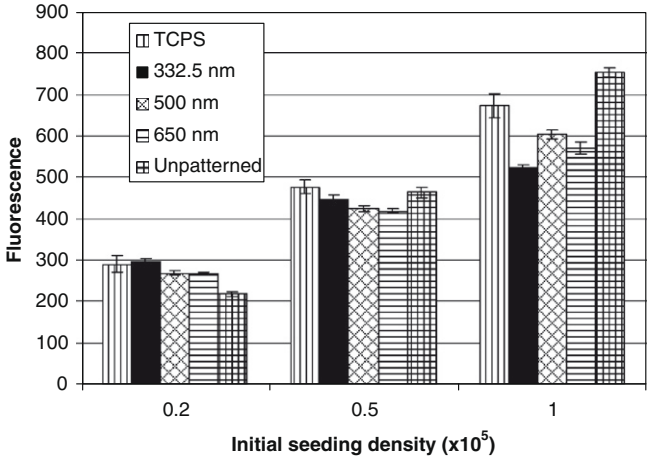

Fig. 3. Alamar Blue results showing the effect of seeding with HMEC with different initial seeding densities (at 48 h) on cell proliferation on nanopatterned and unpatterned collagen films.

to examine the influence of nanopatterns on cell alignment. No such alignment was observed on any of the three nanopatterned film types. Cells were randomly oriented on the surface of these films, as they were on the unpatterned film (Fig. 4). Endothelial cell alignment has been previously studied using micropatterns but not on nanochannels. Wu et al. [20] showed alignment with 15, 30 and 60 μm wide channels, while Vartanian et al. [16] showed the same effect with 25 μm wide channels. Nanoscale topographies that were used to modulate endothelial cells were in the form of islands rather than channels, and aimed to increase adhesion, spreading and proliferation rather than to achieve alignment [30,31]. Alignment on nanoscale patterns was, however, shown by other types of cells. For example, alignment of vascular smooth muscle cells was achieved with the nanoscale dimension patterns [26]. In the literature there are also data showing that fibroblastic cells align with patterns in the nano-range [32]. In the recent study by Lu et al. [22], endothelial cell alignment was shown on both micro- and nanoscale features, but here the channel dimension ranged from 750 nm to 5 μm, which is much larger than the largest dimension used in the current study. This implies that endothelial cells can certainly respond to physical surface features, but only when the feature dimension is around 1 μm or larger. SEM images did support these observations. Although there are a few aligned cells on the nanopatterned films (Fig. 5a), there was no extensive cell alignment on majority of the samples (Fig. 5b). Cell coverage of the films can be seen when micrographs of samples with different initial seeding densities at 48 h are compared (Fig. 5c–e).

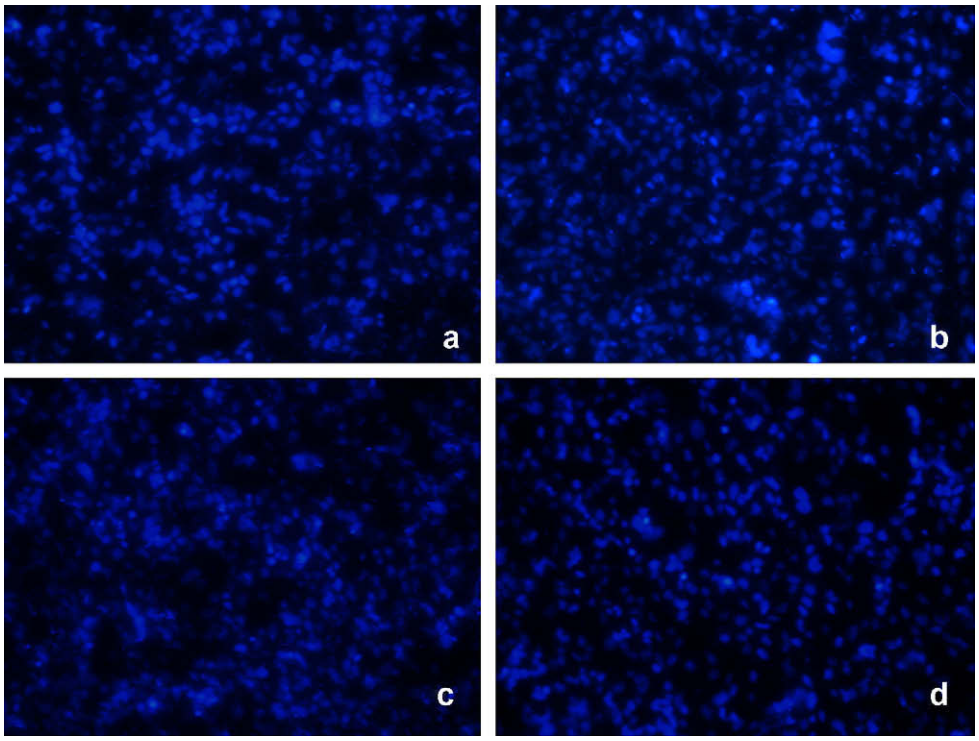

Fig. 4. DAPI staining of HMECs on collagen films at 24 h. (a) Unpatterned; (b) 332.5 nm patterned; (c) 500 nm patterned; (d) 650 nm patterned (×20).

3.5. Diffusivity

The diffusion coefficients for the collagen films were calculated after fitting the simulated amperometric currents to experimental data based on Fick's second law. Representative curves for 4-acetaminophenol diffusivity of each test group are given in Fig. 6a–d and for oxygen in Fig. 6a, c and d. In these experiments oxygen diffusion reached the equilibrium earlier than 4-acetaminophenol, so in the combined figures the lines for oxygen diffusivity appear shorter. From these figures it can be seen that the calculated data fit well with the experimental curves. Table 1 shows the calculated mean diffusion coefficients. The diffusion coefficient for 4-acetaminophenol of unseeded films (crosslinked once) was calculated as $1.86 \times 10^{-7} \pm 0.39 \times 10^{-7}\ cm^2\ s^{-1}$. This value is in the range of biological diffusion coefficients for glucose, which vary between 1.6×10^{-6} and $3.8 \times 10^{-7}\ cm^2\ s^{-1}$ [33]. When treated as in cell fixation, this value dropped to nearly half that of the unseeded samples. Among cell-seeded only and cell-seeded and fixed films there was also a similar 2-fold decrease caused by this second fixation of the collagen. When cell-seeded and cell-seeded and fixed samples were compared, their diffusion coefficient values were nearly four times higher than those of unseeded, and unseeded and fixed samples, respectively. A possible explanation for the higher diffusivity observed with cell seeding could be the contraction of the collagen fibers of the film by the endothelial cells, thus increasing the diffusivity. The support for this comes from Kelley et al. [34], who have shown that microvascular endothelial cells can contract collagen substrates by up to 50%, depending on the cell number and the amount of fetal calf serum in the medium. Even though the diffusivities of the collagen films are within the physiological range, cell seeding appears to further enhance this.

The diffusion coefficient for oxygen in unseeded films was calculated as $5.41 \times 10^{-7} \pm 2.14 \times 10^{-7}\ cm^2\ s^{-1}$. These values were much higher than for 4-acetaminophenol. Upon further fixation, the values dropped as before, but less dramatically, possibly because oxygen is a smaller molecule than 4-acetaminophenol and is less affected by scaffold porosity. Also similar to 4-acetaminophenol results, the cell-seeded samples had higher oxygen diffusivity values than the unseeded ones.

3.6. Flow-shear test

The data presented earlier in this study refer to cell seeding and incubation under static conditions. The data presented in this section are the result when incubation was under shear-flow conditions. In contrast to the microscopy and proliferation results, shear studies showed a significant difference ($p < 0.05$) between unpatterned, 332.5 nm patterned and 650 nm patterned films in terms of endothelial cell retention on the surface after application of shear stress, whereas the cell numbers on the controls for these groups (static culture) were almost the same ($p > 0.05$), indicating that the presence and dimensions of the nanopatterns affect cell number only under flow-shear conditions (Fig. 7). Cell retention on unpatterned films was $35 \pm 10\%$, while it was $75 \pm 4\%$ on 332.5 nm patterned films and even higher, $91 \pm 5\%$, on 650 nm patterned films

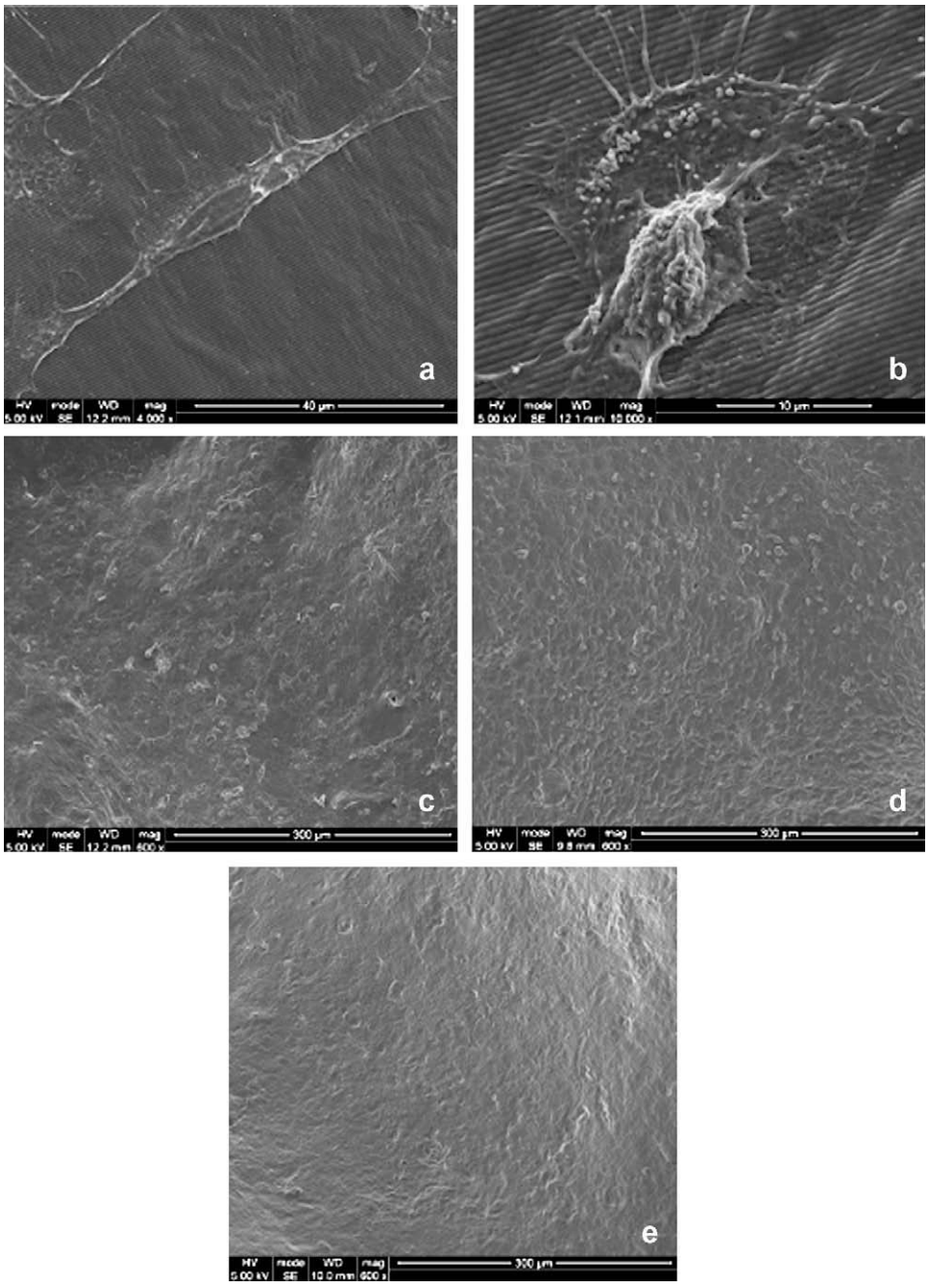

Fig. 5. SEM images of HMECs seeded on 500 nm nanopatterned collagen films at 48 h. (a) A single aligned cell; (b) a single unaligned cell; (c) initial seeding density of 2×10^4; (d) initial seeding density of 5×10^4; (e) initial seeding density of 1×10^5.

($p < 0.05$). This increase in cell retention is probably due to an increase in the level or strength of individual cell attachment zones. Certainly the nanopatterned surfaces present a greater surface area for cells to interact with or attach to, and thus resist the flow-shear. There was more cell retention on the 650 nm patterned films than on the 332.5 nm films, probably due not just to the higher width but also to the lower depth of the 332.5 nm films. The narrower channels might just be too shallow for the cells to cling to. Karuri et al. [35] have previously shown with corneal epithelial cells that nanoscale grooves enhance cell retention under shear stress by increasing the strength of cell attachment, and proposed that this was due to mimicking of the natural ECM. In the present study the increased surface area and higher molecular interaction between the cells and the surface appear to have helped the cells resist the flow.

4. Conclusion

Cell culture studies with HMECs show that, although the presence of nanopatterns does not affect endothelial cell

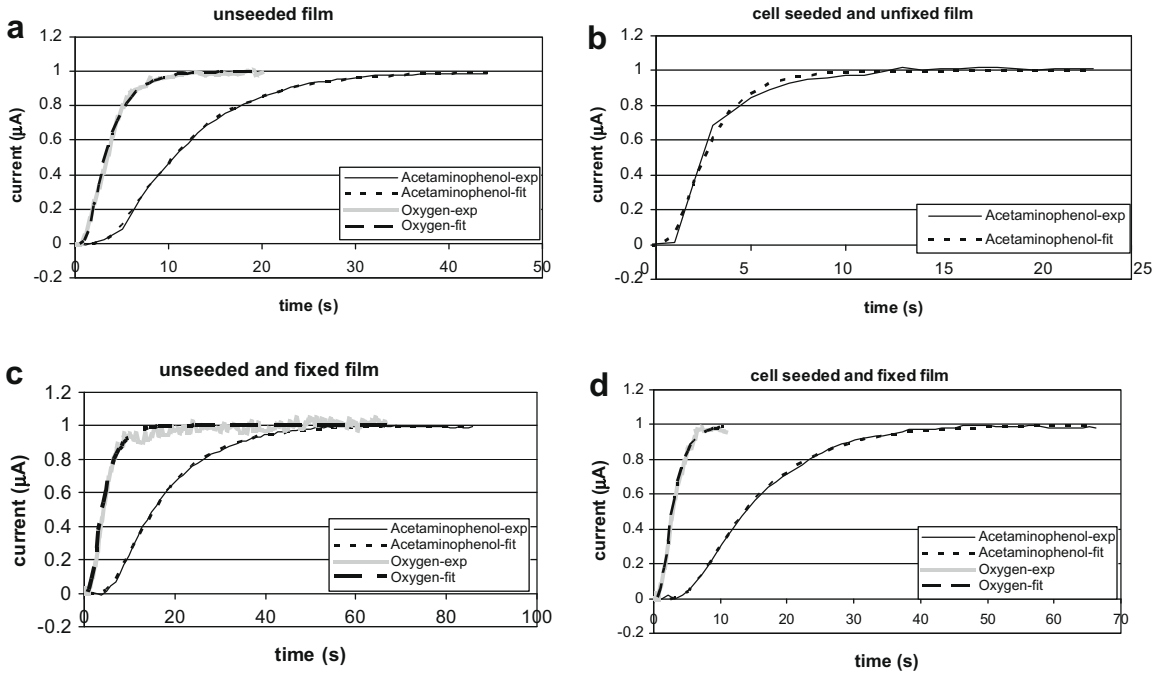

Fig. 6. 4-Acetaminophenol and oxygen diffusivity of collagen films. (a) Unseeded film; (b) HMEC seeded and unfixed film; (c) unseeded and fixed film; (d) HMEC seeded and fixed film.

Table 1
Diffusivity of cell-seeded, unseeded, fixed and unfixed collagen films to 4-acetaminophenol and oxygen.

Specimen	Average diffusivity $\times 10^{-7}$ ($cm^2\ s^{-1}$)	
	4-Acetaminophenol	O_2
Unseeded film	1.86 ± 0.39	5.41 ± 2.14
Unseeded, fixed film	1.12 ± 0.01	4.77 ± 0.78
Cell-seeded, unfixed film	8.09 ± 1.81	–
Cell-seeded, fixed film	4.37 ± 1.51	8.48 ± 2.45

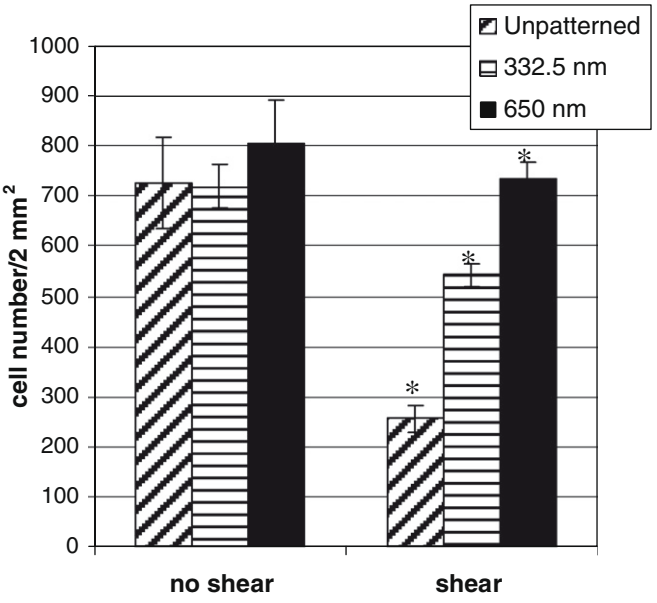

Fig. 7. Cell numbers on flow-shear applied HMECs on nanopatterned and unpatterned films compared to cell numbers on films that were not subjected to shear. * indicates significantly different values ($p < 0.05$).

proliferation and has a minimal effect on cell alignment, it significantly enhances cell retention under flow-shear conditions. Films proved to have high diffusion coefficients for microsolutes, hence they are promising as scaffolds in tubular form for the co-culture of endothelial and smooth muscle cells for vascular tissue engineering. The presence of cells improved O_2 and 4-acetaminophenol diffusivity, indicating that when the films are used in a bottom-up approach to build a three-dimensional scaffold they would allow sufficient oxygen and nutrient transfer to keep the cells alive. This would be especially important when the films are rolled into tubes, thus creating concentric multilayer structures such as that of a tissue engineered blood vessel.

Acknowledgements

We acknowledge Prof. Atilla Aydinli and Askin Kocabas of Bilkent University (Ankara, Turkey) for providing the patterned templates. We also gratefully acknowledge the support of State Planning Organization of Turkey (DPT) through the Project BAP 01.08.DPT. 2003K120920-20 and the Scientific and Technical Research Council of Turkey (TUBITAK) grant to P.Z. through METUNANOBIOMAT (TBAG 105T508).

References

[1] Benditt EP, Schwartz SM. Blood vessels. In: Rubbin E, Faber JL, editors. Pathology. Philadelphia, PA: JP Lippincott; 1988. p. 452–95.
[2] Thomas AC, Campbell GR, Campbell JH. Advances in vascular tissue engineering. Cardiovasc Pathol 2003;12:271–6.

[3] Geeracrt AJ, Callaghan JC. Experimental study of selected small calibre arterial grafts. J Cardiovasc Surg 1977;18:155.
[4] Nunn DB, Freeman MN, Hudgkins PC. Post-operative alterations in the size of Dacron grafts: an ultrasonic evaluation. Ann Surg 1979;189:741–5.
[5] Chakfe N, Kretz JG, Petit H. Albumin impregnated polyester vascular prosthesis for abdominal aortic surgery: an improvement? Eur J Vasc Endovasc Surg 1996;12:346–53.
[6] Kannan RY, Salacinski HJ, Butler PE, Hamilton G, Seifalian AM. Current status of prosthetic bypass grafts: a review. J Biomed Mater Res B Appl Biomater 2005;74(1):570–81.
[7] Henze U, Kaufmann M, Klein B, Handt S, Klosterhalfen B. Endothelium and biomaterials: morpho-functional assessments. Biomed Pharmacother 1996;50(8):388.
[8] Rhee RY, Gloviezki P, Camria RA, Miller VM. Experimental evaluation of bleeding complications, thorombogenicity neo intimal characteristics of prosthetic patch materials used for carotid angioplasty. Cardiovasc Surg 1996;4:746–52.
[9] Thompson MM, Budd JS, Bell PRF. Use of freshly isolated capillary endothelial cells for the immediate establishment of a monolayer on a vascular graft at surgery. Surgery 1994;100:392–9.
[10] Sarkar SJ, Sales KM, Hamilton G, Seifalian AM. Addressing thrombogenicity in vascular graft construction. Biomed Mater Res B Appl Biomater 2007;82(1):100–8.
[11] Ratcliffe A. Tissue engineering of vascular grafts. Matrix Biol 2000;19:353–7.
[12] Mitchell SL, Niklason LE. Requirements for growing tissue-engineered vascular grafts. Cardiovasc Pathol 2003;12(2):59–64.
[13] Kwon K, Kidoaki S, Matsuda T. Electrospun nano- to microfiber fabrics made of biodegradable copolyesters: structural characteristics, mechanical properties and cell adhesion potential. Biomaterials 2005;26:3929–39.
[14] Miller DC, Thapa A, Haberstroh KM, Webster TJ. Endothelial and vascular smooth muscle cell function on poly(lactic-co-glycolic acid) with nano-structured surface features. Biomaterials 2004;25(1):53–61.
[15] Bondar B, Fuchs S, Motta A, Migliaresi C, Kirkpatrick CJ. Functionality of endothelial cells on silk fibroin nets: comparative study of micro- and nanometric fibre size. Biomaterials 2008;29(5):561–72.
[16] Vartanian KB, Kirkpatrick SJ, Hanson SR, Hinds MT. Endothelial cell cytoskeletal alignment independent of fluid shear stress on micropatterned surfaces. Biochem Bioph Res Co 2008;371(4):787–92.
[17] Li YJ, Haga JH, Chien S. Molecular basis of the effects of shear stress on vascular endothelial cells. J Biomech 2005;38:1949–71.
[18] Duncan AC, Rouais F, Lazare S, Bordenave L, Baquey Ch. Effect of laser modified surface microtopochemistry on endothelial cell growth. Colloid Surf B 2007;54:150–9.
[19] Hu S, Eberhard L, Chen J, Love JC, Butler JP, Fredberg JJ, et al. Mechanical anisotropy of adherent cells probed by a three-dimensional magnetic twisting device. Am J Physiol Cell Physiol 2004;287:1184–91.
[20] Wu CC, Li Y, Haga JH, Kaunas R, Chiu J, Su F, et al. Directional shear flow and Rho activation prevent the endothelial cell apoptosis induced by micropatterned anisotropic geometry. Proc Natl Acad Sci USA 2007;104(4):1254–9.
[21] Punshon G, Vara DS, Sales KM, Kidane AG, Salacinski HJ, Seifalian AM. Interactions between endothelial cells and a poly(carbonate-silsesquioxane-bridge-urea)urethane. Biomaterials 2005;26:6271–9.
[22] Lu J, Rao MP, MacDonald NC, Khang D, Webster TJ. Improved endothelial cell adhesion and proliferation on patterned titanium surfaces with rationally designed, micrometer to nanometer features. Acta Biomater 2008;4:192–201.
[23] Kader KN, Yoder CM. Endothelial cell death on biomaterials: theoretical and practical aspects of investigation. Mater Sci Eng C 2008;28:387–91.
[24] Lee CH, Singla A, Lee Y. Biomedical applications of collagen. Int J Pharm 2001;221(1–2):1–22.
[25] Boccafoschi F, Habermehl J, Vesentini S, Mantovani D. Biological performances of collagen-based scaffolds for vascular tissue engineering. Biomaterials 2005;26(35):7410–7.
[26] Zorlutuna P, Hasirci N, Hasirci V. Nanopatterned collagen tubes for vascular tissue engineering. J Tissue Eng Regen Med 2008;2(6):373–7.
[27] Rong Z, Rashid S, Vadgama P. A bipartite expression for transient amperometric current at a membrane covered planar electrode to characterize solute diffusion through the membrane. Electroanal 2006;17:1703–9.
[28] Staros JV, Wright RW, Swingle DM. Enhancement by *N*-hydroxysulfosuccinimide of water-soluble carbodiimide-mediated coupling reactions. Anal Biochem 1986;156:220–2.
[29] Nerem RM, Alexander RW, Chappell DC, Medford RM, Varner SE, Taylor RW. The study of the influence of flow on vascular endothelial biology. Am J Med Sci 1998;316:169–75.
[30] Dalby MJ, Riehle MO, Johnstone H, Affrossman S, Curtis ASG. In vitro reaction of endothelial cells to polymer demixed nanotopography. Biomaterials 2002;23(14):2945–54.
[31] Tajima S, Chu JS, Li S, Komvopoulos K. Differential regulation of endothelial cell adhesion, spreading, and cytoskeleton on low-density polyethylene by nanotopography and surface chemistry modification induced by argon plasma treatment. J Biomed Mater Res A 2008;84(3):828–36.
[32] van Delft FCMJM, van den Heuvel FC, Loesberg WA, te Riet J, Schön P, Figdor CG, et al. Manufacturing substrate nano grooves for studying cell alignment and adhesion. Microelectron Eng 2008;85(5–):1362–6.
[33] Rong Z, Cheema U, Vadgama P. Needle enzyme electrode based glucose diffusive transport measurement in a collagen gel and validation of a simulation model. Analyst 2006;131:816–21.
[34] Kelley C, D'Amore P, Hechtman HB, Shepro D. Microvascular pericyte contractility in vitro: comparison with other cells of the vascular wall. J Cell Biol 1987;104:483–90.
[35] Karuri NW, Liliensiek S, Teixeira AI, Abrams G, Campbell S, Nealey PF, et al. Biological length scale topography enhances cell-substratum adhesion of human corneal epithelial cells. J Cell Sci 2004;117(15):3153–64.

Nanopatterns are Important in Vascular Tissue Engineering Applications

P. Zorlutuna[1], Z. Rong[2], A. Elsheikh[3], P. Vadgama[2], V. Hasirci[1]
[1]METU, BIOMAT, Department of Biotechnology, Biotechnology Research Unit, Ankara, Turkey
[2]IRC in Biomedical Materials, Queen Mary University of London, Mile End Road, London E1 4NS, UK
[3] University of Dundee, Division of Civil Engineering, Dundee DD1 4HN, UK.

INTRODUCTION

Patency of a tissue engineered vascular graft depends on several conditions; most important ones being that it should consist of a continuous layer of endothelium to prevent thrombosis and consequent clogging and adequate mechanical properties that approach that of to native vessels. Therefore, a tissue engineered graft must mimic the highly organized vascular ECM. In this study, nanopatterned collagen films were used for this end. Results showed that presence of nanopattterns on the scaffolds improved the mechanical properties and flow-shear resistance of vascular cells. Therefore, nanopatterning is a promising approach in vascular tissue engineering applications.

MATERIALS AND METHODS

X-ray interference lithography was used to create the templates with nano-size channels on silicon wafers and then transferred to PDMS. Patterned films were produced by solvent casting collagen Type I, isolated from rat tails, on the templates with subsequent crosslinking using chemical crosslinkers (EDC/NHS). These films were seeded with human vascular smooth muscle cells (VSMC) and human microvascular endothelial cells (HMEC) in order to assess the effect of nanopatterns on vascular cell behavior and to test the scaffolds for their suitability for vascular tissue engineering. VSMC proliferation on nanopatterned and unpatterned collagen films were determined by Alamar Blue, and cell phenotype and functionality were confirmed by immunostaining and other fluorescence stainings (i.e. DAPI). Fluorescence microscopy and SEM examination were used to show cell guidance by nanopatterns of different sizes. The films were subjected to tensile testing to study their mechanical properties. Similar films were seeded with HMECs and cell alignment and viability, cell proliferation and cell retention following shear stress were studied.

RESULTS AND DISCUSSION

VSMCs were aligned on the nanopatterns of all the 3 films with different nanopattern dimensions and also retained their phenotype for the whole cell culture duration (Fig. 1). Presence of nanopatterns increased the UTS from 0.55 ± 0.11 to as much as 1.63 ± 0.46 MPa at the end of 75 days, which is a value within the range of natural arteries and veins (Fig. 2). Similarly, Young's Modulus values were calculated to be around 4 MPa, again in the range of natural vessels.

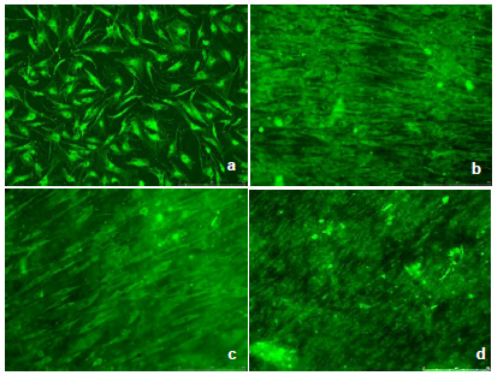

Figure 1. VSMC on collagen films. a) unpatterned, b) 332.5 nm, c) 500 nm, d) 650 nm (x 100). Day 21 anti-a-smooth muscle actin stain.

In the static culture, majority of HMECs were not aligned with nanopatterns (Fig. 3). The presence of the nanopatterns however significantly improved HMEC retention under shear of 12 dynes/cm^2 ($p<0.05$) (Fig. 4). Cell retention on unpatterned films was 35 ± 10 %, while it was 75 ± 4 % on 332.5 nm patterns and even higher, 91 ± 5 %, on 650 nm patterns. Although the presence of the nanopatterns did not affect cell proliferation or viability for both VSMCs and HMECs, they significantly improved mechanical properties of the scaffolds and cell retention under flow shear.

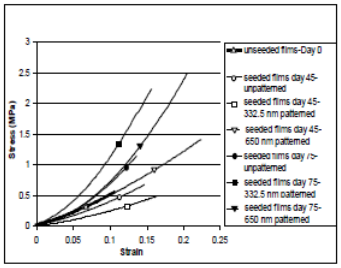

Figure 2. Stress-Strain plots of unseeded and VSMC seeded nanopatterned and unpatterned collagen films after 45 and 75 days of incubation *(n=6)*.

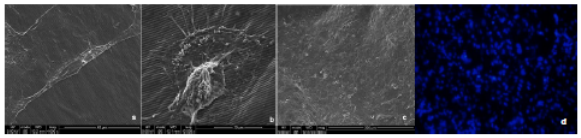

Figure 3. HMECs on nanopatterned collagen films (650 nm). SEM of (a) an aligned cell, (b) an unaligned cell, (c) HMECs on the film. Fluorescence micrograph of HMEC (Stained with DAPI, x 100).

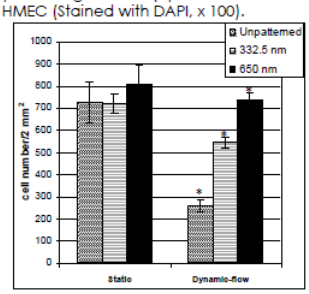

Figure 4. Cell numbers on flow-shear applied HMECs on nanopatterned and unpatterned films compared with cell numbers on films that were not subjected to shear. * indicates significantly different values ($p<0.05$).

It was observed that the nanopatterned collagen films could support and align human VSMC isolated from human saphenous vein biopsy samples. The cell guidance is especially important since natural VSMC in vessels are all oriented in one direction and alignment of cells improved the construct strength. Although the presence of nanopatterns did not affect endothelial cell proliferation and had a minimal effect on cell alignment, they significantly enhanced cell retention under shear. As a conclusion, nanopatterns were shown to be important in vascular tissue engineering applications through enhanced mechanical properties and adhesion strength.

ACKNOWLEDGMENTS

We acknowledge the contributions of Prof. A.Aydinli and A.Kocabas of Bilkent University (Ankara, Turkey) who provided the patterned templates. We also gratefully acknowledge the support of METU through project BAP2007-01-08-02 and TUBITAK through projects TBAG105T508 and 108T576 (including the grant to PZ).

The Role of Nanopillars on Adhesion and Orientation of Saos-2 and Bone Marrow Stem Cells

H. Özçelik[1], J. Ziegler[2], A. Schleunitz[2], M. Bednarzik[2], C. Padeste[2], V. Hasırcı[1]
[1]METU, BIOMAT, Department of [1]Biological Sciences, Biotechnology Research Unit, Ankara 06531, Turkey
[2]Lab for Micro- and Nanotechnology, Paul Scherrer Institut, 5232 Villigen PSI, Switzerland

Introduction

For cell biology and in tissue engineering it is important to understand cell behavior in nanoscale. Recently, it became clear that nanotopography can elicit strong and different effects such as changes in migration, adhesion, cytoskeletal organisation and gene regulation, on a range of cell types [1]. The nanoworld deals with various interfacial forces that have different effective ranges and the prediction of the response of a cell to nanofeatures is difficult. However, remarkable effects on cell adhesion have already been reported. The aim of the present study was to investigate the influence of well defined nanoscale structures on the behavior of Bone Marrow Stem Cells (BMSCs) and Saos-2 cells in order to gain insight into the mechanism of nano-topographical guidance.

Materials and Methods

Square millimeter sized arrays of nanopillars of up to 900 nm height and 200 nm diameter and with a pillar-to-pillar distance of 1 µm to 10 µm were produced on a silicon wafer by e-beam lithography, chromium deposition and lift-off followed by reactive ion etching (Figure 1). From this template a negative replicate was formed by polydimethylsiloxane (PDMS) casting. The final replicates were produced by solvent casting from 1-4% solutions of poly(L-D,L-lactic acid) (P(L-D,L)LA) on PDMS templates. Films were examined by SEM and AFM. Human osteosarcoma cell line cells, Saos-2, were cultured in RPMI medium with 10% fetal calf serum. Mouse Bone Marrow Stem Cells (BMSCs) were cultured in DMEM high glucose medium supplemented with 10% (v/v) FBS. The cells were stained with FITC labelled Phalloidin and DAPI in order to investigate the orientation of the cells using fluorescence microscopy.

Results and Discussion

Behavior of BMSC and Saos-2 showed differences in terms of positioning, orientation and elongation on the P(L-D,L-LA surfaces. Almost all BMSCs avoided the nanopatterned area independent of the spacing of the nanopillars (Figure 2). Our data supports the findings in the literature (2) that regular nanotopography reduces cell adhesion very markedly. It is possible that the cells react on differences in the mechanical stresses produced by the internal contractile mechanisms of the cell and those imposed by other cells and events on the substratum. Reduction in cell adhesion could be due to lowered adhesive forces generated by the surface. Saos-2 cells adhered to patterned fields and aligned in compliance with the gaps between the nanopillars (Figure 3). When pillars were closer in one direction that became the alignment direction. The differences in adhesion behavior of the two cell types might be due to the deformable character of cancerous cells [3,4].

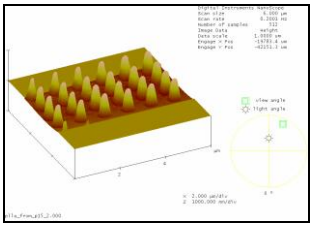

Figure 1. AFM micrograph of nanopillars on PLLA film.

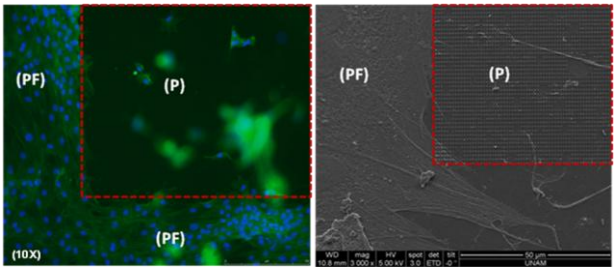

Figure 2. Fluorescence and SEM micrographs of BMSC occupying pattern free regions (PF) on the P(L-D,L-LA) film avoding the nanopillars of the pattern (P). Scale bar of fluorescence micrograph corresponds to 250 µm.

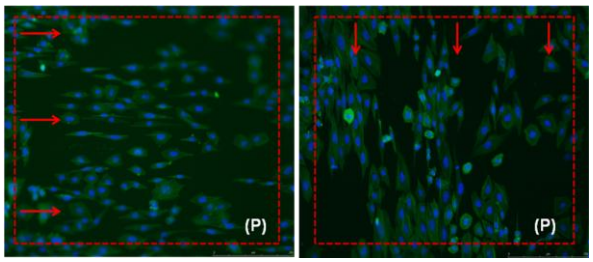

Figure 3. Saos-2 cells positioned and elongated on the nanopillar-based patterned areas (P) along the x or y direction depending on the distance between the nanopillars. Nuclei were DAPI stained and cytoskeleton were Phalloidin stained. Magnification is (10x), scale bar corresponds to 250 µm.

Conclusions

The results on size and type of packing of nanopillars on cell adhesion suggest that the cells may be able to sense relative distances on such topographies. Cell size, shape and deformability determined the attachment behavior of the cells. The differences in adhesion between BMSC and Saos-2 might be due to the specific reaction of the cell to mechanical properties of the substratum and to surface forces.

References

1. Leong K.W. *et al.* (2005) Nanomedicine: Nanotechnology, Biology, and Medicine 1, 10–2.
2. Curtis A. *et al.* (2004) IEEE Transactions on Nanobioscience, 3 (1), 61-65.
3. Ben-Ze'ev A. (1985) Biochim Biophys Acta.780, 197–212.
4. Anselme K. *et al.* (2009) J. Mater Sci: Mater Med DOI 10.1007/s10856-009-3950-7.

Replication of nano-pillar array structures for tissue engineering applications

H. Özçelik[1], C. Padeste[2], J. Ziegler[2], A. Schleunitz[2], M. Bednarzik[2], V. Hasırcı[1]

[1]*METU, BIOMAT, Department of Biological Sciences, Ankara 06531, Turkey*

[2]*Lab for Micro- and Nanotechnology, Paul Scherrer Institut, 5232 Villigen PSI, Switzerland*

INTRODUCTION: For cell biology and in tissue engineering it is important to understand cell behaviour on the nanoscale. Recently, it became clear that nanotopography can elicit strong and different effects such as changes in migration, adhesion, cytoskeletal organisation and gene regulation, on a range of cell types. The technology to produce structures, e.g. in silicon substrates, of dimensions interesting for studying interactions with cells is well established. However, to make such structures attractive for cell growth studies they need to be replicated in high numbers into biologically relevant materials. Here we present a two-step replication process which allows the reproduction of high aspect ratio nanopillar arrays into biocompatible polymers which are soluble in organic solvents.

METHODS: Square millimeter sized arrays of nanopillars of up to 900 nm height and 200 nm diameter and with a pillar-to-pillar distance of 1 µm to 10 µm were produced on a silicon wafer by e-beam lithography, chromium deposition and lift-off followed by reactive ion etching (Fig. 1). The replication process is schematically shown in Fig. 2. A negative replicate was first formed by polydimethylsiloxane (PDMS) casting. The final replicates were produced by solvent casting from 1-4% solutions of poly(L-D,L-lactic acid) (PLLA) on PDMS templates. On the replicated structures human osteosarcoma cell line cells, SaOs-2, as well as Mouse Bone Marrow Stem Cells (BMSCs) were cultured. The cells were stained with FITC labeled Phalloidin and DAPI in order to investigate their orientation using fluorescence microscopy.

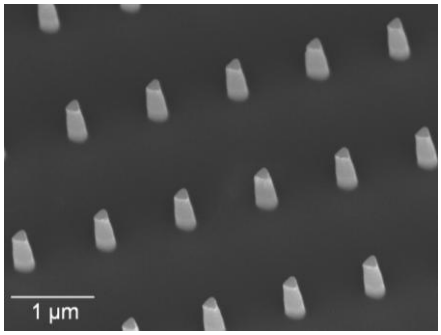

Fig. 1: Array of nanopillars (900 nm high) dry-etched into silicon.

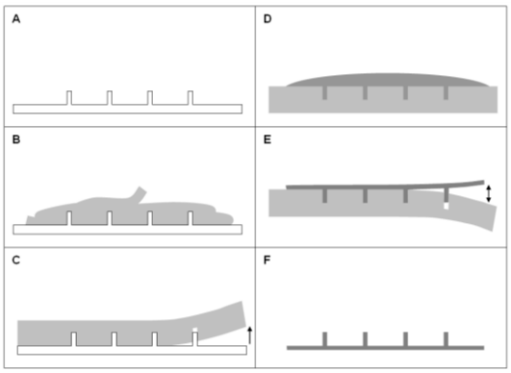

Fig. 2: Scheme of the replication procedure: Silicon nanopillar arrays (A) are embedded in PDMS (B). After curing the PSMS is separated from the master(C) and covered with a droplet of PLLA solution (D). After slow evaporation of the solvent the replicate is separated from the PDMS (E/F).

RESULTS: The replication process proved to be suitable for nano-sized pillar structures with aspect ratios as high as 4-5. AFM measurements confirmed the same height of the pillars of the master and the replicates. The flexibility of the PDMS cast facilitates the detachment in both replication steps. Furthermore, a considerable solvent uptake of the PDMS appears beneficial in the second step, resulting in high enough polymer concentration in the cavities to form solid pillars.

In first cell culture experiments it was found that different types of cells react very differently on the surface topography: While BMSC cells appeared to avoid contact with the nanopillar arrays, the SaOs-2 cells tried to adapt to the structured surfaces as they elongated along the axes with the shortest pillar-to-pillar distance (arrows in Fig. 3).

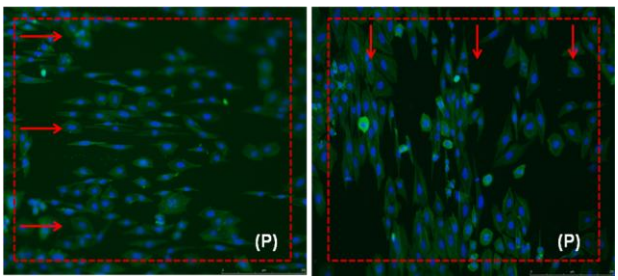

Fig. 3: SaOs-2 cells positioned and elongated on the nanopillar- patterned areas (P).

The Effect of Surface Nanotopography on Neural Stem Cell Alignment

Hayriye Özçelik[1] , Deniz Yücel[1,2], Celestino Padeste[3], Vasıf Hasırcı[1*]
[1]*METU, BIOMAT, Department of 1Biological Sciences, Biotechnology Research Unit, Ankara 06531, Turkey*
[2]*METU, Central Laboratory, Ankara 06531, Turkey*
[3]*Lab for Micro- and Nanotechnology, Paul Scherrer Institut, 5232 Villigen PSI, Switzerland*

Abstract— Surface topography is one of the main parameters used to control the design of biomedical devices, implants, high throughput cell-arrays, and basic cell biology. Square millimeter sized arrays of nanopillars of up to 900 nm height, 200 nm diameter and a pillar-to-pillar distance of 1 µm to 10 µm were produced. The effect of these nanopillars on neural stem cells (NSCs) was studied *in vitro* and the cell attachment, alignment, and morphology were analyzed. NSCs were aligned along the ridge-like structures formed by nanopillars.

Cells in their natural environment are surrounded by and are in interaction with nanostructures, when contacting with other cells or with the extracellular matrix (ECM) that is formed by biomolecules configured in a variety of geometrical arrangements and forms (nanopores, nanofibers, nanogrooves, nanoposts). Fabricated nanotopography can also influence cell morphology, guidance, adhesion, migration, proliferation, and cytoskeletal organization [1]. This ability to control orientation of cells can be very useful in biomaterial and tissue engineering applications in order to create more advanced products.

It has recently been shown that nanotopography can have strong effects on a range of cell types [2]. Since the nerve cells in native tissue are either unidirectionally aligned or form networks, patterning of scaffold surfaces has been used extensively to study and control the interactions of various neuronal cell types with surfaces [3].

The aim of the present study was to investigate the influence of well defined nanoscale structures, nanopillars, on the behavior of NSC in order to gain insight into the mechanism of nanotopographical guidance.

Nanopillars were produced on a silicon wafer by e-beam lithography, chromium deposition and lift-off followed by reactive ion etching. From this template a negative replica of polydimethylsiloxane (PDMS) was cast. The final replica was produced by solvent casting of a 2% solution of poly(L-D,L-lactic acid) (P(L-D,L)LA) on PDMS templates. Films were examined by SEM and AFM. Mouse NSCs were cultured in the growth medium of (DMEM)/F12 containing human transferrin, bovine insulin, chemically defined lipids, sodium selenite, streptomycin/penicillin and a supplement of epidermal growth factor. The cells were seeded on polymeric films with adsorbed fibronectin. The fixed cells were stained with FITC labelled Phalloidin and propidium iodide (PI) in order to investigate the orientation of the cells using fluorescence microscopy. They were examined with SEM to determine their location on the field patterned with nanopillars.

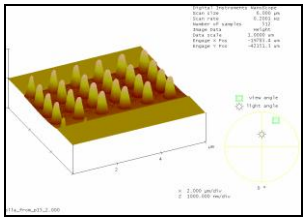

Figure 1: AFM micrograph of nanopillars on PLLA film

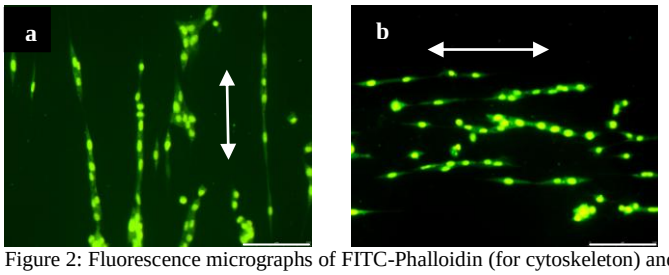

Figure 2: Fluorescence micrographs of FITC-Phalloidin (for cytoskeleton) and PI (for nuclei) stained NSCs on the nanopillar patterns (x20, scale bar: 100 µm). Nanopillars orientations are shown with arrows.

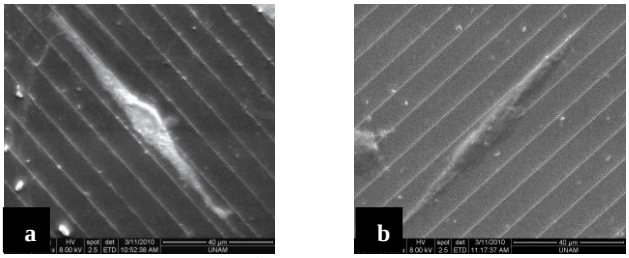

Figure 3: SEM micrographs of aligned NSCs on patterned regions on the P(L-D,L-LA) films. Nanopillars orientations are shown with arrows.

AFM studies showed that nanopillar patterns of the template was successfully reproduced on the P(L-D,L-LA) films with PDMS replica serving as the intermediary template (Figure 1). In Figure 2 the nuclear and cytoskeletal orientation of NSCs showed that the cells were positioned and elongated on the nanopillar-based patterned areas controlled by the distance between the nanopillars; the cells followed the pillars separated by shorter distances. This tendency was also supported by SEM (Figure 3). Moreover, mouse NSCs were localized between the ridge-like structures (900 nm in height) formed by nanopillars. However, these cells were randomly oriented on the fields of symmetrically distributed nanopillars (data not shown).

In conclusion, the results on size and type of organization of nanopillars on cell alignment suggest that the cells are able to sense relative distances on such small topograph.

This work was partially supported by TUBITAK under Grant No. TBAG-108T576.

*Corresponding author: vhasirci@metu.edu.tr

[1] C. J. Bettinger, R. Langer, J. T. Borenstein. Angew Chem Int Ed Engl. **48**(30), 5406 (2009).
[2] E. Martinez, E. Engel, J. A. Planel, J. Samitiera. Ann Anat 191, **126** (2009).
[3] L. A. Cyster, K. G. Parker, T. L. Parker, D. M. Grant. Biomaterials **25**(1),97 (2004).